

Aspects of High Field Theory in Relativistic Plasmas

Haibao Wen

BSc (Shanxi University, China) MSc (Graduate University
of the Chinese Academy of Sciences, China)

Date submitted

March 2012

A thesis submitted in fulfilment of the
requirements of the degree of Doctor of
Philosophy at Lancaster University

Some of the results in the present thesis have been published. Here is the list of the publications and the corresponding calculations:

- | | |
|------------------|--|
| Ref [6] | kinetic calculation of the 3 – D gourd waterbag in Chapter II |
| Ref [52] | fluid calculation of the 3 – D gourd waterbag in Chapter III |
| Ref [60][65][70] | kinetic calculation of the cold Born – Infeld plasmas in Chapter V |

Declaration

This thesis is the author's own work and has not been submitted in substantially the same form for the award of a higher degree elsewhere.

Haibao Wen

March 2012

Abstract

This thesis is concerned with plasmas and high field physics. We investigate the oscillations of relativistic plasmas using a kinetic description (Chapter II), a macroscopic fluid moment description (Chapter III), a quantum description (Chapter IV as a brief exploration) and Born-Infeld electrodynamics (Chapter V).

Using a kinetic description, we examine the non-linear electrostatic oscillations of waterbag-distributed plasmas and obtain the maximum electric field E_{\max} (Chapter II).

Using a macroscopic fluid moment description with the closure of the Equations Of State (EOSs), we obtain the maximum electric field E_{\max} of electrostatic oscillations for various waterbag-distributed electron fluids, which may imply the advantages of some fluids with particular EOSs in the aspect of particle acceleration. Furthermore, we find that fluids with a more general class of EOSs may have the same advantages (Chapter III).

A brief numerical calculation of an ODE system originating from the Maxwell equations and a Madelung decomposition of the Klein-Gorden equation with a $U(1)$ field shows that electrostatic oscillations decay in a Klein-Gorden plasma due to quantum effects (Chapter IV).

With calculations using the Born-Infeld equations and the Lorentz equation, we investigate the electrostatic and electromagnetic oscillations in cold plasmas in Born-Infeld electrodynamics (Chapter V).

For the electrostatic oscillations we find that the electric field of Born-Infeld electrodynamics behaves differently from that of Maxwell electrodynamics. However, Born-Infeld electrodynamics gives the same prediction as Maxwell electrodynamics for the maximum energy that a test electron may obtain in an electrostatic wave (Section V A).

For electromagnetic waves, the dispersion relation and the cutoff frequencies of the “R”, “L” and “X” modes of electromagnetic waves in Born-Infeld cold plasma are deduced to be different from those in Maxwell cold plasma. The cutoff frequencies (when the index of refraction $n \rightarrow 0$) are also obtained, showing the advantage of “O” mode waves for the acceleration of particles (Section VB).

Keywords: relativistic plasmas, high fields, non-linear electrostatic oscillations, electromagnetic waves, wave-breaking limits, trapped particles, waterbag-distributed warm plasmas, Maxwell-moments method, cold Born-Infeld plasmas

Acknowledgements

This thesis would not have been possible without the help and support of many kind people.

My deepest gratitude goes to my supervisor, Dr. David Burton. His guidance, patience, encouragement, enlightenment and valuable advice from the preliminary to the concluding level enabled me to shape this project and develop an understanding of the subject. I am also grateful to his wife, Anne, who has kindly offered to help me with my English. I am particularly thankful for their enthusiastic help during my stay in Lancaster.

Without the studentship provided by the Cockcroft Institute, I would not have had the opportunity to do a PhD in Lancaster.

I am heartily grateful to Prof. Robin Tucker and Dr. Jonathan Gratus, for their valuable advice and insightful comments on my work, as well as for the kind communication from their families.

Thanks also go to all the members in the mathematical physics group in Lancaster University. Special thanks go to Dr. Volker Perlick, Dr. Adam Noble, Dr. Shin Goto, Dr. Timothy Walton and Dr. Ricardo Gallego Torrome for their help in various ways.

I am indebt to Dr. Raoul Trines from Rutherford-Appleton Laboratory for his insightful discussions on my work, and Dr. Costas Gabrielatos for helping me with my English. I am also grateful to Dr. Min Yin for his great support.

I would also like to thank other staff in the Department of Physics for their assistance, as well as all my friends who have supported me in various ways.

Last, but by no means least, I am extremely grateful to my parents and other family members for their unconditional love and continuous support through the duration of my studies.

Contents

I. Introduction	11
A. Plasma Physics	11
1. Vlasov Equation	13
2. Applications of Plasmas in Particle Acceleration	15
B. Fundamental Theoretical Descriptions	17
1. (Single Particle) Kinetic Description	17
2. Macroscopic Fluid Description	18
3. Advantages of Macroscopic Fluid Description & its Relationship with the Kinetic Description	20
C. Waterbag Distribution	21
D. Wave-Breaking Limits	22
1. Oscillations and Waves of Plasma	22
2. Wave-Breaking	23
3. Applications of Wave-Breaking Limits	25
4. Mathematical Wave-Breaking and Physical Wave-Breaking	25
E. High Field & Non-Linear Electrodynamics	27
1. A Brief Introduction to Born-Infeld Electrodynamics	27
F. Cold Born-Infeld Plasmas	29
1. Wave-Breaking Limit	30
2. Dispersion Relation	30
II. Electrostatic Oscillations in the Kinetic Description	32
A. Cold Plasma	33
B. Waterbag-Distributed Warm Plasma	33
1. Shape of the Waterbag Distributions	33

2. Non-Linear Electrostatic Oscillations	35
3. Electrostatic Wave-breaking in 3-D Waterbag	37
III. Velocity Moments Method in the Fluid Model	43
A. Framework	43
1. Introduction	43
2. Moments Method for Plasma Fluid	44
3. Closure of the Moments Hierarchy with a Waterbag Distribution	46
B. Calculation of Moments	47
1. Parameterised Description of the Boundary of the Waterbag	47
2. Integrals of Moments	48
C. ODE System	57
D. Original Results	61
1. Properties of Non-Linearities for a Large Proper Density	61
2. Wave-Breaking Limits	66
3. Trapped Particles	73
4. The Fraction of the Trapped Particles in the 3-D Ellipsoid Waterbag-Distributed Fluid	74
IV. A Brief Exploration of a Quantum Plasma	79
V. Born-Infeld Plasmas	88
A. Wave-Breaking Limit and Period of a Maximum Electrostatic Oscillation	88
1. Wave-Breaking Limit	91
2. Period of the Maximum Amplitude Oscillation	94
3. Comparison of the Maximum Energy Gain with Maxwell Theory	97
B. Dispersion Relation in Born-Infeld Electrodynamics	97

1. Wave Traveling Parallel to the External Magnetic Field	98
2. Wave Traveling Perpendicular to the External Magnetic Field	106
C. Comparisons with Cold Maxwell Plasmas	109
1. Wave-Breaking Limits and Dispersion Relations	109
2. Decelerating and particle trapping for “O” modes	110
VI. Summary of the Original Results	112
A. Electrostatic Oscillations & Bounds on the Electric Field in the Kinetic Description	112
B. Wave-Breaking Limits Calculated in a Maxwell-Moments Model	112
C. A Brief Exploration of a Klein-Gorden Plasma	113
D. Wave-Breaking Limits and Dispersion Relations for Cold Plasmas in Born-Infeld Theory	113
References	115

List of Figures

Page Fig.

20 Fig.1 1-D waterbag distribution showing the boundary of the indicator-type function $f(x, \dot{x})$ (see [50])

31 Fig.2 A schematic illustration of a 3-D gourd waterbag

34 Fig.3 A schematic illustration of E and μ as functions of ζ (the solid and the dashed line show E and μ respectively, see [61])

49 Fig.4 A schematic illustration of a 3-D ellipsoid waterbag

63 Fig.5 E and n with respect to ζ (the upper one is E and the lower one is n)

68 Fig.6 The relation between l and l_W

69 Fig.7 The relation between l and l_W when $l_W < l$

70 Fig.8 The fraction of trapped particles with respect to l (upper) and l_W (lower)

76 Fig.9 The relation between μ and ζ when $\hbar = 0$

77 Fig.10 ν (upper graph) and E (lower graph) with respect to ζ , re-

spectively

79 Fig.11 a (upper graph) and $\frac{1}{f^2}$ (lower graph) with respect to ζ , respectively

82 Fig.12 E and μ with respect to ζ (the solid and the dashed line show E and μ , respectively, see [6])

86 Fig.13 Electric field calculated in Maxwell electrodynamics

87 Fig.14 Electric field calculated in Born-Infeld electrodynamics

88 Fig.15 $\kappa E_{\max}^{\text{BI}}$ with respect to $\kappa E_{\max}^{\text{M}}$ when κBc takes the value 0.1 (black solid), 1 (red dashed) and 10 (blue dotted), respectively

89 Fig.16 $\kappa E_{\max}^{\text{BI}}$ with respect to κBc when $\kappa E_{\max}^{\text{M}}$ takes the value 0.1 (black solid), 1 (red dashed) and 10 (blue dotted), respectively

I. INTRODUCTION

A. Plasma Physics

Astronomical observations suggest that most visible matter is in the plasma state [1]. Actually, “plasma” has different meanings in different situations. Originated from the investigation into ionised gases, the plasma state is called “the fourth state of matter” in addition to the states of “solid”, “liquid” and “gas”. However, the free electrons in metals and free ions in liquids can also be regarded as plasmas, though they inhabit matter in the traditional solid or liquid state. The common property behind the above so-called plasmas is that the local interactions between particles in a plasma are negligible compared with the long range collective effects that are caused by the force fields (combination of external fields and the fields generated by the plasma particles, sometimes called “self-consistent fields”).

The term “plasma” was explicitly introduced by Langmuir in 1928 [2] during his investigations of the oscillations in ionised gases, which had been extensively studied by scientists including Pluecker, Goldstein, Thomson and John Sealy Townsend [3] during the late 19th century. The strict use of the term “plasma” describes particles with collective effects (rather than collisions) as the dominant effects, although “plasma” is also loosely used when collective effects are not that obvious. Considering “electric-field screening”, electric fields damping caused by the electrostatic interaction between charged particles, the term “plasma” is strictly used for the “electric-field screened” case. In other words, a sufficiently high number of particles are in the Debye sphere of any particle, where Debye sphere is the region outside which a typical electric fields damping happens. The name “Debye sphere” was named after Peter Debye as the electric-field screening was first theo-

retically treated by Debye and Hueckelin 1923 [4]. The Debye radius corresponding to the Debye sphere is the length $\lambda_D = \sqrt{\frac{\varepsilon_0 k_B T}{n_0 e^2}}$, where T is the temperature, n_0 is the average density of electrons and the constants k_B and e are the Boltzmann constant and the charge of a proton, respectively. In this thesis, the term “plasma” is used in the strict way, which refers precisely to a cluster of particles with an average distance much shorter than the Debye length and the macroscopic system scale much larger than the Debye length to screen the external fields.

In general, a plasma may consist of various types of positive and negative charged particles. In this thesis the properties of plasma oscillations and waves in a neutral plasma consisting of electrons and single-type massive ions are emphasised. Time scales (so that also length scales) considered throughout the thesis are always much shorter than typical two body collisions between the plasma particles so that collision terms are not considered, while they are longer than typical interactions between electric fields and particles so that (electrostatic or electromagnetic) oscillations are included. We regard the ions as “pinned” (also rest to the lab) and this allows us to introduce an inertial frame of reference adapted to the lab-background ions. Thus, if unspecified, the term “plasma” is used to refer to “neutral plasma” consisting of electrons and single-type massive ions.

For a general plasma, there is a spread in the velocities of the electrons. According to the velocity distribution of particles within a coarse grained cell (small from a macroscopic viewpoint but still containing a large number of particles), plasmas are divided into cold and finite temperature plasmas. A “cold” plasma has a uniform velocity distribution within a coarse grained cell and a “finite temperature” plasma has a non-uniform one. The term “warm plasma” is used when the width of the distribution is narrow. “Thermal” plasma is usually used to describe a plasma consisting of Maxwellian distributed particles in any coarse grained cell (see [5] [6] for exceptions).

Additionally, quantum effects are briefly discussed in Chapter IV, whereas relativistic effects are applied without exception. The Einstein summation convention is applied whenever an upper and lower occurrence of the same index appears. Unless otherwise specified, conventions $\varepsilon_0 = 1, \mu_0 = 1, c = 1$ are used for simplicity of the calculation and constants m and q are regarded as the mass and charge of an electron in Section IB1, Chapter II, III and V, of a scalar field particle in Chapter IV, and of an unspecified particle elsewhere.

1. Vlasov Equation

The general case of a cluster of particles with local interactions regarded as collisions (as interactions between particles outside their neighborhood are already counted in their contribution to the long range self-consistent force field \mathbf{F}) is described by the following Boltzmann equation,

$$\frac{\partial f}{\partial t} + \frac{\partial f}{\partial \mathbf{x}} \cdot \frac{\mathbf{p}}{m} + \frac{\partial f}{\partial \mathbf{p}} \cdot \mathbf{F} = \left. \frac{\partial f}{\partial t} \right|_{\text{col}}, \quad (1)$$

where $f d^3\mathbf{x} d^3\mathbf{p}$ is the number of particles with positions in the range $[\mathbf{x}, \mathbf{x} + d\mathbf{x}]$ and momenta in the range $[\mathbf{p}, \mathbf{p} + d\mathbf{p}]$, $F(\mathbf{x}, \mathbf{p}, t)$ is the force field acting on the particles, and $\left. \frac{\partial f}{\partial t} \right|_{\text{col}}$ is the collision term. We require the Boltzmann equation to respect the conservation law of particle number in circumstances with a changing force field and local interactions. The problem of existence and uniqueness of solutions to the Boltzmann equation is still not fully resolved. For a covariant and compact description, we use the exterior differential language, in which the Boltzmann equation can be written in the following compact form,

$$Lf = C[f], \quad (2)$$

where $C[f]$ is a collision term and

$$L = \dot{x}^\mu \left[\left(\frac{\partial}{\partial x^\mu} \right)^{\text{H}} - \left(\frac{q}{m} F^\nu{}_\mu \frac{\partial}{\partial x^\nu} \right)^{\text{V}} \right] \quad (3)$$

$$\left(\frac{\partial}{\partial x^\mu} \right)^{\text{H}} = \frac{\partial}{\partial x^\mu} - (\Gamma^\nu{}_{\mu\alpha})^{\text{V}} \dot{x}^\alpha \frac{\partial}{\partial \dot{x}^\nu}, \quad (4)$$

where x^μ and \dot{x}^ν , $\mu = 0, 1, 2, 3$ are the Lorentz coordinates of the spacetime manifold \mathcal{M} and its tangent bundle $(T\mathcal{M}, \Pi, \mathcal{M})$, $^{\text{H}}$ and $^{\text{V}}$ are the horizontal and vertical lifts from the manifold \mathcal{M} to the tangent bundle $T\mathcal{M}$, which is defined in the next paragraph, and $\Gamma^\nu{}_{\mu\alpha}$ are the Christoffel symbols defined as follows,

$$\begin{aligned} \Gamma_{\gamma\alpha\beta} &= g_{\gamma\delta} \Gamma_{\alpha\beta}^\delta \\ &= \frac{1}{2} (g_{\gamma\alpha,\beta} + g_{\beta\gamma,\alpha} - g_{\alpha\beta,\gamma}), \end{aligned} \quad (5)$$

with $g_{\alpha\beta}$ as the metric tensor of the base manifold \mathcal{M} and $g_{\alpha\beta,\gamma}$ as the partial differential of $g_{\alpha\beta}$ with respect to x^γ .

To obtain the expression for equation (4), we need the definition and rules of the vertical lifts, which can be found in textbooks like ‘‘Tangent and Cotangent bundles’’ written by Yano and Ishihara [7]. Here I list some fundamental formulae. For the projection operator from the total space to the base manifold $\Pi : T\mathcal{M} \rightarrow \mathcal{M}$ and a function on the base manifold $f : \mathcal{M} \rightarrow R$, the vertical lifts f^{V} and ω^{V} of the 0-form f and the 1-form ω are defined as

$$f^{\text{V}} = f \circ \Pi = \Pi^* f, \quad (6)$$

$$\omega^{\text{V}} = \Pi^* \omega. \quad (7)$$

The vertical lift X^{V} of a vector field X on \mathcal{M} is given by the following definition for any 1-form $\omega = \omega_\mu dx^\mu$ on \mathcal{M} ,

$$X^{\text{V}}(\iota\omega) = (\omega(X))^{\text{V}}, \quad (8)$$

where $\iota\omega = \omega_\mu^V \dot{x}^\mu$ is a 0-form on $T\mathcal{M}$. With the above equation (8), the vertical lift term in the definition of L (equation (3)) is rewritten as

$$\left(\frac{q}{m} F^\nu{}_\mu \frac{\partial}{\partial x^\nu} \right)^V = \frac{q}{m} F^{\nu V}{}_\mu \frac{\partial}{\partial \dot{x}^\nu} . \quad (9)$$

Collisionless plasma (where the local interaction terms on the right side of equation (2) is negligible) is described by the following equation without the collision term

$$Lf = 0 , \quad (10)$$

which is called the (relativistic) Vlasov equation [8]. Combined with the Maxwell equation that electromagnetic fields obey, the Vlasov equation gives a complete description of a classical collisionless plasma. However, the solutions of the Vlasov-Maxwell system are not always easy to obtain. Alternatively, especially when we are only interested in the macroscopic properties of plasma, we express moments of f in velocity (points in $T_X\mathcal{M}$) to a certain order and close the system of moment equations using physical considerations. Such a description in terms of the macroscopic physical quantities is called a “fluid description”. We will discuss the Vlasov and the fluid description in detail in Section IB and carry out calculations with them in the later chapters.

2. Applications of Plasmas in Particle Acceleration

Particles in particle accelerators are actually in a plasma state, and will show their collective properties. Often the particle beams in traditional accelerators have a complex collective behaviour and therefore kinetic and fluid models are useful [9].

There have been proposed new generations of more efficient accelerators with advantages such as a much higher energy gain per distance. One of them is called

a “(laser) wakefield”, “laser driven” or “(laser) plasma” accelerator which was first proposed by Toshiki Tajima and John Dawson in 1979 [10] and first experimentally demonstrated in 1988 [11]. We will use the term “plasma accelerator” throughout this thesis. A typical plasma accelerator consists of a laser pulse and a waveguide containing electron-ion plasma. When the laser pulse passes through the electron-ion plasma, it displaces the electrons following the laser pulse and there will be a neighborhood in the plasma lacking electrons, which causes an extremely intense local electrostatic field to accelerate the subsequent particle beam. Theoretically, plasma accelerators have an extremely intense local electrostatic field and a very high energy gain per distance. However, such acceleration could not be achieved over a large distance (at least at an order larger than 1m until recently) because it is difficult to control particle beams or laser beams over long distances. In fact, the physics in plasma accelerators becomes much more complex with the increase of the acceleration distance and the presence of non-linear effects [12]. In typical recent plasma accelerators, GeV-order energy was gained through a cm-order distance. For example, the Lawrence Berkeley National Laboratory (LBNL) accelerated an electron beam by 1GeV along a 3.3cm hydrogen-based capillary discharge waveguide in 2006 [13]. The Stanford Linear Accelerator Center (SLAC), on the other hand, even doubled the energy of electrons with an initial energy of 42GeV along a distance of 85cm in 2007 [14]. Obviously, these experiments have shown the merit of plasma accelerators in their much higher energy gain per distance as compared with traditional accelerators.

In the astrophysical area, the study of plasmas has long established since a lot of intensive phenomena occur in extreme circumstances [15]. Plasma is the dominant state in the cosmos [1], and therefore we can view astrophysical objects as plasmas. Moreover, we may expect similar mechanisms in astrophysical objects as in plasma accelerators. As an example, in order to explain how energetic electrons may be

ejected from the interior of neutron stars to their atmosphere, Diver et al. [17] estimated the energy gain of accelerated electrons by assuming that strong electric fields arising from density gradients in the conduction electrons drive electrostatic plasma waves in neutron star crusts. The mechanism of the acceleration is similar to that of a plasma accelerator, where the laser pulse is replaced by the magnetic field line curvature as the cause of the density wave.

B. Fundamental Theoretical Descriptions

1. (Single Particle) Kinetic Description

When we consider the physics of a typical neutral plasma consisting of electrons massed m charged $q \equiv -e$ and ions charged $-q$, we are interested in processes with time scales that are much shorter than the time of a typical (local binary) collision. In other words, the term “plasma” in the present study always refers to a collisionless plasma.

In the collisionless plasma, the local interaction term is negligible so that the particles satisfy the Vlasov-Maxwell system consisting of the Vlasov equation [8] and the Maxwell equations. In the Vlasov equation (10), L is defined in Section I A 1 as $L = \dot{x}^\mu \left(\frac{\partial}{\partial x^\mu}{}^H - \frac{q}{m} F^{\nu V}{}_\mu \frac{\partial}{\partial \dot{x}^\nu} \right)$. The coordinates x^μ and \dot{x}^ν , $\mu = 0, 1, 2, 3$ are coordinates of the spacetime manifold \mathcal{M} and the fiber of its tangent bundle $(T\mathcal{M}, \Pi, \mathcal{M})$.

The other constraints (in this thesis the term “constraint” is used in a general sense, as an alternative to “equation”), namely Maxwell equations, are as follows [18] (see [19] for Maxwell’s equations written in the language of exterior

calculus),

$$dF = 0 \quad (11)$$

$$d \star F = -q \star \tilde{N} + q \star \widetilde{N_{\text{ion}}} \quad (12)$$

where F is the electromagnetic 2-form, N and N_{ion} are the number 4-current fields of electrons and ions, respectively, $\tilde{N} = g(N, -) = g_{\mu\nu} dx^\mu(N) dx^\nu$ is the metric dual of N with respect to the metric tensor g of the spacetime manifold, and

$$N_{\text{ion}} = n_{\text{ion}} \frac{\partial}{\partial x^0} = n_{\text{ion}} \partial_0, \quad (13)$$

where n_{ion} is the number density of ions. We can define the 4-velocity field V so that

$$N = nV = \left(\int \dot{x}^\mu f \frac{d\dot{x}^1 \wedge d\dot{x}^2 \wedge d\dot{x}^3}{\sqrt{1 + |\dot{x}|^2}} \right) \frac{\partial}{\partial x^\mu}, \quad (14)$$

$$g(V, V) = -1, \quad (15)$$

where $|\dot{x}|^2 = |\dot{x}^1|^2 + |\dot{x}^2|^2 + |\dot{x}^3|^2$.

The Vlasov-Maxwell system, though not always easy to solve, is a “kinetic description” of the plasma and gives a more complete description of a plasma than a fluid description.

2. Macroscopic Fluid Description

The Vlasov-Maxwell system is often difficult to solve and in some circumstances we are only interested in the macroscopic fluid properties of plasma with a certain equation of state (EOS). In these cases there is no need to solve the Vlasov-Maxwell system completely. We simply need the “macroscopic fluid description” which is generally easier to analyse.

The idea of the macroscopic fluid description is to average microscopic physical quantities in a local neighborhood of a point in space to give macroscopic physical fluid quantities. The macroscopic quantities at a point x in \mathcal{M} are the different orders of moments of f in velocity over a subset of the tangent fiber $T_X\mathcal{M}$. The base manifold \mathcal{M} is the Minkowski spacetime manifold coordinated with the Lorentz coordinates $\{x^\mu, \mu = 0, 1, 2, 3\}$ with metric

$$g = -dx^0 \otimes dx^0 + dx^1 \otimes dx^1 + dx^2 \otimes dx^2 + dx^3 \otimes dx^3 \quad (16)$$

and the total space $T\mathcal{M}$ is coordinated by $\{x^\mu, \dot{x}^\nu, \mu = 0, 1, 2, 3\}$.

The volume 4-form $\star 1$ on \mathcal{M} is

$$\star 1 = dx^0 \wedge dx^1 \wedge dx^2 \wedge dx^3 \quad (17)$$

and the 4-form $\sharp 1$

$$\sharp 1 = d\dot{x}^0 \wedge d\dot{x}^1 \wedge d\dot{x}^2 \wedge d\dot{x}^3 \quad (18)$$

is on $T\mathcal{M}$. The state of a plasma electron is a point in the unit hyperboloid sub-bundle $(\mathcal{E}, \Pi, \mathcal{M})$ of the tangent bundle $(T\mathcal{M}, \Pi, \mathcal{M})$, where \mathcal{E} is the set of timelike, future-directed, unit normalised tangent vectors on \mathcal{M} ,

$$\mathcal{E} = \{(x, \dot{x}) \in T\mathcal{M} \mid \varphi = 0 \text{ and } \dot{x}^0 > 0\} \quad (19)$$

where

$$\varphi = \eta_{\mu\nu} \dot{x}^\mu \dot{x}^\nu + 1. \quad (20)$$

The zeroth, first and second order moments of velocity are [20]

$$h(x) = \int_{\Pi^{-1}(x)} f \iota_X \sharp 1 \quad (21)$$

$$S_I^\mu(x) = \int_{\Pi^{-1}(x)} f \dot{x}^\mu \iota_X \sharp 1 \quad (22)$$

$$S_{II}^{\mu\nu}(x) = \int_{\Pi^{-1}(x)} f \dot{x}^\mu \dot{x}^\nu \iota_X \sharp 1, \quad (23)$$

where $f = f(x^\mu, \dot{x}^\mu)$ is a 0-form in the spacetime manifold \mathcal{M} known as the single particle distribution of electrons, $X = \dot{x}^\mu \frac{\partial}{\partial \dot{x}^\mu} \in \Gamma T\mathcal{M}$ and

$$\iota_X \#1 \Big|_\varepsilon = \frac{d\dot{x}^1 \wedge d\dot{x}^2 \wedge d\dot{x}^3}{\sqrt{1 + |\dot{x}|^2}} . \quad (24)$$

We then have

$$N \Big|_x = \left(\int_{\Pi^{-1}(x)} \dot{x}^\mu f \iota_X \#1 \right) \frac{\partial}{\partial x^\mu} . \quad (25)$$

The left sides of moment equations (21)-(23) are macroscopic fluid quantities. The ‘‘macroscopic fluid description’’, also called ‘‘Maxwell-Moments system’’, consists of some orders of the above moment equations (21)-(23), Maxwell equation (11), (12) and some other physical constraints (equations) to close the system.

3. *Advantages of Macroscopic Fluid Description & its Relationship with the Kinetic Description*

From moment equations (21)-(23) we get macroscopic fluid currents $\sigma_I = \star \tilde{S}_I = \star \tilde{N}$, $\sigma_{II}^\mu = \star S_{II}(\widetilde{-, dx^\mu})$, $N = S_I = S_I^\mu \frac{\partial}{\partial x^\mu}$ and $S_{II} = S_{II}^{\mu\nu} \frac{\partial}{\partial x^\mu} \otimes \frac{\partial}{\partial x^\nu}$, where S_I and S_{II} are 1st and 2nd order velocity moment tensor currents with direct physical interpretations. Hence, the macroscopic fluid description naturally leads to a solution including macroscopic fluid quantities, which forms a direct physical picture. The kinetic description, however, does not share this merit.

The complete series of equations of the moment integrals from the first to the infinite order is equivalent to the kinetic description. Clearly, it is impossible to solve such a system with an infinite number of moments. We have to cut off at a certain order, which loses information and leaves more unknowns than equations. The corresponding physical picture for such a system with a finite number of moment equations is that there are degrees of freedom to be determined

by certain physical assumptions such as an Equation of State (EOS). It shows that the macroscopic fluid description is easier to solve.

Due to the advantages of the macroscopic fluid description and the macroscopic fluid properties of the plasma in different specified EOSs, we will perform calculations in the “fluid description” to a certain order in the moments. The field system will be closed by different specified EOSs in Chapter III. It should be noted that the Vlasov equation is not generally satisfied in the macroscopic fluid description, which will be discussed after the corresponding calculation.

C. Waterbag Distribution

As was mentioned in Section IB2, some physical constraints are required to close the Maxwell-Moments system. Such constraints can be imposed by assuming an EOS or a form for the velocity distribution function. We now use a waterbag distribution, which was first introduced by DePackh [21] and Hohl [22] and is a simple description of a warm plasma. The waterbag (labelled as $\mathcal{U} \subset \mathcal{E}$) distribution $f(x, \dot{x})$, i.e., a function with respect to \dot{x} in the tangent fiber space, is an indicator-type function of the form

$$f(x, \dot{x}) = \begin{cases} \alpha & \text{if } (x, \dot{x}) \in \mathcal{U} \\ 0 & \text{otherwise} \end{cases} \quad (26)$$

in the tangent bundle $T\mathcal{M} = \Pi^{-1}\mathcal{M}$ where α is a constant. For clarity, Fig. 1 describes a 1-dimensional waterbag distribution.

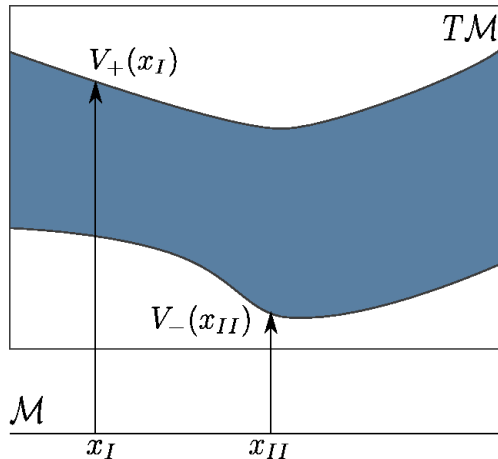


FIG. 1: 1-D waterbag distribution showing the boundary of the indicator-type function $f(x, \dot{x})$ (see [50])

D. Wave-Breaking Limits

1. Oscillations and Waves of Plasma

Plasma oscillations were presented in 1925 by Langmuir [23] as a possible explanation for the behaviour of electrons scattering in ionised gases. In 1929, Tonks and Langmuir [24] gave a systematic calculation of the plasma-electron and plasma-ion oscillations, named “electrostatic oscillations” or “Langmuir oscillations”. The Langmuir wave formed by the Langmuir oscillations is longitudinal. The reason is that the electric field caused by the displacement of a large number of electrons is parallel to the direction of the displacement. The wave propagates in the direction of the displacement.

In the case of a cold plasma, electron electrostatic oscillations are driven by the restoring electrostatic force caused by a superposition of number densities of electrons and ions with a small displacement of electrons with the same magnitude and direction. Then the electrostatic potential energy becomes kinetic energy and vice versa so that electrons run back and forth around the nearby ions. Such

small displacement can be regarded as a perturbation so that the system can be linearised and the frequency of such oscillation is obtained as $\omega_{pe} = \sqrt{\frac{q^2 n_{\text{ion}}}{m \epsilon_0}}$ [24]. Oscillations in a warm plasma were also studied in [24]. Some extended topics were investigated, including the oscillations and waves in variable density plasmas [26] and stationary plasma oscillations [27] in the framework of linear theories. The processes of the setting up of the electron electrostatic oscillations, and even the trapping of particles were discussed in [25].

Situations become complicated as non-linear effects may occur when the displacement is too large to be regarded as a linear perturbation. Dawson [28] investigated non-linear electron oscillations in a cold plasma. As a major point, non-linear electron oscillations and waves in various plasmas have been investigated and will be shown in Chapters II, III, IV, & V.

2. *Wave-Breaking*

So far there has been much interest in plasma accelerators in which wave-breaking in a plasma is stimulated by an intense laser pulse (see Section I A 2) and the particles in such plasmas are relativistic. This thesis, therefore, will be focusing on relativistic plasmas.

In a cold plasma, Dawson's results [28] showed that plane oscillations are stable below a critical amplitude (the so-called "wave-breaking limit"). Unstable (multi-stream) phenomena occur beyond this critical amplitude in plane oscillations, and in most spherically or cylindrically symmetric oscillations as well, regardless of the amplitude. The stability in a plane oscillation breaks down when the peak fluid velocity equals the phase speed of the plasma wave [28] [29].

In the case of a warm plasma, wave-breaking is generally regarded as the trapping of electrons in the wave [30]. However, it was observed in some cases that

there is electron trapping but the wave is still stable [31] [32]. The practical reason is that the trapped electrons are too few to break down the wave. Such a situation was also supported by simulations [33]- [39] and experiments [40]- [46] of self injected monoenergetic electron bunches in the “bubble regime”. In 1990, Mori and Katsouleas [47] developed a general method to study the wave-breaking of longitudinal plasma oscillations in all the combinations of plasmas consisting of cold non-relativistic fluid, cold relativistic fluid, warm 1D non-relativistic waterbag and warm 1D relativistic waterbag. In terms of a relativistic warm plasma, some other calculations using fluid models were conducted to study the wave-breaking limit by Katsouleas and Mori [5], Schroeder et al. [49], Trines and Norreys [48], Burton and Noble [50], and Burton and Wen [51].

The wave-breaking limit of a cold plasma is straightforward as all the electrons within a given coarse grained cell travel at a certain speed, however, it is much more complicated for a warm plasma. In 2006, Trines and Norreys [48] discussed the calculation of the wave-breaking limit and its physical implications. To do this, it is necessary to understand under what conditions the wave actually breaks. For the calculation using macroscopic fluid model like [5] [47]- [50], “breaking down” happens in the fluid model and the corresponding distribution or EOS. Such “wave-breaking” is also termed the “hydrodynamic” definition for wave-breaking [48]. It is still not clear, however, what exactly happens when the top speed of electrons exceeds the phase speed of the wave.

Concerning a 1-D waterbag model, Katsouleas and Mori [5] and Burton and Noble [50] obtained a travelling solution with all the physical quantities dependent only on $\zeta = x - vt$ (namely the “quasi-static assumption”), where v is the phase speed. When electrons are trapped, the quasi-static assumption is violated for waterbag solutions to the Vlasov equation. However, it is not clear whether or not the wave actually breaks.

Taking the ultra-relativistic approximation, Katsouleas and Mori [5], Burton and Noble [50] found that E_{\max} diverges logarithmically for the 1D waterbag. For a 3-D gourd waterbag model, Burton and Noble [50] obtained an E_{\max} independent of the Lorentz factor γ of the phase speed v of the electrostatic wave in the regime $\gamma \gg 1$. These behaviours show that the results Burton and Noble [50] obtained are similar to that of Schroeder's [49] and Rosenzweig's [11], but not Katsouleas and Mori's [5].

3. Applications of Wave-Breaking Limits

It is usually beyond simple models to describe the details of what will really happen when the waves break, however, certain properties of the plasma may still be accessible to the models.

For an oscillation in a plasma stimulated by a travelling wave, once an oscillating particle catches up with the wave, it will not continue its oscillation by going back and forth, but will be accelerated by the travelling wave. As a result, energy will shift from the wave to the trapped particle. A considerable number of trapped particles will consume much of the energy of the wave. Therefore, we consider a oscillating plasma with a stronger maximum electric field E_{\max} to be more likely a candidate in which physically meaningful "particle-trapping" is allowed. Results of the wave-breaking limits include the maximum electric field E_{\max} . This enables us to estimate whether it is more likely or unlikely that "particle-trapping" is allowed in the models, and predict the maximum energy gain a test electron may obtain.

4. Mathematical Wave-Breaking and Physical Wave-Breaking

Since the interpretation of the relation between wave-breaking and the trapped particles varies among different cases or researchers, to make it clearer, in this thesis

we will make a distinction between “mathematical wave-breaking” and “physical wave-breaking”. “Mathematical wave-breaking” represents exactly the “model dependent wave-breaking”, showing when the model fails to describe the situation. As examples, later chapters with the calculations for different models will show that the electric field never goes beyond the maximum electric field E_{\max} . Hence, “mathematical wave-breaking limit” is not able to tell whether or not the wave actually collapses, which is termed “physical wave-breaking”.

As was mentioned in the previous subsection, in the case where trapped particles exist, energy shifts from the wave to the trapped particles. Even though the wave loses energy due to the energy shift, whether the wave collapses physically or not depends on two factors. One is the strength of the electric field (which is proportional to the wave energy density) and the other is the fraction of trapped particles over the whole fluid. The wave does collapse when the fraction of trapped particles is large enough to consume too much of the wave energy density. Or in other words, wave collapses when the electric field is too weak to offer enough wave energy for a certain fraction of trapped particles.

It should be reminded what are the preferences in the situation of physical experiments and theoretical modeling work. In physical experiments, meaningful particle acceleration requires a large fraction of trapped particles while the wave is always there without collapse. In theoretical modeling work, we need the model to work well in the largest possible region. As a result, a model with a larger maximum electric field E_{\max} tends to support a larger fraction of trapped particles before the wave actually collapses.

For convenience, the abbreviated term “trapped particles” is used in this thesis to describe the actual physics of “trapped particles before the system reaches the limit of a physical wave-collapsing”. Therefore, the term “wave-breaking” will be used exclusively to refer to “mathematical wave-breaking” hereafter.

E. High Field & Non-Linear Electrodynamics

As was stated in Section IA2, the theory of plasma physics has been widely applied to laser-pulsed plasma accelerators of the new type. There are high fields that may lead to nonlinearities of vacuum (Schwinger limit 10^{18}V/m) in such extreme experimental circumstances [52]. However, Maxwell electrodynamics is linear, which may not be applicable to extreme situations with nonlinearities such as extreme high fields in high-intensity physical experiments or astronomical observations. It would, therefore, be helpful to explore non-linear effective theory of electrodynamics. Among the different effective theories of non-linear electrodynamics, Euler-Heisenberg theory [53] arising from QED vacuum effects, or Born-Infeld electrodynamics proposed in 1930's [54] and found to arise from low energy string field theory [55] [56] have been extensively studied. We will focus on Born-Infeld electrodynamics due to convenience and its advantages over other theories, which will be explicated in Chapter V. Interpretations and predictions on experiments and observations will also be given.

1. *A Brief Introduction to Born-Infeld Electrodynamics*

Born-Infeld electrodynamics, which was first presented in the 1930s [54] as a description of the classical electron entirely in terms of its electromagnetic field, has attracted considerable interest recently [57]- [61] since Born-Infeld-type theories have been shown to arise from low energy string field theory [56]. Born-Infeld electrodynamics has also some other advantages. Particularly, like the vacuum Maxwell equations, the solutions to the vacuum Born-Infeld equations have an exceptionally causal behaviour [62], [63]. The vacuum Maxwell and Born-Infeld field equations are the only physical theories with a single light cone obtainable from a local Lagrangian constructed solely from the two Lorentz invariants associated

with the electromagnetic field strength tensor and the metric tensor. It is well known that Maxwell electrodynamics exhibits an infinite self energy for a point charge [64]. Even though the electron is regarded as a point charge in classical theory, Born-Infeld electrodynamics, however, gives a finite self energy for a point charge like a classical electron.

Below we will give a short introduction to Born-Infeld electrodynamics, particularly its fundamental field equations, expressed in our symbols and conventions that will be used through the whole thesis. To satisfy the following principle of general invariance in the following variational equation

$$\delta \int \mathcal{L} \star 1 = 0 , \quad (27)$$

we take the simplest Lagrangian [61] in the following form,

$$\mathcal{L} = \frac{1}{\kappa^2} \left(1 - \sqrt{1 - \kappa^2 X - \frac{\kappa^4}{4} Y^2} \right) , \quad (28)$$

where the functions X and Y in equation (28) are

$$X = \star(F \wedge \star F) \quad (29)$$

$$Y = \star(F \wedge F) , \quad (30)$$

where F is the electromagnetic field strength tensor, from which the excitation 2-form G is defined as

$$\star G = 2 \left(\frac{\partial \mathcal{L}}{\partial X} \star F + \frac{\partial \mathcal{L}}{\partial Y} F \right) . \quad (31)$$

The first order derivatives of the Lagrangian with respect to X and Y are

$$\frac{\partial \mathcal{L}}{\partial X} = \frac{1}{2} \frac{1}{\sqrt{1 - \kappa^2 X - \frac{\kappa^4}{4} Y^2}} , \quad (32)$$

$$\frac{\partial \mathcal{L}}{\partial Y} = \frac{\kappa^2}{4} \frac{Y}{\sqrt{1 - \kappa^2 X - \frac{\kappa^4}{4} Y^2}} . \quad (33)$$

From an action principle based on the Lagrangian (28) [61], we obtain the field equations that the electromagnetic field and excitation tensors satisfy in Born-Infeld electrodynamics below,

$$dF = 0 \tag{34}$$

$$d \star G = j , \tag{35}$$

where \star is the Hodge map and j is the electric current 3-form, which will be specified in the Chapter V. Equations (34)-(35) are the fundamental field equations in Born-Infeld electrodynamics.

F. Cold Born-Infeld Plasmas

It is interesting to introduce Born-Infeld electrodynamics into the study of plasma waves. For cold plasmas, we will show [61] [65] that the maximum electric field (the wave-breaking limit) and the period of the electron waves are different from the solutions calculated using Maxwell electrodynamics. This may lead to a different prediction for experimental or observational tests about the motion of electrons in such plasmas that might be applicable in high field environments in the laboratory and in astrophysical systems. However, it should be pointed out that certain predictions are independent of the Born-Infeld constant κ . A comparison will be given between the dispersion relations of different modes of electro-magnetic waves in Born-Infeld electrodynamics and in Maxwell electrodynamics. A further comparison of the phase speed of the electro-magnetic waves in Born-Infeld and Maxwell plasmas shows the differences in the aspects of decelerating and particle trapping.

1. Wave-Breaking Limit

The laser plasma accelerator proposed by Tajima and Dawson [10] has been widely studied for its advantage of acceleration per distance. In such an accelerator, a density gradient which drives the electrostatic wave is created by an intense laser pulse. The laser pulse drives the electrons away from the ions, which are then electrostatically attracted back to the ions and overshoot, leading to an electrostatic wave. There is a similar acceleration mechanism by the strong electric fields in neutron stars, where the density gradient which drives the electrostatic wave is created by magnetic field line curvature since the electrons are confined to travel along the magnetic field lines. Diver et al. [66] estimated the energies of accelerated electrons in neutron stars in traditional Maxwell electrodynamics. In both of the above cases, the behaviour of the plasma waves plays a key role in understanding the process of the acceleration. In the traditional Maxwell framework, the maximum electrical field strength for the plasma waves is calculated by Akhiezer and Polovin [29]. Burton et al. [61] explored the calculation of the maximum electrical field strength of Born-Infeld plasma in a zero external magnetic field. Here we generalise the calculation to the cases in nonzero external magnetic fields, which is applicable in the strong magnetic fields in magnetars. This allows us to explore consequences of Born-Infeld electrodynamics for electron acceleration in magnetars. As a result, we are able to get the result in Born-Infeld electrodynamics and compare it with the one in Maxwell electrodynamics.

2. Dispersion Relation

It is also interesting to find out the dispersion relation at different frequencies of plasma waves in Born-Infeld electrodynamics and compare it with that in Maxwell electrodynamics. We will explore the dispersion relations and the cutoff frequency

for different modes of electromagnetic waves in Born-Infeld plasmas.

II. ELECTROSTATIC OSCILLATIONS IN THE KINETIC DESCRIPTION

We now consider electrons moving in a homogeneous background of ions at rest. For simplicity we will try to look for a travelling wave solution with all the physical quantities dependent only on

$$\zeta = x^3 - vx^0 \quad (36)$$

with a constant phase speed v (in the rest frame of the ions).

As stated in Section IB, the Vlasov-Maxwell system is not always easy to solve. It is a complete description of a collisionless plasma (i.e. discrete particle effects are neglected). Here we carry out some calculations for simple cases such as cold and waterbag-distributed warm plasmas formulated by (26). For such simple cases we get solutions satisfying the Vlasov equation. One choice is to reduce the Vlasov equation (10) to the Lorentz equation

$$\nabla_V \tilde{V} = \frac{q}{m} \iota_V F , \quad (37)$$

where the velocity vector field V is normalised as

$$g(V, V) = -1 . \quad (38)$$

Equation (37) describes a cold fluid. In fact, (37) can be shown to hold for waterbag distributions where V is replaced by a family of vector fields. The permission for such a reduction is given based on the fact that the Vlasov equation (10) will lead to the Lorentz equation (37) (see [6]), although it is not true vice versa. We then look for solutions to the Lorentz-Maxwell system consisting of (11), (12), (37), (38). If we do find such solutions, they are also solutions to the distributional Vlasov-Maxwell system (10), (11), (12).

In the structure of the tangent bundle $(T\mathcal{M}, \Pi, \mathcal{M})$ where the calculation is carried out, we restrict the “total space” $T\mathcal{M}$ to $\mathcal{E} \subset T\mathcal{M}$ so that the “total space” \mathcal{E} is the set consisting of all future-pointing timelike unit normalised vectors.

A. Cold Plasma

For a cold plasma, a section of the bundle (\mathcal{E}, Π, M) is a velocity vector field V normalised by $g(V, V) = -1$. In the following we will consider electrostatic oscillation and assume an electromagnetic 2-form

$$F = E(\zeta)dx^0 \wedge dx^3, \quad (39)$$

which is purely longitudinal and depends on $\zeta = x^3 - vx^0$ only. We then get the solution [20] by substituting the above 2-form F (39) and an input parameter $N_{\text{ion}} = n_{\text{ion}} \frac{\partial}{\partial x^0}$ into the Lorentz-Maxwell system (11), (12), (37), where n_{ion} is the proper number density of the ions.

B. Waterbag-Distributed Warm Plasma

1. Shape of the Waterbag Distributions

We now consider the case of a 1-D waterbag-distributed plasma. The velocity is distributed over an interval with the upper and lower limits of the interval determined by the Vlasov-Maxwell system. A physically meaningful 1-D waterbag requires smooth upper and lower boundaries, each represented by a vector field on spacetime ($V_+(x)$ and $V_-(x)$). $V_+(x)$ and $V_-(x)$ satisfy the Lorentz equation (when acting as V in equation (37)).

The conclusion can be generalised to an arbitrary dimension. In the case of an n -D waterbag-distributed plasma, the velocity is distributed over a set whose boundary is determined by the Vlasov-Maxwell system. A physically meaningful

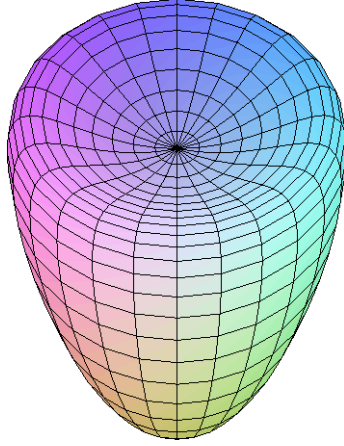


FIG. 2: A schematic illustration of a 3-D gourd waterbag

waterbag requires a smooth boundary. For example, a waterbag over spacetime is 3-D and the Vlasov-Maxwell system determines the evolution of its boundary. When the boundary of the waterbag is written in terms of a parameter set \mathcal{D} as $V_\xi(x)$ with $\xi \in \mathcal{D}$, the family of velocity fields $V_\xi(x)$ describing the boundary satisfies the Lorentz equation (when acting as V in equation (37)). For example, \mathcal{D} is the 2-D surface for the 3-D gourd waterbag illustrated in Fig. 2, which will be investigated in this chapter. The physical meaning for the boundary of the waterbag is a bit complicated and we will dwell on it in the next section.

Here we give a general definition of a waterbag distribution function $f(x, \dot{x})$ (with respect to velocity \dot{x}) as follows

$$f(x, \dot{x}) = \begin{cases} \alpha & \text{if } \dot{x} \in \mathcal{U}_x \subset \mathcal{E}_x \\ 0 & \text{otherwise,} \end{cases} \quad (40)$$

where \mathcal{U}_x is the waterbag restricted to $T_X\mathcal{M}$. In the following parts of this thesis, we will carry out calculations on the boundary $\partial\mathcal{U}_x$ of the waterbag.

2. Non-Linear Electrostatic Oscillations

A waterbag-distributed plasma is specified by the boundary of the support of the distribution. Each point ξ in the boundary of the waterbag has the velocity field $V_\xi(x)$. It can be shown that

$$\nabla_{V_\xi} \tilde{V}_\xi = \frac{q}{m} \iota_{V_\xi} F, \quad (41)$$

where $\xi = (\xi^1, \xi^2)$, follows from the Vlasov equation (10).

For a 3-D gourd waterbag illustrated in Fig. 2, we introduce

$$e^1 = v dx^3 - dx^0, \quad (42)$$

$$e^2 = dx^3 - v dx^0, \quad (43)$$

and decompose \tilde{V}_ξ with the test form that we choose due to its solvability as [6]

$$\tilde{V}_\xi = [\mu(\zeta) + A(\xi^1)]e^1 + \psi(\xi^1, \zeta)e^2 + R \sin(\xi^1) \cos(\xi^2) dx^1 + R \sin(\xi^1) \sin(\xi^2) dx^2 \quad (44)$$

for $0 < \xi^1 < \pi, 0 \leq \xi^2 < 2\pi$ where $R > 0$ is constant.

We see that $(\gamma e^1, \gamma e^2, dx^1, dx^2)$, with $\gamma = 1/\sqrt{1-v^2}$, is orthonormal. Physical considerations of causality require future-directed and timelike velocity fields, from which follows $e^1(V_\xi) < 0$ and therefore $\mu + A(\xi^1) > 0$.

From the normalisation condition $g(V_\xi, V_\xi) = -1$ we get the following component ψ [6],

$$\psi = -\sqrt{[\mu(\zeta) + A(\xi^1)]^2 - \gamma^2[1 + R^2 \sin^2(\xi^1)]}, \quad (45)$$

where we choose the negative square root so that the condition that none of the electrons moves faster than the wave along x^3 is satisfied, since we are calculating in the wave frame.

As stated in Section II A, physical quantities depend on ζ only, we then assume the following formal solution of a purely longitudinal electric field,

$$F = E(\zeta)dx^0 \wedge dx^3, \quad (46)$$

along with the ansatz (44) into Lorentz force equation (37), and the property

$$\nabla_V \tilde{V} = \iota_V d\tilde{V} \quad (47)$$

according to the metric tensor g chosen here, we get [6]

$$E = \frac{1}{\gamma^2} \frac{m}{q} \frac{d\mu}{d\zeta}. \quad (48)$$

We then use the above equation (48), the electron number current for the waterbag and the Maxwell equations (11), (12) to obtain the following differential equation for μ ,

$$\begin{aligned} \frac{1}{\gamma^2} \frac{d^2\mu}{d\zeta^2} &= -\frac{q^2}{m} n_{\text{ion}} \gamma^2 - \frac{q^2}{m} 2\pi R^2 \alpha \\ &\times \int_0^\pi ([\mu(\zeta) + A(\xi^1)]^2 - \gamma^2 [1 + R^2 \sin^2(\xi^1)])^{\frac{1}{2}} \sin(\xi^1) \cos(\xi^1) d\xi^1 \end{aligned} \quad (49)$$

and

$$2\pi R^2 \int_0^\pi A(\xi^1) \sin(\xi^1) \cos(\xi^1) d\xi^1 = -\frac{n_{\text{ion}} \gamma^2 v}{\alpha}. \quad (50)$$

The next subsection will show that when we specify the generator $A(\xi^1)$ of the boundary $\partial\mathcal{U}$ (of the waterbag) subject to the normalisation condition (50), the first integral of equation (49) is solved according to integral intervals with specific values of physical quantities.

3. Electrostatic Wave-breaking in 3-D Waterbag

The definiteness of the square root in the integrand of (49) requires that when ζ is running over its possible intervals, at least the largest μ is physically meaningful for equation (49). We define the largest μ with respect to its argument ζ as μ_{wb} , which matches a vanishing square root in equation (49). Hence

$$\mu_{\text{wb}} = \max \left\{ -A(\xi^1) + \gamma \sqrt{1 + R^2 \sin^2(\xi^1)} \mid 0 \leq \xi^1 \leq \pi \right\}, \quad (51)$$

as $\mu < \mu_{\text{wb}}$ will lead to an imaginary integrand in (49) for some ξ^1 . We also choose the positive square root in (51) to satisfy $\mu + A(\xi^1) > 0$ which leads to $\mu_{\text{wb}} + A(\xi^1) > 0$ as required.

Behaviours of E and μ with respect to ζ are schematically illustrated in Fig. 3, where the wave-breaking value of μ , $\mu_{\text{wb}} \equiv \mu(\zeta_{\text{I}})$ corresponds to a vanishing $E(\zeta_{\text{I}}) = 0$ and the equilibrium value of μ as a constant $\mu_{\text{eq}} \equiv \mu(\zeta_{\text{II}})$ is at a (positive or negative) maximum electric field $E_{\text{max}} \equiv -E(\zeta_{\text{II}})$, i.e., $\mu = \mu_{\text{eq}}$ when $\zeta = \zeta_{\text{II}}$ so that

$$\left. \frac{d^2 \mu}{d\zeta^2} \right|_{\zeta=\zeta_{\text{II}}} = 0. \quad (52)$$

Setting μ equals to μ_{eq} in (49), and using the corresponding result to eliminate α , we get the following equation for μ_{eq} ,

$$\begin{aligned} & \frac{1}{v} \int_0^\pi A(\xi^1) \sin(\xi^1) \cos(\xi^1) d\xi^1 \\ &= \int_0^\pi \left([\mu_{\text{eq}} + A(\xi^1)]^2 - \gamma^2 [1 + R^2 \sin^2(\xi^1)] \right)^{\frac{1}{2}} \sin(\xi^1) \cos(\xi^1) d\xi^1, \end{aligned} \quad (53)$$

with

$$\int_0^\pi A(\xi^1) \sin(\xi^1) \cos(\xi^1) d\xi^1 < 0 \quad (54)$$

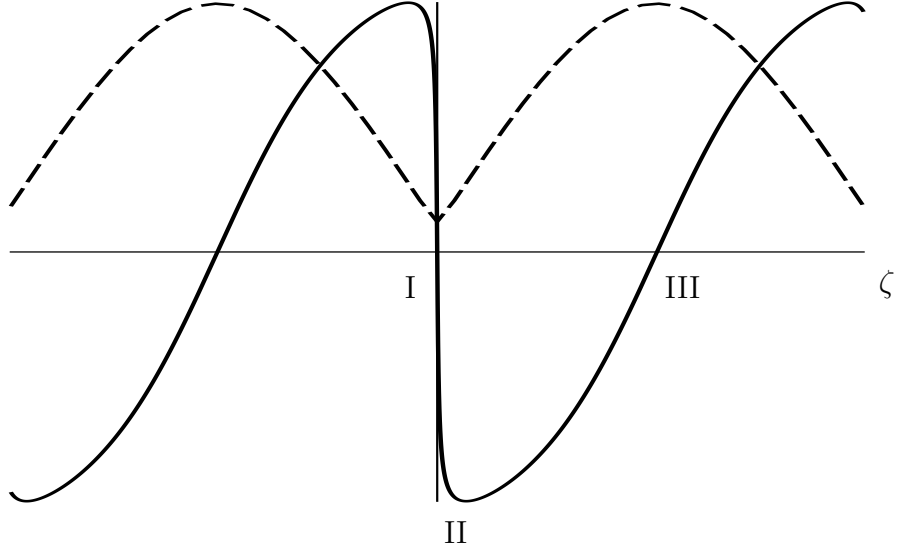


FIG. 3: A schematic illustration of E and μ as functions of ζ (the solid and the dashed line show E and μ respectively, see [61])

since $\alpha, v > 0$.

To get the wave-breaking limit E_{\max} , we now integral $d(E(\zeta))^2 = 2E(\zeta)dE(\zeta)$ obtained by multiplying equation (48) to 2 times of equation (49) over the integral interval from ζ_I to ζ_{II} . The maximum value of E , i.e., $E_{\max} = E_I$, is therefore obtained as follows,

$$E_{\max}^2 = 2mn_{\text{ion}} \left[-\mu_{\text{eq}} + \mu_{\text{wb}} + \frac{v}{\int_0^\pi A(\xi^{1'}) \sin(\xi^{1'}) \cos(\xi^{1'}) d\xi^{1'}} \times \int_{\mu_{\text{wb}}}^{\mu_{\text{eq}}} d\mu \int_0^\pi ([\mu + A(\xi^1)]^2 - \gamma^2[1 + R^2 \sin^2(\xi^1)])^{\frac{1}{2}} \sin(\xi^1) \cos(\xi^1) d\xi^1 \right] \quad (55)$$

The exact expression for E_{\max} (55) is not easy to solve. We obtain (loose) lower and upper bounds on E_{\max} , however. Considering that the two intervals of the

integration in the right side of (55) satisfy [6]

$$\begin{aligned}
& (\mu_{\text{eq}} - \mu_{\text{wb}}) \int_0^{\frac{\pi}{2}} \sin(\xi^1) \cos(\xi^1) \sqrt{[\mu_{\text{wb}} + A(\xi^1)]^2 - \gamma^2[1 + R^2 \sin^2(\xi^1)]} d\xi^1 \\
\leq & \int_{\mu_{\text{wb}}}^{\mu_{\text{eq}}} \left\{ \int_0^{\frac{\pi}{2}} \sin(\xi^1) \cos(\xi^1) \sqrt{[\mu(\zeta) + A(\xi^1)]^2 - \gamma^2[1 + R^2 \sin^2(\xi^1)]} d\xi^1 \right\} d\mu \\
\leq & (\mu_{\text{eq}} - \mu_{\text{wb}}) \int_0^{\frac{\pi}{2}} \sin(\xi^1) \cos(\xi^1) \sqrt{[\mu_{\text{eq}} + A(\xi^1)]^2 - \gamma^2[1 + R^2 \sin^2(\xi^1)]} d\xi^1 \quad (56) \\
& (\mu_{\text{eq}} - \mu_{\text{wb}}) \int_{\frac{\pi}{2}}^{\pi} \sin(\xi^1) \cos(\xi^1) \sqrt{[\mu_{\text{eq}} + A(\xi^1)]^2 - \gamma^2[1 + R^2 \sin^2(\xi^1)]} d\xi^1 \\
\leq & \int_{\mu_{\text{wb}}}^{\mu_{\text{eq}}} \left\{ \int_{\frac{\pi}{2}}^{\pi} \sin(\xi^1) \cos(\xi^1) \sqrt{[\mu(\zeta) + A(\xi^1)]^2 - \gamma^2[1 + R^2 \sin^2(\xi^1)]} d\xi^1 \right\} d\mu \\
\leq & (\mu_{\text{eq}} - \mu_{\text{wb}}) \int_{\frac{\pi}{2}}^{\pi} \sin(\xi^1) \cos(\xi^1) \sqrt{[\mu_{\text{wb}} + A(\xi^1)]^2 - \gamma^2[1 + R^2 \sin^2(\xi^1)]} d\xi^1 \quad (57)
\end{aligned}$$

and the factor

$$\frac{v}{\int_0^{\pi} A(\xi) \sin(\xi) \cos(\xi) d\xi} = -\frac{2\pi R^2 \alpha}{n_{\text{ion}} \gamma^2} \quad (58)$$

is negative, we get $E_{\text{max, lb}}^2$, one of the lower bounds of E_{max}^2 and $E_{\text{max, ub}}^2$, one of

the upper bounds of E_{\max}^2 as [6]

$$\begin{aligned}
& E_{\max, \text{lb}}^2 \\
&= 2mn_{ion} \left\{ -\mu_{\text{eq}} + \mu_{\text{wb}} + \frac{v}{\int_0^\pi A(\xi) \sin(\xi) \cos(\xi) d\xi} \times \right. \\
&\quad \left[(\mu_{\text{eq}} - \mu_{\text{wb}}) \int_0^{\frac{\pi}{2}} \sqrt{[\mu_{\text{eq}} + A(\xi^1)]^2 - \gamma^2[1 + R^2 \sin^2(\xi^1)]} \sin(\xi^1) \cos(\xi^1) d\xi^1 \right. \\
&\quad \left. + (\mu_{\text{eq}} - \mu_{\text{wb}}) \int_{\frac{\pi}{2}}^\pi \sqrt{[\mu_{\text{wb}} + A(\xi^1)]^2 - \gamma^2[1 + R^2 \sin^2(\xi^1)]} \sin(\xi^1) \cos(\xi^1) d\xi^1 \right] \left. \right\} \\
&= 2mn_{ion} \left\{ -\mu_{\text{eq}} + \mu_{\text{wb}} + \frac{v}{\int_0^\pi A(\xi) \sin(\xi) \cos(\xi) d\xi} \times \right. \\
&\quad \left[(\mu_{\text{eq}} - \mu_{\text{wb}}) \int_0^\pi \sqrt{[\mu_{\text{eq}} + A(\xi^1)]^2 - \gamma^2[1 + R^2 \sin^2(\xi^1)]} \sin(\xi^1) \cos(\xi^1) d\xi^1 \right. \\
&\quad \left. + (\mu_{\text{eq}} - \mu_{\text{wb}}) \int_{\frac{\pi}{2}}^\pi \sin(\xi^1) \cos(\xi^1) d\xi^1 \times \right. \\
&\quad \left. \left(\sqrt{[\mu_{\text{wb}} + A(\xi^1)]^2 - \gamma^2[1 + R^2 \sin^2(\xi^1)]} - \sqrt{[\mu_{\text{eq}} + A(\xi^1)]^2 - \gamma^2[1 + R^2 \sin^2(\xi^1)]} \right) \right] \left. \right\} \\
&\leq E_{\max}^2 \\
&\leq E_{\max, \text{ub}}^2 \\
&= 2mn_{ion} \left\{ -\mu_{\text{eq}} + \mu_{\text{wb}} + \frac{v}{\int_0^\pi A(\xi) \sin(\xi) \cos(\xi) d\xi} \times \right. \\
&\quad \left[(\mu_{\text{eq}} - \mu_{\text{wb}}) \int_0^{\frac{\pi}{2}} \sqrt{[\mu_{\text{wb}} + A(\xi^1)]^2 - \gamma^2[1 + R^2 \sin^2(\xi^1)]} \sin(\xi^1) \cos(\xi^1) d\xi^1 \right. \\
&\quad \left. + (\mu_{\text{eq}} - \mu_{\text{wb}}) \int_{\frac{\pi}{2}}^\pi \sqrt{[\mu_{\text{eq}} + A(\xi^1)]^2 - \gamma^2[1 + R^2 \sin^2(\xi^1)]} \sin(\xi^1) \cos(\xi^1) d\xi^1 \right] \left. \right\} \\
&= 2mn_{ion} \left\{ -\mu_{\text{eq}} + \mu_{\text{wb}} + \frac{v}{\int_0^\pi A(\xi) \sin(\xi) \cos(\xi) d\xi} \times \right. \\
&\quad \left[(\mu_{\text{eq}} - \mu_{\text{wb}}) \int_0^\pi \sqrt{[\mu_{\text{eq}} + A(\xi^1)]^2 - \gamma^2[1 + R^2 \sin^2(\xi^1)]} \sin(\xi^1) \cos(\xi^1) d\xi^1 \right. \\
&\quad \left. + (\mu_{\text{eq}} - \mu_{\text{wb}}) \int_0^{\frac{\pi}{2}} \sin(\xi^1) \cos(\xi^1) d\xi^1 \times \right. \\
&\quad \left. \left(\sqrt{[\mu_{\text{wb}} + A(\xi^1)]^2 - \gamma^2[1 + R^2 \sin^2(\xi^1)]} - \sqrt{[\mu_{\text{eq}} + A(\xi^1)]^2 - \gamma^2[1 + R^2 \sin^2(\xi^1)]} \right) \right] \left. \right\} .
\end{aligned} \tag{59}$$

With the property $\left. \frac{d^2 \mu}{d\xi^2} \right|_{\mu_{\text{eq}}} = 0$, we get a simpler expression as [6]

$$\begin{aligned}
& E_{\text{max, lb}}^2 \\
= & -\frac{4m\pi R^2 \alpha}{\gamma^2} (\mu_{\text{eq}} - \mu_{\text{wb}}) \int_{\frac{\pi}{2}}^{\pi} \sin(\xi^1) \cos(\xi^1) d\xi^1 \times \\
& \left(\sqrt{[\mu_{\text{wb}} + A(\xi^1)]^2 - \gamma^2[1 + R^2 \sin^2(\xi^1)]} - \sqrt{[\mu_{\text{eq}} + A(\xi^1)]^2 - \gamma^2[1 + R^2 \sin^2(\xi^1)]} \right) \\
\leq & E_{\text{max}}^2 \\
\leq & E_{\text{max, ub}}^2 \\
= & -\frac{4m\pi R^2 \alpha}{\gamma^2} (\mu_{\text{eq}} - \mu_{\text{wb}}) \int_0^{\frac{\pi}{2}} \sin(\xi^1) \cos(\xi^1) d\xi^1 \times \\
& \left(\sqrt{[\mu_{\text{wb}} + A(\xi^1)]^2 - \gamma^2[1 + R^2 \sin^2(\xi^1)]} - \sqrt{[\mu_{\text{eq}} + A(\xi^1)]^2 - \gamma^2[1 + R^2 \sin^2(\xi^1)]} \right).
\end{aligned} \tag{60}$$

For example, when $A(\xi^1) = -a \cos(\xi^1)$ where a is a positive constant ($a > 0$ ensures (54) is satisfied), we determine an upper bound on E_{max} as follows [6],

$$E_{\text{max}}^2 \leq \frac{3v}{2a} \frac{m^2 \omega_p^2}{q^2} (\mu_{\text{eq}} - \mu_{\text{wb}}) \sqrt{\mu_{\text{eq}}^2 - \gamma^2}, \tag{61}$$

where $\omega_p = \sqrt{n_{\text{ion}} q^2 / m}$ is the plasma angular frequency.

Substituting $A(\xi^1) = -a \cos(\xi^1)$ into equation (49) and considering $\mu'' = 0$ at the equilibrium value $\mu = \mu_{\text{eq}}$, we get the following expression for μ_{eq} [50],

$$\mu_{\text{eq}} \approx \gamma^2. \tag{62}$$

From Fig. 3 and the behaviour of the function $\sqrt{[\mu_{\text{wb}} + A(\xi^1)]^2 - \gamma^2[1 + R^2 \sin^2(\xi^1)]}$ in equation (60), we obtain that

$$\mu_{\text{wb}} = a + \gamma, \tag{63}$$

where

$$a = \frac{3n_{\text{ion}}\gamma^2 v}{4\pi R^2 \alpha} . \quad (64)$$

With equations (62) and (63) we get the further expression for the upper bound of E_{max}^2 as

$$E_{\text{max}}^2 \leq \frac{3v}{2a} mn_{\text{ion}} (\gamma^2 - a - \gamma) \gamma \sqrt{\gamma^2 - 1} . \quad (65)$$

We can fix the constant a in terms of the ‘‘longitudinal temperature’’

$$T_{\parallel \text{eq}} = \frac{1}{n_{\text{ion}} k_{\text{B}}} \mathcal{T}_{\text{eq}}^{33} \quad (66)$$

of the state $\mu = \mu_{\text{eq}}$ since

$$\begin{aligned} p_{\parallel \text{eq}} &= n_{\text{ion}} k_{\text{B}} T_{\parallel \text{eq}} \\ &= \mathcal{T}_{\text{eq}}^{33} \\ &= \frac{1}{5} mn_{\text{ion}} \left(\frac{a}{\gamma^2 v} \right)^2 , \end{aligned} \quad (67)$$

where k_{B} is the Boltzmann constant and $\mathcal{T}_{\text{eq}}^{\mu\nu}$ are the components of the stress-energy-momentum tensor

$$\mathcal{T}_{\text{eq}}^{\mu\nu} = m\alpha n_{\text{ion}} \int_{\mathcal{U}_{\text{eq}}} \dot{x}^\mu \dot{x}^\nu \iota_X \#1 , \quad (68)$$

where \mathcal{U}_{eq} is the support of the waterbag distribution $\mu = \mu_{\text{eq}}$.

We then get the final expression for the upper bound of E_{max}^2 in a relativistic approximation ($\gamma \gg 1$)

$$E_{\text{max}}^2 \leq \frac{\sqrt{9m}}{\sqrt{20k_{\text{B}}T_{\parallel \text{eq}}}} mn_{\text{ion}} \gamma^2 . \quad (69)$$

The expression for E_{max}^2 of the form (69) shows a relation between the maximum electric field E_{max}^2 and the ‘‘longitudinal temperature’’ $T_{\parallel \text{eq}}$ that accords with the results obtained for $\gamma \gg 1$ by Katsouleas and Mori [5] $E_{\text{max}}^2 \approx \frac{m^2 \omega_p^2 c^2}{2q^2} \left(\frac{mc^2}{3k_{\text{B}}T_{\text{eq}}} \right)^{\frac{1}{2}} \ln \gamma$ and Burton and Noble [50] $E_{\text{max}}^2 \approx \frac{m^2 \omega_p^2 c^2}{q^2} \left(\frac{9mc^2}{20k_{\text{B}}T_{\parallel \text{eq}}} \right)^{\frac{1}{2}}$.

III. VELOCITY MOMENTS METHOD IN THE FLUID MODEL

A. Framework

As we have demonstrated in Section I B, solving the entire Vlasov equation can be very complicated. One possible way, however, would be to start from the different orders of central moments of the distribution f in velocity and close the system by assuming that the distribution has a particular form. Again in this thesis, we will be focusing on the case of a waterbag distribution.

1. Introduction

The maximum sustainable amplitude (the “wave-breaking limit”) of non-linear electrostatic oscillations has attracted considerable interest for over half a century [5] [6] [28] [48] [49] [67]. Recently, there has been a resurgence of interest in the wave-breaking limit of relativistic warm plasma oscillations based on macroscopic fluid (hydrodynamic) models of plasmas [49]. Recent work [6] was motivated by the observation that the wave-breaking limit is highly sensitive to the details of the macroscopic fluid model [48].

Plasmas dominated by collisions can be close to thermodynamic equilibrium. However, an intense and ultrashort laser pulse propagating through an under-dense plasma will drive the plasma anisotropically over a plasma oscillation period, and the plasma is effectively collisionless over such timescales. To describe the dynamics of a collisionless plasma one can employ the collisionless Vlasov equation to evolve the plasma forward in time. With such methods, however, it is difficult to obtain explicit analytical formulae for wave-breaking limits from the non-linear Vlasov-Maxwell system for general initial conditions. The reason is that the equations for the moments are equivalent to the Vlasov equation only if moment equa-

tions at all the orders are included. Furthermore, the moment equation at any order is related to its next higher order moment via new unknowns. Therefore, it is never complete if we cut off the moment equations at any finite order, as we do when we practice the moments method. In other words, to make up the constraints from higher order equations, we need to make assumptions as constraints to close the hierarchy of moment equations. In this chapter, we will assume that electrons are waterbag-distributed as in [6] and get solutions of the behaviour of such electrons.

The calculations in [6] tackle the Vlasov-Maxwell system directly and retain the details of the shape of the waterbag, while an alternative approach introduced here employs a covariant macroscopic fluid model and is designed to isolate generic properties of wave-breaking limits in the ultra-relativistic limit. Our main goal in this chapter is to try to gain a better understanding of how trapped particles influence E_{\max} .

2. Moments Method for Plasma Fluid

As before, we introduce the Minkowski spacetime manifold \mathcal{M} coordinated by $\{x^\mu, \mu = 0, 1, 2, 3\}$ with the Lorentz coordinates $\{x^\mu, \mu = 0, 1, 2, 3\}$ with metric

$$g = -dx^0 \otimes dx^0 + dx^1 \otimes dx^1 + dx^2 \otimes dx^2 + dx^3 \otimes dx^3 \quad (70)$$

and the tangent bundle $T\mathcal{M}$ coordinated by $\{x^\mu, \dot{x}^\nu, \mu, \nu = 0, 1, 2, 3\}$.

The volume 4-form $\star 1$ on \mathcal{M} is

$$\star 1 = dx^0 \wedge dx^1 \wedge dx^2 \wedge dx^3 \quad (71)$$

and the 4-form $\sharp 1$

$$\sharp 1 = d\dot{x}^0 \wedge d\dot{x}^1 \wedge d\dot{x}^2 \wedge d\dot{x}^3 \quad (72)$$

is on $T\mathcal{M}$. The state of a plasma electron is a point in the unit hyperboloid sub-bundle $(\mathcal{E}, \Pi, \mathcal{M})$ of the tangent bundle $(T\mathcal{M}, \Pi, \mathcal{M})$.

The set \mathcal{E} contains all timelike, future-directed, unit normalised tangent vectors on \mathcal{M} ,

$$\mathcal{E} = \{(x, \dot{x}) \in T\mathcal{M} \mid \varphi = 0 \text{ and } \dot{x}^0 > 0\} \quad (73)$$

where

$$\varphi = \eta_{\mu\nu} \dot{x}^\mu \dot{x}^\nu + 1. \quad (74)$$

The zeroth, first, second and third order moments of velocity are

$$h(x) = \int_{\Pi^{-1}(x)} f \iota_X \#1 \quad (75)$$

$$S_I^\mu(x) = \int_{\Pi^{-1}(x)} f \dot{x}^\mu \iota_X \#1 \quad (76)$$

$$S_{II}^{\mu\nu}(x) = \int_{\Pi^{-1}(x)} f \dot{x}^\mu \dot{x}^\nu \iota_X \#1 \quad (77)$$

$$S_{III}^{\mu\nu\chi}(x) = \int_{\Pi^{-1}(x)} f \dot{x}^\mu \dot{x}^\nu \dot{x}^\chi \iota_X \#1 , \quad (78)$$

where $f = f(x^\mu, \dot{x}^\mu)$ is a 0-form on $T\mathcal{M}$ describing the spacetime position and velocity of electrons and

$$X = \dot{x}^\mu \frac{\partial}{\partial \dot{x}^\mu} . \quad (79)$$

The electromagnetic 2-form F is determined from Maxwell's equations

$$dF = 0 \quad (80)$$

$$d \star F = -q \star \tilde{N} + q \star \widetilde{N_{\text{ion}}} = -q \sigma_I + q \star \widetilde{N_{\text{ion}}} , \quad (81)$$

where q is the charge of electron and $\widetilde{N_{\text{ion}}} = n_{\text{ion}} \frac{\partial}{\partial x^0}$.

For the first order moments

$$\sigma_I = \star \tilde{S}_I = \star \tilde{N} \quad (82)$$

$$S_I = S_I^\mu \frac{\partial}{\partial x^\mu} , \quad (83)$$

we can obtain the following first order field equation for the 4-velocity moments of f directly from the Maxwell equation (81),

$$d\sigma_{\text{I}} = 0 . \quad (84)$$

Similarly, for the second order moments

$$\sigma_{\text{II}}^{\mu} = \star S_{\text{II}}(\widetilde{-, dx^{\mu}}) \quad (85)$$

$$S_{\text{II}} = S_{\text{II}}^{\mu\nu} \frac{\partial}{\partial x^{\mu}} \otimes \frac{\partial}{\partial x^{\nu}} , \quad (86)$$

from the Vlasov equation (10), i.e.,

$$Lf = 0 , \quad (87)$$

where

$$L = \dot{x}^{\mu} \left[\left(\frac{\partial}{\partial x^{\mu}} \right)^{\text{H}} - \left(\frac{q}{m} F^{\nu}_{\mu} \right)^{\text{V}} \frac{\partial}{\partial \dot{x}^{\nu}} \right] \quad (88)$$

(with m as the mass of electron and labels H and V as horizontal and vertical lift from \mathcal{M} to $T\mathcal{M}$), we can obtain the following second order field equation for the 4-velocity moments of f ,

$$D\sigma_{\text{II}}^{\mu} + \frac{q}{m} F^{\mu} \wedge \sigma_{\text{I}} = 0 , \quad (89)$$

where $F^{\mu} = F^{\mu}_{\nu} dx^{\nu}$.

3. Closure of the Moments Hierarchy with a Waterbag Distribution

We now close the hierarchy of moments using a waterbag distribution $f(x, \dot{x})$ (about velocity \dot{x}) as follows

$$f(x, \dot{x}) = \begin{cases} \alpha & \text{if } \dot{x} \in \mathcal{U}_x \subset \mathcal{E}_x \\ 0 & \text{otherwise .} \end{cases} \quad (90)$$

We will use (the EOS of) the waterbag distribution as constraints rather than higher order moment equations. Then the moment equations which are cut off, and therefore incomplete, are closed by such a waterbag distribution.

B. Calculation of Moments

1. Parameterised Description of the Boundary of the Waterbag

The boundary $\partial\mathcal{C}_x$ of the chain $\mathcal{C}_x : \mathcal{D} \rightarrow \mathcal{E}_x$ representing the waterbag is written as follows,

$$\begin{aligned} \partial\mathcal{C}_x &= \Sigma_x : \mathcal{D} \rightarrow \mathcal{E}_x \\ \xi &\mapsto (\Sigma_x^0(\xi), \dots, \Sigma_x^3(\xi)) , \end{aligned} \quad (91)$$

where $\xi = (\xi^1, \xi^2)$ is a point in the parameter space \mathcal{D} and $\partial\mathcal{C}_x^\mu(\xi) = \Sigma_x^\mu(\xi) = V_\xi^\mu(x)$. Equation (91) shows how the boundary $\partial\mathcal{U}_x$ of the waterbag \mathcal{U}_x is parameterised. The parameter space representation $\Sigma_x^\mu(\xi)$ (of the boundary operator $\partial\mathcal{C}_x$) runs over the parameter space ξ to create the boundary $\partial\mathcal{U}_x$ (of the waterbag). From another viewpoint, the base manifold spacetime representation $V_\xi^\mu(x)$ (of the boundary operator $\partial\mathcal{C}_x$) runs over the base manifold spacetime point x to create the worldline of a point on the waterbag boundary.

With the above parameterised description of the boundary (of the waterbag) in the tangent fiber space \mathcal{E}_x , we can transform an integral of an arbitrary function $h(\dot{x}, \xi)$ from the fiber space \mathcal{E}_x to the parameter space as follows,

$$\begin{aligned} \int_{\partial\mathcal{C}_x} h(\dot{x}, \xi) d\dot{x}^\mu \wedge d\dot{x}^\nu &= \int_{\mathcal{D}} h(\dot{x}, \xi) \partial\mathcal{C}_x^\star d\dot{x}^\mu \wedge \partial\mathcal{C}_x^\star d\dot{x}^\nu \\ &= \int_{\mathcal{D}} h(\dot{x}, \xi) d(\partial\mathcal{C}_x^\star \dot{x}^\mu) \wedge d(\partial\mathcal{C}_x^\star \dot{x}^\nu) \\ &= \int_{\mathcal{D}} h(\dot{x}, \xi) d(\partial\mathcal{C}_x^\mu) \wedge d(\partial\mathcal{C}_x^\nu) \\ &= \int_{\mathcal{D}} h(\dot{x}, \xi) d\Sigma_x^\mu \wedge d\Sigma_x^\nu . \end{aligned} \quad (92)$$

Integrals in the parameter space is easy to be done. We will carry out such integrals in a spherical parameter system for the moments calculation in the next subsection.

2. Integrals of Moments

For simplicity, we focus on waterbags whose boundaries $\partial\mathcal{U}_x$ are axially asymmetric about the \dot{x}^3 axis and abbreviate the following combinations $\beta^2 = 1 + (\dot{x}^1)^2 + (\dot{x}^2)^2 \in \Gamma\Lambda^0\mathcal{E}$ and $\underline{\beta}^2 = 1 + (\Sigma_x^1)^2 + (\Sigma_x^2)^2$ with the labels $\beta^2 \in \Gamma\Lambda^0\mathcal{E}$ and $\underline{\beta}^2 \in \Gamma\Lambda^0\mathcal{D}$. We then write the first, second and third order moments of velocity in the fluid model of plasmas as follows,

$$S_{\text{I}}^\mu(x) = \int_{\Pi^{-1}(x)} f(x, \dot{x}) \dot{x}^\mu \iota_X \#1 , \quad (93)$$

$$S_{\text{II}}^{\mu\nu}(x) = \int_{\Pi^{-1}(x)} f(x, \dot{x}) \dot{x}^\mu \dot{x}^\nu \iota_X \#1 , \quad (94)$$

$$S_{\text{III}}^{\mu\nu\chi}(x) = \int_{\Pi^{-1}(x)} f(x, \dot{x}) \dot{x}^\mu \dot{x}^\nu \dot{x}^\chi \iota_X \#1 . \quad (95)$$

We now parameterise the above integrals over the tangent fiber space $T_X\mathcal{M}$. In the following subsection, the lab inertial coordinate system x^μ on \mathcal{M} is chosen so that the waterbag on $T\mathcal{M}$ is axisymmetric about the \dot{x}^3 axis over the origin of x^μ on \mathcal{M} . It should be commented that the choice of the inertial coordinate system $\{x^\mu\}$ on \mathcal{M} is simply to determine which fiber to choose as $T_0\mathcal{M} \equiv T_{x=0}\mathcal{M}$ so that the waterbag with the axis pointing to the direction of \dot{x}^3 can be placed in that fiber. From now on in this section we will use (0) instead of $(x=0)$ to specify the values the physical quantities take at the origin of x^μ . And further, we define $\mathcal{C} \equiv \mathcal{C}_{x=0}$ and $\Sigma \equiv \Sigma_{x=0}$ for convenience.

For the waterbag distribution described by formula (90) with the boundary $V_\xi(0)$ axially asymmetric about the \dot{x}^3 axis and therefore all the moments vanish when they are perpendicular to \dot{x}^3 , we obtain the following first, second and third order centered moments of velocity (all the moments are symmetric in the superscripts so we only list one ordering of the superscripts):

$$S_{\text{I}}^1(0) = S_{\text{I}}^2(0) = S_{\text{I}}^3(0) = 0 , \quad (96)$$

$$S_{\text{II}}^{01}(0) = S_{\text{II}}^{02}(0) = S_{\text{II}}^{12}(0) = S_{\text{II}}^{13}(0) = S_{\text{II}}^{23}(0) = 0, \quad (97)$$

$$\begin{aligned} S_{\text{I}}^0(0) &= \int_{\Pi^{-1}(0)} f(0, \dot{x}) \dot{x}^0 \iota_X \# 1 \\ &= \alpha \int_{\mathcal{C}} \dot{x}^0 \frac{d\dot{x}^1 \wedge d\dot{x}^2 \wedge d\dot{x}^3}{\sqrt{1 + (\dot{x}^1)^2 + (\dot{x}^2)^2 + (\dot{x}^3)^2}} \\ &= \alpha \int_{\mathcal{C}} d\dot{x}^1 \wedge d\dot{x}^2 \wedge d\dot{x}^3 \\ &= \alpha \int_{\partial\mathcal{C}} \dot{x}^3 d\dot{x}^1 \wedge d\dot{x}^2 \\ &= \alpha \int_{\mathcal{D}} \Sigma^3 d\Sigma^1 \wedge d\Sigma^2, \end{aligned} \quad (98)$$

$$\begin{aligned} S_{\text{II}}^{00}(0) &= \int_{\Pi^{-1}(0)} f(0, \dot{x}) \dot{x}^0 \dot{x}^0 \iota_X \# 1 \\ &= \alpha \int_{\mathcal{C}} \dot{x}^{02} \frac{d\dot{x}^1 \wedge d\dot{x}^2 \wedge d\dot{x}^3}{\sqrt{1 + (\dot{x}^1)^2 + (\dot{x}^2)^2 + (\dot{x}^3)^2}} \\ &= \alpha \int_{\mathcal{C}} \sqrt{1 + (\dot{x}^1)^2 + (\dot{x}^2)^2 + (\dot{x}^3)^2} d\dot{x}^1 \wedge d\dot{x}^2 \wedge d\dot{x}^3 \\ &= \alpha \int_{\mathcal{C}} \sqrt{\beta^2 + (\dot{x}^3)^2} d\dot{x}^1 \wedge d\dot{x}^2 \wedge d\dot{x}^3 \\ &= \alpha \int_{\partial\mathcal{C}} d\dot{x}^1 \wedge d\dot{x}^2 \frac{1}{2} \left[\dot{x}^3 \sqrt{\beta^2 + (\dot{x}^3)^2} + \beta^2 \ln \left(\dot{x}^3 + \sqrt{\beta^2 + (\dot{x}^3)^2} \right) \right] \\ &= \alpha \int_{\mathcal{D}} d\Sigma^1 \wedge d\Sigma^2 \frac{1}{2} \left[\Sigma^3 \sqrt{\beta^2 + \Sigma^{32}} + \beta^2 \ln \left(\Sigma^3 + \sqrt{\beta^2 + \Sigma^{32}} \right) \right], \end{aligned} \quad (99)$$

$$\begin{aligned} S_{\text{II}}^{03}(0) &= \int_{\Pi^{-1}(0)} f(0, \dot{x}) \dot{x}^0 \dot{x}^3 \iota_X \# 1 \\ &= \alpha \int_{\mathcal{C}} \dot{x}^0 \dot{x}^3 \frac{d\dot{x}^1 \wedge d\dot{x}^2 \wedge d\dot{x}^3}{\sqrt{1 + (\dot{x}^1)^2 + (\dot{x}^2)^2 + (\dot{x}^3)^2}} \\ &= \alpha \int_{\mathcal{C}} \dot{x}^3 d\dot{x}^1 \wedge d\dot{x}^2 \wedge d\dot{x}^3 \\ &= \alpha \int_{\partial\mathcal{C}} d\dot{x}^1 \wedge d\dot{x}^2 \frac{1}{2} \dot{x}^3^2 \\ &= \alpha \int_{\mathcal{D}} d\Sigma^1 \wedge d\Sigma^2 \frac{1}{2} \Sigma^{32}, \end{aligned} \quad (100)$$

$$\begin{aligned}
S_{\text{II}}^{11}(0) &= \int_{\Pi^{-1}(0)} f(0, \dot{x}) \dot{x}^1 \dot{x}^1 \iota_X \#1 \\
&= \alpha \int_{\mathcal{C}} (\dot{x}^1)^2 \frac{d\dot{x}^1 \wedge d\dot{x}^2 \wedge d\dot{x}^3}{\sqrt{1 + (\dot{x}^1)^2 + (\dot{x}^2)^2 + (\dot{x}^3)^2}} \\
&= \alpha \int_{\mathcal{C}} \dot{x}^{12} \frac{d\dot{x}^1 \wedge d\dot{x}^2 \wedge d\dot{x}^3}{\sqrt{\beta^2 + (\dot{x}^3)^2}} \\
&= \alpha \int_{\partial\mathcal{C}} d\dot{x}^1 \wedge d\dot{x}^2 (\dot{x}^1)^2 \ln(\dot{x}^3 + \sqrt{\beta^2 + (\dot{x}^3)^2}) \\
&= \alpha \int_{\mathcal{D}} d\Sigma^1 \wedge d\Sigma^2 \Sigma^{12} \ln(\Sigma^3 + \sqrt{\underline{\beta}^2 + \Sigma^{32}}), \tag{101}
\end{aligned}$$

$$\begin{aligned}
S_{\text{II}}^{22}(0) &= \int_{\Pi^{-1}(0)} f(0, \dot{x}) \dot{x}^2 \dot{x}^2 \iota_X \#1 \\
&= \alpha \int_{\mathcal{C}} (\dot{x}^2)^2 \frac{d\dot{x}^1 \wedge d\dot{x}^2 \wedge d\dot{x}^3}{\sqrt{1 + (\dot{x}^1)^2 + (\dot{x}^2)^2 + (\dot{x}^3)^2}} \\
&= \alpha \int_{\mathcal{C}} \dot{x}^{22} \frac{d\dot{x}^1 \wedge d\dot{x}^2 \wedge d\dot{x}^3}{\sqrt{\beta^2 + \dot{x}^{32}}} \\
&= \alpha \int_{\partial\mathcal{C}} d\dot{x}^1 \wedge d\dot{x}^2 (\dot{x}^2)^2 \ln(\dot{x}^3 + \sqrt{\beta^2 + (\dot{x}^3)^2}) \\
&= \alpha \int_{\mathcal{D}} d\Sigma^1 \wedge d\Sigma^2 \Sigma^{22} \ln(\Sigma^3 + \sqrt{\underline{\beta}^2 + \Sigma^{32}}), \tag{102}
\end{aligned}$$

$$\begin{aligned}
S_{\text{II}}^{33}(0) &= \int_{\Pi^{-1}(0)} f(0, \dot{x}) \dot{x}^3 \dot{x}^3 \iota_X \#1 \\
&= \alpha \int_{\mathcal{C}} \dot{x}^{32} \frac{d\dot{x}^1 \wedge d\dot{x}^2 \wedge d\dot{x}^3}{\sqrt{1 + (\dot{x}^1)^2 + (\dot{x}^2)^2 + (\dot{x}^3)^2}} \\
&= \alpha \int_{\mathcal{C}} \dot{x}^{32} \frac{d\dot{x}^1 \wedge d\dot{x}^2 \wedge d\dot{x}^3}{\sqrt{\beta^2 + (\dot{x}^3)^2}} \\
&= \alpha \int_{\partial\mathcal{C}} d\dot{x}^1 \wedge d\dot{x}^2 \frac{1}{2} \left[\dot{x}^3 \sqrt{\beta^2 + (\dot{x}^3)^2} - \beta^2 \ln \left(\dot{x}^3 + \sqrt{\beta^2 + (\dot{x}^3)^2} \right) \right] \\
&= \alpha \int_{\mathcal{D}} d\Sigma^1 \wedge d\Sigma^2 \frac{1}{2} \left[\Sigma^3 \sqrt{\underline{\beta}^2 + \Sigma^{32}} - \underline{\beta}^2 \ln \left(\Sigma^3 + \sqrt{\underline{\beta}^2 + \Sigma^{32}} \right) \right] \tag{103}
\end{aligned}$$

$$\begin{aligned}
S_{\text{III}}^{001}(0) &= S_{\text{III}}^{002}(0) = S_{\text{III}}^{012}(0) = S_{\text{III}}^{013}(0) = S_{\text{III}}^{023}(0) \\
&= S_{\text{III}}^{112}(0) = S_{\text{III}}^{123}(0) = S_{\text{III}}^{133}(0) = S_{\text{III}}^{233}(0) \\
&= 0, \tag{104}
\end{aligned}$$

$$\begin{aligned}
S_{\text{III}}^{000}(0) &= \int_{\Pi^{-1}(0)} f(0, \dot{x}) \dot{x}^0 \dot{x}^0 \dot{x}^0 \iota_X \#1 \\
&= \alpha \int_C \dot{x}^{03} \frac{d\dot{x}^1 \wedge d\dot{x}^2 \wedge d\dot{x}^3}{\sqrt{1 + (\dot{x}^1)^2 + (\dot{x}^2)^2 + (\dot{x}^3)^2}} \\
&= \alpha \int_C (1 + (\dot{x}^1)^2 + (\dot{x}^2)^2 + (\dot{x}^3)^2) d\dot{x}^1 \wedge d\dot{x}^2 \wedge d\dot{x}^3 \\
&= \alpha \int_C (\beta^2 + (\dot{x}^3)^2) d\dot{x}^1 \wedge d\dot{x}^2 \wedge d\dot{x}^3 \\
&= \alpha \int_{\partial C} d\dot{x}^1 \wedge d\dot{x}^2 \left(\beta^2 \dot{x}^3 + \frac{1}{3} \dot{x}^{33} \right) \\
&= \alpha \int_{\mathcal{D}} d\Sigma^1 \wedge d\Sigma^2 \left(\underline{\beta}^2 \Sigma^3 + \frac{1}{3} \Sigma^{33} \right) , \tag{105}
\end{aligned}$$

$$\begin{aligned}
S_{\text{III}}^{003}(0) &= \int_{\Pi^{-1}(0)} f(0, \dot{x}) \dot{x}^0 \dot{x}^0 \dot{x}^3 \iota_X \#1 , \\
&= \alpha \int_C \dot{x}^3 \dot{x}^{02} \frac{d\dot{x}^1 \wedge d\dot{x}^2 \wedge d\dot{x}^3}{\sqrt{1 + (\dot{x}^1)^2 + (\dot{x}^2)^2 + (\dot{x}^3)^2}} \\
&= \alpha \int_C \dot{x}^3 \sqrt{1 + (\dot{x}^1)^2 + (\dot{x}^2)^2 + (\dot{x}^3)^2} d\dot{x}^1 \wedge d\dot{x}^2 \wedge d\dot{x}^3 \\
&= \alpha \int_C \dot{x}^3 \sqrt{\beta^2 + (\dot{x}^3)^2} d\dot{x}^1 \wedge d\dot{x}^2 \wedge d\dot{x}^3 \\
&= \alpha \int_{\partial C} d\dot{x}^1 \wedge d\dot{x}^2 \frac{1}{3} (\beta^2 + (\dot{x}^3)^2)^{\frac{3}{2}} \\
&= \alpha \int_{\mathcal{D}} d\Sigma^1 \wedge d\Sigma^2 \frac{1}{3} \left(\underline{\beta}^2 + \Sigma^{32} \right)^{\frac{3}{2}} , \tag{106}
\end{aligned}$$

$$\begin{aligned}
S_{\text{III}}^{011}(0) &= \int_{\Pi^{-1}(0)} f(0, \dot{x}) \dot{x}^0 \dot{x}^1 \dot{x}^1 \iota_X \#1 \\
&= \alpha \int_C (\dot{x}^1)^2 \dot{x}^0 \frac{d\dot{x}^1 \wedge d\dot{x}^2 \wedge d\dot{x}^3}{\sqrt{1 + (\dot{x}^1)^2 + (\dot{x}^2)^2 + (\dot{x}^3)^2}} \\
&= \alpha \int_C (\dot{x}^1)^2 d\dot{x}^1 \wedge d\dot{x}^2 \wedge d\dot{x}^3 \\
&= \alpha \int_{\partial C} d\dot{x}^1 \wedge d\dot{x}^2 (\dot{x}^1)^2 \dot{x}^3 \\
&= \alpha \int_{\mathcal{D}} d\Sigma^1 \wedge d\Sigma^2 \Sigma^{12} \Sigma^3 , \tag{107}
\end{aligned}$$

$$\begin{aligned}
S_{\text{III}}^{022}(0) &= \int_{\Pi^{-1}(0)} f(0, \dot{x}) \dot{x}^0 \dot{x}^2 \dot{x}^2 \iota_X \#1 \\
&= \alpha \int_{\mathcal{D}} d\Sigma^1 \wedge d\Sigma^2 \Sigma^{22} \Sigma^3, \tag{108}
\end{aligned}$$

$$\begin{aligned}
S_{\text{III}}^{033}(0) &= \int_{\Pi^{-1}(0)} f(0, \dot{x}) \dot{x}^0 \dot{x}^3 \dot{x}^3 \iota_X \#1 \\
&= \alpha \int_c (\dot{x}^3)^2 \dot{x}^0 \frac{d\dot{x}^1 \wedge d\dot{x}^2 \wedge d\dot{x}^3}{\sqrt{1 + (\dot{x}^1)^2 + (\dot{x}^2)^2 + (\dot{x}^3)^2}} \\
&= \alpha \int_c (\dot{x}^3)^2 d\dot{x}^1 \wedge d\dot{x}^2 \wedge d\dot{x}^3 \\
&= \alpha \int_{\partial c} d\dot{x}^1 \wedge d\dot{x}^2 \frac{1}{3} \dot{x}^{33} \\
&= \alpha \int_{\mathcal{D}} d\Sigma^1 \wedge d\Sigma^2 \frac{1}{3} \Sigma^{33}, \tag{109}
\end{aligned}$$

$$\begin{aligned}
S_{\text{III}}^{113}(0) &= \int_{\Pi^{-1}(0)} f(0, \dot{x}) \dot{x}^1 \dot{x}^1 \dot{x}^3 \iota_X \#1 \\
&= \alpha \int_c (\dot{x}^1)^2 \dot{x}^3 \frac{d\dot{x}^1 \wedge d\dot{x}^2 \wedge d\dot{x}^3}{\sqrt{1 + (\dot{x}^1)^2 + (\dot{x}^2)^2 + (\dot{x}^3)^2}} \\
&= \alpha \int_c (\dot{x}^1)^2 \dot{x}^3 \frac{d\dot{x}^1 \wedge d\dot{x}^2 \wedge d\dot{x}^3}{\sqrt{\beta^2 + (\dot{x}^3)^2}} \\
&= \alpha \int_{\partial c} d\dot{x}^1 \wedge d\dot{x}^2 (\dot{x}^1)^2 \sqrt{\beta^2 + (\dot{x}^3)^2} \\
&= \alpha \int_{\mathcal{D}} d\Sigma^1 \wedge d\Sigma^2 \Sigma^{12} \sqrt{\underline{\beta}^2 + \Sigma^{32}}, \tag{110}
\end{aligned}$$

$$\begin{aligned}
S_{\text{III}}^{223}(0) &= \int_{\Pi^{-1}(0)} f(0, \dot{x}) \dot{x}^2 \dot{x}^2 \dot{x}^3 \iota_X \#1 \\
&= \alpha \int_{\mathcal{D}} d\Sigma^1 \wedge d\Sigma^2 \Sigma^{22} \sqrt{\underline{\beta}^2 + \Sigma^{32}}, \tag{111}
\end{aligned}$$

$$\begin{aligned}
S_{\text{III}}^{333}(0) &= \int_{\Pi^{-1}(0)} f(0, \dot{x}) \dot{x}^3 \dot{x}^3 \dot{x}^3 \iota_X \#1 \\
&= \alpha \int_c \dot{x}^{33} \frac{d\dot{x}^1 \wedge d\dot{x}^2 \wedge d\dot{x}^3}{\sqrt{1 + (\dot{x}^1)^2 + (\dot{x}^2)^2 + (\dot{x}^3)^2}} \\
&= \alpha \int_c \dot{x}^{33} \frac{d\dot{x}^1 \wedge d\dot{x}^2 \wedge d\dot{x}^3}{\sqrt{\beta^2 + (\dot{x}^3)^2}} \\
&= \alpha \int_{\partial c} d\dot{x}^1 \wedge d\dot{x}^2 \left[\frac{1}{3} (\beta^2 + (\dot{x}^3)^2)^{\frac{3}{2}} - \beta^2 (\beta^2 + (\dot{x}^3)^2)^{\frac{1}{2}} \right] \\
&= \alpha \int_{\mathcal{D}} d\Sigma^1 \wedge d\Sigma^2 \left[\frac{1}{3} (\underline{\beta}^2 + \Sigma^{32})^{\frac{3}{2}} - \underline{\beta}^2 (\underline{\beta}^2 + \Sigma^{32})^{\frac{1}{2}} \right], \tag{112}
\end{aligned}$$

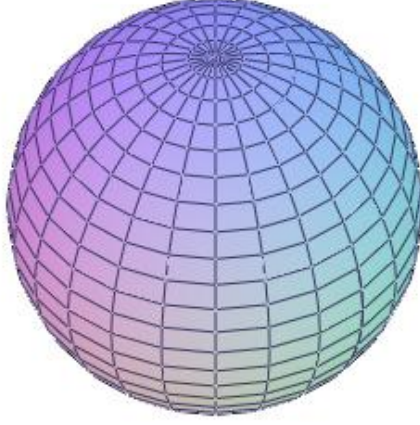


FIG. 4: A schematic illustration of a 3-D ellipsoid waterbag

where we have used Stokes Theorem.

For further calculation, we choose a 3-D ellipsoid waterbag illustrated in Fig. 4 and parameterised as follows,

$$\Sigma^0(\xi) = \sqrt{1 + R^2 \sin^2(\xi^1) + l^2 \cos^2(\xi^1)} \quad (113)$$

$$\Sigma^3(\xi) = l \cos(\xi^1) \quad (114)$$

$$\Sigma^1(\xi) = R \sin(\xi^1) \cos(\xi^2) \quad (115)$$

$$\Sigma^2(\xi) = R \sin(\xi^1) \sin(\xi^2) \quad (116)$$

$$\begin{aligned} \underline{\beta}^2 &= 1 + \Sigma^{1^2} + \Sigma^{2^2} = 1 + V_\xi^{1^2}(x) + V_\xi^{2^2}(x) \\ &= 1 + R^2 \sin^2(\xi^1) . \end{aligned} \quad (117)$$

And the boundary of the above 3-D ellipsoid waterbag is parameterised accord-

ingly below,

$$\frac{\dot{x}^1{}^2}{R^2} + \frac{(\dot{x}^2)^2}{R^2} + \frac{\dot{x}^3{}^2}{l^2} = 1 . \quad (118)$$

From the integral of

$$\begin{aligned} d\Sigma^1(\xi) \wedge d\Sigma^2(\xi) &= d[R \sin(\xi^1) \cos(\xi^2)] \wedge d[R \sin(\xi^1) \sin(\xi^2)] \\ &= R^2 [\cos(\xi^2) d \sin(\xi^1) + \sin(\xi^1) d \cos(\xi^2)] \\ &\quad \wedge d[\sin(\xi^1) d \sin(\xi^2) + \sin(\xi^2) d \sin(\xi^1)] \\ &= R^2 [\cos(\xi^1) \cos(\xi^2) d\xi^1 - \sin(\xi^1) \sin(\xi^2) d\xi^2] \\ &\quad \wedge [\sin(\xi^2) \cos(\xi^1) d\xi^1 + \sin(\xi^1) \cos(\xi^2) d\xi^2] \\ &= R^2 \sin(\xi^1) \cos(\xi^1) [\cos^2(\xi^2) + \sin^2(\xi^2)] d\xi^1 \wedge d\xi^2 \\ &= R^2 \sin(\xi^1) \cos(\xi^1) d\xi^1 \wedge d\xi^2 , \end{aligned} \quad (119)$$

over the boundary of the waterbag distribution, and choosing the orientation of $*1 = d\xi^1 \wedge d\xi^2$, we get the leading order terms about R (in the neighborhood of $R = 0$) of the non-zero velocity moments below.

1st order moment:

$$\begin{aligned} S_1^0(0) &= \alpha R^2 \int_0^{2\pi} d\xi^2 \int_0^\pi d\xi^1 l \sin(\xi^1) \cos^2(\xi^1) \\ &= \frac{4\pi\alpha R^2 l}{3} , \end{aligned} \quad (120)$$

2nd order moments (where the integral transforms $u = -\cos(\xi^1)$ and $\sinh w =$

lu are used):

$$\begin{aligned}
S_{\text{II}}^{00}(0) &= \alpha R^2 \int_0^{2\pi} d\xi^2 \int_0^\pi d\xi^1 \sin(\xi^1) \cos(\xi^1) \frac{1}{2} [l \cos(\xi^1) \sqrt{1 + R^2 \sin^2(\xi^1) + l^2 \cos^2(\xi^1)} \\
&\quad + (1 + R^2 \sin^2(\xi^1)) \ln(l \cos(\xi^1) + \sqrt{1 + R^2 \sin^2(\xi^1) + l^2 \cos^2(\xi^1)})] \\
&= \pi \alpha R^2 \int_{-1}^1 du (-u) [-lu \sqrt{1 + l^2 u^2} + \ln(-lu + \sqrt{1 + l^2 u^2})] \\
&= \pi \alpha R^2 \int_{-\sinh^{-1} l}^{\sinh^{-1} l} dw \left(-\frac{1}{l^2}\right) \cosh w \sinh w [-\sinh w \sqrt{1 + \sinh^2 w} \\
&\quad + \ln(-\sinh w + \sqrt{1 + \sinh^2 w})] \\
&= \pi \alpha R^2 \left[\left(\frac{l}{2} - \frac{1}{4l} \right) \sqrt{1 + l^2} + \left(1 + \frac{1}{4l^2} \right) \sinh^{-1} l \right], \tag{121}
\end{aligned}$$

$$\begin{aligned}
S_{\text{II}}^{03}(0) &= \alpha R^2 \int_0^{2\pi} d\xi^2 \int_0^\pi d\xi^1 \frac{1}{2} \sin(\xi^1) \cos(\xi^1)^3 l^2 \\
&= -\alpha R^2 \int_0^{2\pi} d\xi^2 \int_1^{-1} d \cos(\xi^1) \frac{1}{2} \cos(\xi^1)^3 l^2 \\
&= 0, \tag{122}
\end{aligned}$$

$$\begin{aligned}
S_{\text{II}}^{11}(0) &= \alpha R^4 \int_0^{2\pi} d\xi^2 \cos^2(\xi^2) \int_0^\pi d\xi^1 \sin^3(\xi^1) \cos(\xi^1) \\
&\quad \ln[l \cos(\xi^1) + \sqrt{1 + R^2 \sin^2(\xi^1) + l^2 \cos^2(\xi^1)}] \\
&= \pi \alpha R^4 \int_{-1}^1 du (u^3 - u) \ln[-lu + \sqrt{1 + l^2 u^2}] \\
&= \pi \alpha R^4 \left[\left(-\frac{3}{8l} - \frac{3}{16l^3} \right) \sqrt{1 + l^2} + \left(\frac{1}{2} + \frac{1}{2l^2} + \frac{3}{16l^4} \right) \sinh^{-1} l \right], \tag{123}
\end{aligned}$$

$$\begin{aligned}
S_{\text{II}}^{22}(0) &= \alpha R^4 \int_0^{2\pi} d\xi^2 \sin^2(\xi^2) \int_0^\pi d\xi^1 \sin^3(\xi^1) \cos(\xi^1) \\
&\quad \ln[l \cos(\xi^1) + \sqrt{1 + R^2 \sin^2(\xi^1) + l^2 \cos^2(\xi^1)}] \\
&= \pi \alpha R^4 \left[\left(-\frac{3}{8l} - \frac{3}{16l^3} \right) \sqrt{1 + l^2} + \left(\frac{1}{2} + \frac{1}{2l^2} + \frac{3}{16l^4} \right) \sinh^{-1} l \right], \tag{124}
\end{aligned}$$

$$\begin{aligned}
S_{\text{II}}^{33}(0) &= \alpha R^2 \int_0^{2\pi} d\xi^2 \int_0^\pi d\xi^1 \sin(\xi^1) \cos(\xi^1) \frac{1}{2} [l \cos(\xi^1) \sqrt{1 + R^2 \sin^2(\xi^1) + l^2 \cos^2(\xi^1)} \\
&\quad - (1 + R^2 \sin^2(\xi^1)) \ln(l \cos(\xi^1) + \sqrt{1 + R^2 \sin^2(\xi^1) + l^2 \cos^2(\xi^1)})] \\
&= \pi \alpha R^2 \int_{-1}^1 du (-u) [-lu \sqrt{1 + l^2 u^2} - \ln(-lu + \sqrt{1 + l^2 u^2})] \\
&= \pi \alpha R^2 \int_{-\sinh^{-1} l}^{\sinh^{-1} l} dw \left(-\frac{1}{l^2}\right) \cosh w \sinh w [-\sinh w \sqrt{1 + \sinh^2 w} \\
&\quad - \ln(-\sinh w + \sqrt{1 + \sinh^2 w})] \\
&= \pi \alpha R^2 \left[\left(\frac{l}{2} + \frac{3}{4l}\right) \sqrt{1 + l^2} - \left(1 + \frac{3}{4l^2}\right) \sinh^{-1} l \right], \tag{125}
\end{aligned}$$

3rd order moments:

$$\begin{aligned}
S_{\text{III}}^{000}(0) &= \alpha R^2 \int_0^{2\pi} d\xi^2 \int_0^\pi d\xi^1 \sin(\xi^1) \cos(\xi^1) \{ [1 + R^2 \sin^2(\xi^1)] l \cos(\xi^1) + \frac{1}{3} l^3 \cos^3(\xi^1) \} \\
&= 2\pi \alpha R^2 \int_{-1}^1 du (lu^2 + \frac{1}{3} l^3 u^4) \\
&= \frac{4\pi \alpha R^2}{15} l^3 + \frac{4\pi \alpha R^2}{3} l, \tag{126}
\end{aligned}$$

$$\begin{aligned}
S_{\text{III}}^{003}(0) &= \frac{1}{3} \alpha R^2 \int_0^{2\pi} d\xi^2 \int_0^\pi d\xi^1 \sin(\xi^1) \cos(\xi^1) [1 + R^2 \sin^2(\xi^1) + l^2 \cos^2(\xi^1)]^{\frac{3}{2}} \\
&= \frac{2\pi \alpha R^2}{3} \int_{-1}^1 du (-u) (1 + l^2 u^2)^{\frac{3}{2}} \\
&= 0, \tag{127}
\end{aligned}$$

$$\begin{aligned}
S_{\text{III}}^{011}(0) &= \alpha R^4 \int_0^{2\pi} d\xi^2 \cos^2(\xi^2) \int_0^\pi d\xi^1 \sin^3(\xi^1) \cos(\xi^1) l \cos(\xi^1) \\
&= \pi \alpha R^4 \int_{-1}^1 du (u^2 - u^4) l \\
&= \frac{4\pi \alpha R^4}{15} l, \tag{128}
\end{aligned}$$

$$\begin{aligned}
S_{\text{III}}^{022}(0) &= \alpha R^4 \int_0^{2\pi} d\xi^2 \sin^2(\xi^2) \int_0^\pi d\xi^1 \sin^3(\xi^1) \cos(\xi^1) l \cos(\xi^1) \\
&= \pi \alpha R^4 \int_{-1}^1 du (u^2 - u^4) l \\
&= \frac{4\pi \alpha R^4}{15} l, \tag{129}
\end{aligned}$$

$$\begin{aligned}
S_{\text{III}}^{033}(0) &= \frac{\alpha R^2}{3} \int_0^{2\pi} d\xi^2 \int_0^\pi d\xi^1 \sin(\xi^1) \cos(\xi^1) l^3 \cos^3(\xi^1) \\
&= \frac{2\alpha R^2}{3} \int_{-1}^1 du u^4 l^3 \\
&= \frac{4\pi\alpha R^2}{15} l^3 ,
\end{aligned} \tag{130}$$

$$\begin{aligned}
S_{\text{III}}^{113}(0) &= \alpha R^4 \int_0^{2\pi} d\xi^2 \cos^2(\xi^2) \int_0^\pi d\xi^1 \sin^3(\xi^1) \cos(\xi^1) \sqrt{1 + R^2 \sin^2(\xi^1) + l^2 \cos^2(\xi^1)} \\
&= \pi\alpha R^4 \int_{-1}^1 du (u^3 - u) \sqrt{1 + l^2 u^2} \\
&= 0 ,
\end{aligned} \tag{131}$$

$$\begin{aligned}
S_{\text{III}}^{223}(0) &= \alpha R^4 \int_0^{2\pi} d\xi^2 \sin^2(\xi^2) \int_0^\pi d\xi^1 \sin^3(\xi^1) \cos(\xi^1) \sqrt{1 + R^2 \sin^2(\xi^1) + l^2 \cos^2(\xi^1)} \\
&= \pi\alpha R^4 \int_{-1}^1 du (u^3 - u) \sqrt{1 + l^2 u^2} \\
&= 0 ,
\end{aligned} \tag{132}$$

$$\begin{aligned}
S_{\text{III}}^{333}(0) &= \alpha R^2 \int_0^{2\pi} d\xi^2 \int_0^\pi d\xi^1 \sin(\xi^1) \cos(\xi^1) \\
&\quad \left\{ \frac{1}{3} [1 + R^2 \sin^2(\xi^1) + l^2 \cos^2(\xi^1)]^{\frac{3}{2}} - [1 + R^2 \sin^2(\xi^1)] [1 + R^2 \sin^2(\xi^1) + l^2 \cos^2(\xi^1)]^{\frac{1}{2}} \right\} \\
&= 2\pi\alpha R^2 \int_{-1}^1 du (-u) \left\{ \frac{1}{3} (1 + l^2 u^2)^{\frac{3}{2}} - (1 + l^2 u^2)^{\frac{1}{2}} \right\} \\
&= 0 .
\end{aligned} \tag{133}$$

C. ODE System

In the fluid model of plasmas, the equation for the first order moment of velocity in the fluid model of plasmas

$$d\sigma_{\text{I}} = 0 \tag{134}$$

is automatically satisfied due to the conservation of number 4-current.

Considering the proved (in [50]) properties of the volume in the total space, the

higher order moments equations are

$$D\sigma_{\text{II}}^\mu + \frac{q}{m}F^\mu \wedge \sigma_{\text{I}} = 0 , \quad (135)$$

$$D\sigma_{\text{III}}^{\mu\nu} + \frac{q}{m}F^\mu \wedge \sigma_{\text{II}}^\nu + \frac{q}{m}F^\nu \wedge \sigma_{\text{II}}^\mu = 0 . \quad (136)$$

In the natural coordinate co-frame $\left\{ \frac{\partial}{\partial x^\mu} \right\}$, the second order velocity moments equation (135) can be written as

$$d\sigma_{\text{II}}^\mu + \frac{q}{m}\eta^{\mu\nu}\iota_\nu F \wedge \sigma_{\text{I}} = 0 \quad (137)$$

due to the vanishing connection one forms $\omega^\mu{}_\nu$ on Minkowski spacetime.

For the bulks of waterbags, the following co-moving orthogonal co-frames $\{X_{\hat{\mu}}\}$:

$$X_{\hat{0}} = U = U^\mu \frac{\partial}{\partial x^\mu},$$

$$X_{\hat{1}} = \partial_1,$$

$$X_{\hat{2}} = \partial_2,$$

$$\tilde{X}_{\hat{3}} = \star(dx^1 \wedge dx^2 \wedge \tilde{U}) \quad (138)$$

$$g(U, U) = \eta_{\mu\nu}U^\mu U^\nu = -1 , \quad (139)$$

will be convenient for calculations. To be noted that in the above equation (138), we use U as the velocity vector for the bulks to be distinguishable with the boundaries velocity vector V^ξ of waterbags. We will keep this notation in the rest of this chapter.

With the above co-moving orthogonal co-frames (138), tensor fields representing the moments of f are introduced as follows,

$$\begin{aligned} S_{\text{I}} &= S_{\text{I}}^{\hat{\mu}}(0)X_{\hat{\mu}} \\ S_{\text{II}} &= S_{\text{II}}^{\hat{\mu}\hat{\nu}}(0)X_{\hat{\mu}} \otimes X_{\hat{\nu}} \\ S_{\text{III}} &= S_{\text{III}}^{\hat{\mu}\hat{\nu}\hat{\chi}}(0)X_{\hat{\mu}} \otimes X_{\hat{\nu}} \otimes X_{\hat{\chi}} , \end{aligned} \quad (140)$$

where the orthonormal frame field $\{X_{\hat{\mu}}\}$ encodes the orientation (adapted to flow) of the axes of the waterbag. The frame field $\{X_{\hat{\mu}}\}$ must be determined as part of the fluid model. Indices associated with the frame field are distinguished using hats.

Furthermore, the above moment equation (137) can be expressed with respect to the co-moving orthogonal co-frame (138) as

$$\begin{aligned} d\{S_{\text{II}}^{\hat{0}\hat{0}}U^\mu \star \tilde{U} + S_{\text{II}}^{\hat{3}\hat{3}}[\star(dx^1 \wedge dx^2 \wedge \tilde{U})]^\mu \star \star(dx^1 \wedge dx^2 \wedge \tilde{U})\} \\ + \frac{q}{m}\eta^{\mu\nu}\iota_\nu(\frac{1}{2}F_{\lambda\tau}dx^\lambda \wedge dx^\tau) \wedge S_{\text{I}}^{\hat{0}}\star \tilde{U} = 0 \end{aligned} \quad (141)$$

when we take the approximation of a large l .

For simplicity and clarity in examining the behaviour of electron waves, we start from the case that the electrons are moving in the x^3 direction in a travelling wave and all the physical properties depend on $\zeta = x^3 - vx^0$, where $0 \leq v \leq 1$ is the phase speed of the wave. Unless otherwise specified, ' will be used to express differentiations of functions with respect to ζ . As a result, the 4-velocity U (where $U = X_{\hat{0}}$) and the corresponding normalisation condition turn out to be

$$U = U^0\partial_0 + U^3\partial_3 \quad (142)$$

$$g(U, U) = -(U^0)^2 + (U^3)^2 = -1. \quad (143)$$

With the above specification, as well as one more assumption $F = Edx^0 \wedge dx^3$, we find that the equation for the second order moments turns into

$$\begin{aligned} d[S_{\text{II}}^{\hat{0}\hat{0}}U^\mu(U^0dx^1 \wedge dx^2 \wedge dx^3 - U^3dx^0 \wedge dx^1 \wedge dx^2)] \\ + d[S_{\text{II}}^{\hat{3}\hat{3}}(g^{-1}(-, -U^0 \star dx^0 \wedge dx^1 \wedge dx^2 + U^3 \star dx^1 \wedge dx^2 \wedge dx^3))^\mu \\ \star \star (-U^0dx^0 \wedge dx^1 \wedge dx^2 + U^3dx^1 \wedge dx^2 \wedge dx^3)] \\ + \frac{q}{m}\eta^{\mu\nu}\iota_\nu(Edx^0 \wedge dx^3) \wedge S_{\text{I}}^{\hat{0}}(U^0dx^1 \wedge dx^2 \wedge dx^3 - U^3dx^0 \wedge dx^1 \wedge dx^2) = 0 \end{aligned} \quad (144)$$

where $g^{-1}(-, dx^\tau) = g^{\mu\nu} \frac{\partial}{\partial x^\mu} \otimes \frac{\partial}{\partial x^\nu} (dx^\tau)$ and $\star\star$ act as 1 for 3-forms in the Minkowski spacetime. The above equation (144) will then be furthered into

$$\begin{aligned}
& d[S_{\text{II}}^{\hat{0}\hat{0}} U^\mu (U^0 dx^1 \wedge dx^2 \wedge dx^3 - U^3 dx^0 \wedge dx^1 \wedge dx^2)] \\
& + d[S_{\text{II}}^{\hat{3}\hat{3}} (g^{-1}(-, U^0 dx^3 - U^3 dx^0))^\mu (-U^0 dx^0 \wedge dx^1 \wedge dx^2 + U^3 dx^1 \wedge dx^2 \wedge dx^3)] \\
& + \frac{q}{m} \eta^{\mu\nu} \iota_\nu (E dx^0 \wedge dx^3) \wedge S_{\text{I}}^{\hat{0}} (U^0 dx^1 \wedge dx^2 \wedge dx^3 - U^3 dx^0 \wedge dx^1 \wedge dx^2) = 0 .
\end{aligned} \tag{145}$$

We rewrite the above equation into the following two equations of components,

$$\begin{aligned}
& (S_{\text{II}}^{\hat{0}\hat{0}})' [-v(U^0)^2 + U^0 U^3] \star 1 + S_{\text{II}}^{\hat{0}\hat{0}} [-2vU^0(U^0)' + (U^0 U^3)'] \star 1 \\
& + (S_{\text{II}}^{\hat{3}\hat{3}})' [U^0 U^3 - v(U^3)^2] \star 1 + S_{\text{II}}^{\hat{3}\hat{3}} [(U^0 U^3)' - 2vU^3(U^3)'] \star 1 \\
& - \frac{q}{m} E S_{\text{I}}^{\hat{0}} U^3 \star 1 = 0 ,
\end{aligned} \tag{146}$$

$$\begin{aligned}
& (S_{\text{II}}^{\hat{0}\hat{0}})' [-vU^0 U^3 + (U^3)^2] \star 1 + S_{\text{II}}^{\hat{0}\hat{0}} [-v(U^0 U^3)' + 2U^3(U^3)'] \star 1 \\
& + (S_{\text{II}}^{\hat{3}\hat{3}})' [(U^0)^2 - vU^0 U^3] \star 1 + S_{\text{II}}^{\hat{3}\hat{3}} [2U^0(U^0)' - v(U^0 U^3)'] \star 1 \\
& - \frac{q}{m} E S_{\text{I}}^{\hat{0}} U^0 \star 1 = 0 .
\end{aligned} \tag{147}$$

Since

$$\begin{aligned}
d \star F &= d \star (E dx^0 \wedge dx^3) \\
&= -dE \wedge dx^1 \wedge dx^2 \\
&= E' (v dx^0 \wedge dx^1 \wedge dx^2 - dx^1 \wedge dx^2 \wedge dx^3)
\end{aligned} \tag{148}$$

$$\tilde{N}_{\text{ion}} = n_{\text{ion}} \tilde{\partial}_0 = -n_{\text{ion}} dx^0 \tag{149}$$

$$\tilde{N} = \tilde{S}_{\text{I}} = S_{\text{I}}^{\hat{0}} \tilde{U} = S_{\text{I}}^{\hat{0}} (-U^0 dx^0 + U^3 dx^3) \tag{150}$$

$$q \star (\tilde{N}_{\text{ion}} - \tilde{N}) = q(-S_{\text{I}}^{\hat{0}} U^0 + n_{\text{ion}}) dx^1 \wedge dx^2 \wedge dx^3 + q S_{\text{I}}^{\hat{0}} U^3 dx^0 \wedge dx^1 \wedge dx^2 \tag{151}$$

the Maxwell equations $d \star F = q \star (\tilde{N}_{\text{ion}} - \tilde{N})$ will be

$$-E' = q(-S_{\text{I}}^{\hat{0}} U^0 + n_{\text{ion}}) \tag{152}$$

$$vE' = q S_{\text{I}}^{\hat{0}} U^3 . \tag{153}$$

There are 6 unknown and 5 equations for the ODE system consisting of the following five equations (143), (146), (147), (152) and (153) with respect to U^0, U^3, E , proper number density $n = S_{\text{I}}^{\hat{0}}$, proper mass density $\rho = mS_{\text{II}}^{\hat{0}\hat{0}}$, and relativistic pressure $p = mS_{\text{II}}^{\hat{3}\hat{3}}$ of the electron fluid, respectively. It is a differential-algebraic ODE system because of equation (143). In order to solve such a differential-algebraic ODE system, we need to close it by introducing the 6-th equation. We will show how to close the ODE with a certain Equation Of State (EOS) as the so-called 6-th equation.

D. Original Results

1. Properties of Non-Linearities for a Large Proper Density

We will now show that large number densities are incompatible with small amplitude (linear) oscillations. To do that, we rewrite the ODE system consisting of equations (143), (146), (147), (152) and (153) in the following form,

$$-1 = -(U^0)^2 + (U^3)^2 \quad (154)$$

$$0 = \rho'[-v(U^0)^2 + U^0U^3] + \rho[-2vU^0(U^0)' + (U^0U^3)'] \\ + p'[U^0U^3 - v(U^3)^2] + p[(U^0U^3)' - 2vU^3(U^3)'] - qEnU^3 \quad (155)$$

$$0 = \rho'[-vU^0U^3 + (U^3)^2] + \rho[-v(U^0U^3)' + 2U^3(U^3)'] \\ + p'[-vU^0U^3 + (U^0)^2] + p[-v(U^0U^3)' + 2U^0(U^0)'] - qEnU^0 \quad (156)$$

$$-E' = q(-nU^0 + n_{\text{ion}}) \quad (157)$$

$$vE' = qnU^3. \quad (158)$$

We now close the ODE system consisting of equations (154-158) with a class of Equation Of States (EOSs) with the leading term satisfies the following relation:

$$\rho = p \propto n^2, \quad (159)$$

which is useful for us as it is satisfied for the EOSs of 1-D, 3-D ellipsoid and gourd waterbags, which will be shown in the next subsection. In the present subsection we will show that there are no stable linear solutions to the above ODE for the waterbags whose EOS satisfies equation (159).

From equation (159) we then have

$$p = n \frac{d\rho}{dn} - \rho . \quad (160)$$

We investigate the behaviour of the displacement δE from the equilibrium of the field E caused by a perturbation δn of the number density $n = n_{\text{ion}}$. We now define the subscript $|_{\text{ion}}$ of a function $h(n) \Big|_{\text{ion}} = h(n) \Big|_{n=\text{ion}}$ when $n = n_{\text{ion}}$, or strictly speaking, when ζ takes the value ζ_{ion} where $n(\zeta_{\text{ion}}) = n_{\text{ion}}$.

We find the following constant combination

$$n = n_{\text{ion}} \quad (161)$$

$$E = 0 \quad (162)$$

$$U^3 = 0 \quad (163)$$

$$U^0 = 1 \quad (164)$$

$$\rho = \rho \Big|_{\text{ion}} \quad (165)$$

$$p = p \Big|_{\text{ion}} \quad (166)$$

satisfies the ODE system (155-160).

We then expand the variables as follows,

$$n = n_{\text{ion}} + \delta n \quad (167)$$

$$E = \delta E \quad (168)$$

$$U^3 = \delta U^3 \quad (169)$$

$$U^0 = 1 + O[(\delta U^3)^2] \quad (170)$$

$$\rho = \rho \Big|_{\text{ion}} + \frac{d\rho}{dn} \Big|_{\text{ion}} \delta n + O(\delta n^2) \quad (171)$$

$$p = p \Big|_{\text{ion}} + \frac{dp}{dn} \Big|_{\text{ion}} \delta n + O(\delta n^2) . \quad (172)$$

Substituting the above expansions into equations (157) and (158) we get

$$\delta n = \frac{1}{q} \delta E' \quad (173)$$

$$\delta U^3 = \frac{v}{qn_{\text{ion}}} \delta E' . \quad (174)$$

Further, substituting the above equations (173), (174) and the expansions (167)-(172) into equation (156), we obtain the second order Ordinary Differential Equation (ODE) for δE below,

$$\delta E'' = - \frac{q^2 n_{\text{ion}}}{m \left[-\frac{dp}{dn} \Big|_{\text{ion}} + \frac{v^2}{n_{\text{ion}}} (p + \rho) \Big|_{\text{ion}} \right]} \delta E . \quad (175)$$

The condition

$$\frac{q^2 n_{\text{ion}}}{m \left[-\frac{dp}{dn} \Big|_{\text{ion}} + \frac{v^2}{n_{\text{ion}}} (p + \rho) \Big|_{\text{ion}} \right]} \geq 0 , \quad (176)$$

i.e.

$$-\frac{dp}{dn} \Big|_{\text{ion}} + \frac{v^2}{n_{\text{ion}}} (p + \rho) \Big|_{\text{ion}} \geq 0 \quad (177)$$

should be satisfied for the existence of stable linear oscillating solutions for the ODE (175), or a small $|\delta E|$ will grow up monotonously due to the sign of the first order derivative.

Considering the EOS (160), the condition turns out to be

$$\left(-\frac{dp}{dn} + v^2 \frac{d\rho}{dn} \right) \Big|_{\text{ion}} \geq 0 . \quad (178)$$

From moment equations (120), (121) and (125) we have,

$$n = S_{\text{I}}^0(x) = \frac{4\pi\alpha R^2 l}{3} , \quad (179)$$

$$\begin{aligned} \rho &= mS_{\text{II}}^{00}(x) = m\pi\alpha R^2 \int_{-1}^1 du(-u)[-lu\sqrt{1+l^2u^2} + \ln(-lu + \sqrt{1+l^2u^2})] \\ &= m\pi\alpha R^4 \left[\left(\frac{l}{2} - \frac{1}{4l} \right) \sqrt{1+l^2} + \left(1 + \frac{1}{4l^2} \right) \sinh^{-1} l \right] , \end{aligned} \quad (181)$$

$$\begin{aligned} p &= mS_{\text{II}}^{33}(x) = m\pi\alpha R^2 \int_{-1}^1 du(-u)[-lu\sqrt{1+l^2u^2} - \ln(-lu + \sqrt{1+l^2u^2})] \\ &= m\pi\alpha R^4 \left[\left(\frac{l}{2} + \frac{3}{4l} \right) \sqrt{1+l^2} - \left(1 + \frac{3}{4l^2} \right) \sinh^{-1} l \right] . \end{aligned} \quad (183)$$

The first equation shows that $\frac{dl}{dn} > 0$ so that the condition we need is equivalent to

$$\left(-\frac{dp}{dl} + v^2 \frac{d\rho}{dl} \right) \Big|_{\text{ion}} \geq 0 , \quad (184)$$

where $\frac{d\rho}{dl}$ and $\frac{dp}{dl}$ will be

$$\begin{aligned} \frac{d\rho}{dl} &= m\pi\alpha R^2 \int_{-1}^1 du \left(u^2 \sqrt{1+l^2u^2} + \frac{l^2u^4}{\sqrt{1+l^2u^2}} + \frac{u^2 - \frac{lu^3}{\sqrt{1+l^2u^2}}}{-lu + \sqrt{1+l^2u^2}} \right) \\ &= m\pi\alpha R^2 \int_{-1}^1 du \left(u^2 \sqrt{1+l^2u^2} + \frac{l^2u^4}{\sqrt{1+l^2u^2}} + u^2 \sqrt{1+l^2u^2} - \frac{l^2u^4}{\sqrt{1+l^2u^2}} \right) \\ &= \frac{2m\pi\alpha R^2}{l^3} \int_{-l}^l dy y^2 \sqrt{1+y^2} \\ &= \frac{2m\pi\alpha R^2}{l^3} \left[\frac{y}{4} (1+y^2)^{\frac{3}{2}} - \frac{y}{8} (1+y^2)^{\frac{1}{2}} - \frac{1}{8} \ln(y + (1+y^2)^{\frac{1}{2}}) \right] \Big|_{-l}^l \\ &= \frac{2m\pi\alpha R^2}{l^3} \left[\frac{l}{2} (1+l^2)^{\frac{3}{2}} - \frac{l}{4} (1+l^2)^{\frac{1}{2}} - \frac{1}{8} \ln(1+2l^2+2l(1+l^2)^{\frac{1}{2}}) \right] \\ &= \frac{m\pi\alpha R^2}{l^3} \left[\left(l^3 + \frac{1}{2}l \right) \sqrt{l^2+1} - \frac{1}{2} \ln(\sqrt{l^2+1} + l) \right] , \end{aligned} \quad (185)$$

$$\begin{aligned}
\frac{dp}{dl} &= m\pi\alpha R^2 \int_{-1}^1 du \left(u^2 \sqrt{1+l^2u^2} + \frac{l^2u^4}{\sqrt{1+l^2u^2}} - \frac{u^2 - \frac{lu^3}{\sqrt{1+l^2u^2}}}{-lu + \sqrt{1+l^2u^2}} \right) \\
&= m\pi\alpha R^2 \int_{-1}^1 du \left(u^2 \sqrt{1+l^2u^2} + \frac{l^2u^4}{\sqrt{1+l^2u^2}} - u^2 \sqrt{1+l^2u^2} + \frac{l^2u^4}{\sqrt{1+l^2u^2}} \right) \\
&= \frac{2m\pi\alpha R^2}{l^3} \int_{-l}^l dy \frac{y^4}{\sqrt{1+y^2}} \\
&= \frac{2m\pi\alpha R^2}{l^3} (y^3 \sqrt{1+y^2}) \Big|_{-l}^l - \frac{6\pi\alpha R^2}{l^3} \int_{-l}^l dy y^2 \sqrt{1+y^2} \\
&= \frac{2m\pi\alpha R^2}{l^3} \left[2l^3(1+l^2)^{\frac{1}{2}} - \frac{3l}{2}(1+l^2)^{\frac{3}{2}} + \frac{3l}{4}(1+l^2)^{\frac{1}{2}} + \frac{31}{8} \ln(1+2l^2+2l(1+l^2)^{\frac{1}{2}}) \right] \\
&= \frac{m\pi\alpha R^2}{l^3} \left[(l^3 - \frac{3}{2}l)\sqrt{l^2+1} + \frac{3}{2} \ln(\sqrt{l^2+1}+l) \right], \tag{186}
\end{aligned}$$

where $y = lu$.

We then get the condition for the existence of stable linear oscillating solutions below,

$$\begin{aligned}
v &\geq \sqrt{\frac{dp}{dl} / \frac{d\rho}{dl}} \\
&= \sqrt{\frac{(l^3 - \frac{3}{2}l)\sqrt{l^2+1} + \frac{3}{2} \ln(\sqrt{l^2+1}+l)}{(l^3 + \frac{1}{2}l)\sqrt{l^2+1} - \frac{1}{2} \ln(\sqrt{l^2+1}+l)}}. \tag{187}
\end{aligned}$$

Condition (187) is possible to be satisfied for $l \gg 1$ (representing a large proper density from equation (179)) when $v < 1$. For the EOS of 3-D ellipsoid waterbag, however, when the dominant term in l for $l \gg 1$ is considered only, equation (175) becomes

$$\begin{aligned}
\delta E'' &= -\frac{q^2 n_{\text{ion}}}{m(-\frac{dp}{dn}|_{\text{ion}} + v^2 \frac{d\rho}{dn}|_{\text{ion}})} \delta E \\
&= -\frac{q^2 n_{\text{ion}}}{m(-\frac{dp}{dn}|_{\text{ion}} + v^2 \frac{d\rho}{dn}|_{\text{ion}})} \delta E \\
&= \frac{-4q^2 n_{\text{ion}}}{3m^2} \frac{l^3}{[v^2(l^3 + \frac{l}{2}) - (l^3 - \frac{3}{2}l)]\sqrt{l^2+1} - (\frac{v^2}{2} + \frac{3}{2} \ln(\sqrt{l^2+1}+l))} \Big|_{\text{ion}} \delta E \\
&\approx \frac{-4q^2}{3m^2} \frac{4\pi\alpha R^2}{3} \frac{1}{(v^2-1)} \delta E \\
&\approx -\left[\frac{4qR\sqrt{\pi\alpha}}{3m\sqrt{v^2-1}} \right]^2 \delta E. \tag{188}
\end{aligned}$$

Since $v < 1$ leads to an imaginary $\sqrt{v^2 - 1}$, hence a positive linear relation between $\delta E''$ and δE , this shows that the approximation $l \gg 1$ conflicts with the existence of a stable linear oscillating solution for the ODE system. In other words, non-linear behaviour appears for a sufficiently large proper number density n .

2. Wave-Breaking Limits

As an electric field in an electrostatic oscillation stronger than E_{\max} is beyond our model, it is important to calculate the maximum electric field by solving the ODE system consisting of equations (154)-(158) for a 1-D waterbag, 3-D ellipsoid waterbag and 3-D gourd waterbag. An electrostatic oscillation whose amplitude is close to the maximum electric fields E_{\max} is schematically illustrated in Fig. 5. Fig. 5 shows that $n = n_{\text{ion}}$ when the electric field reaches its maximum value ($E' = 0$), whereas $n = n_{\max}$ or $n = n_{\min}$ when the electric field vanishes ($E = 0$).

To obtain the expression for the maximum electric field E_{\max} in terms of the ion mass density n_{ion} and n_{\max} , the maximum proper number density of electrons, we write the following stress-energy momentum tensor T for an axially symmetric waterbag-distributed electron fluid from the definitions (138) and (140),

$$T = mS_{\text{II}} = \rho \tilde{U} \otimes \tilde{U} + \xi(\tilde{U} \otimes \#_{\parallel} \tilde{U} + \#_{\parallel} \tilde{U} \otimes \tilde{U}) + p \#_{\parallel} \tilde{U} \otimes \#_{\parallel} \tilde{U} + T_{\perp}, \quad (189)$$

$$\rho = mS_{\text{II}}^{\hat{0}\hat{0}}, \quad (190)$$

$$p = mS_{\text{II}}^{\hat{3}\hat{3}}, \quad (191)$$

$$\xi = mS_{\text{II}}^{\hat{0}\hat{3}}, \quad (192)$$

$$T_{\perp} = mS^{\hat{1}\hat{2}} dx^1 \otimes dx^2 \quad (193)$$

where ξ is the heat flux, $\#_{\parallel}$ is the Hodge star operator for the space spanned by $\{\tilde{X}_{\hat{0}}, \tilde{X}_{\hat{3}}\}$, T_{\perp} stands for the projection of stress-energy momentum tensor on the

subspace of covariant tensors spanned by $\{dx^1, dx^2\}$, and the 2-D metric tensor $G = \{-1, 1\}$ is just the pull back of the 4-D metric tensor g of the base manifold \mathcal{M} . For axially symmetric waterbags (about \dot{x}^3), the only non-zero contribution to the heat flux ξ in (189) comes from an integral of $\dot{x}^0 \dot{x}^3$, i.e., formula (100), which vanishes further for the ellipsoid waterbag obtained in equation (122). Equation (189) is satisfied for both 3-D and 1-D waterbag cases if we take $T_{\perp} = 0$ for the 1-D case.

We now consider the total stress-energy momentum tensor $T_{\text{total}} = T + T_{\text{ion}} + T_{\mathcal{EM}}$. Considering no energy input or output in the system we are dealing with, the total stress-energy momentum tensor T_{total} satisfies the following non-divergence equation,

$$\begin{aligned} 0 = \nabla \cdot T_{\text{total}} &= \nabla \cdot (T + T_{\text{ion}} + T_{\mathcal{EM}}) \\ &= \nabla \cdot (T + T_{\text{ion}}) - \iota_{(qnU + qn_{\text{ion}}U_{\text{ion}})} F, \end{aligned} \quad (194)$$

where the following equality (proved in pages 155-159 of [61])

$$\star[T_{\mathcal{EM}}(X_a, -)] = \tau_{a\mathcal{EM}} = \frac{1}{2}(\iota_{X_a} F \wedge \star F - F \wedge \iota_{X_a} \star F), \quad (195)$$

on stress energy 3-form $\tau_{a\mathcal{EM}}$ has been used in the last step of equation (194).

Since the stress-energy momentum tensor T for electrons is independent from n_{ion} , we get that

$$\nabla \cdot T = qn\iota_U F. \quad (196)$$

We then introduce a Killing vector field K and the stress form

$$\tau_K \equiv \star[T(K, -)], \quad (197)$$

which satisfies

$$d\tau_K = qn(\iota_K \iota_U F) \star 1, \quad (198)$$

because of equation (196).

To solve equation (198), we rewrite the velocity vector U in the following form

$$U = \gamma_u(\partial_0 + u\partial_3) , \quad (199)$$

where

$$\gamma_u = \frac{1}{\sqrt{1-u^2}} , \quad (200)$$

and $u = u(\zeta)$ with $\zeta = x^3 - vx^0$.

We then write the left side of equation (198) as

$$d\tau_K = \{(\rho + p)\gamma_u^2(v - u)(1 - uv) - \xi\gamma_u^2[(v - u)^2 + (1 - uv)^2]\}' \star 1 , \quad (201)$$

and its right side as

$$qn\iota_K\iota_U F \star 1 = qn\gamma_u(v - u)E \star 1 . \quad (202)$$

Equating the above two equations leads to that

$$\begin{aligned} qn_{\text{ion}}vE &= qn\gamma_u(v - u)E \\ &= \{(\rho + p)\gamma_u^2(v - u)(1 - uv) - \xi\gamma_u^2[(v - u)^2 + (1 - uv)^2]\}' . \end{aligned} \quad (203)$$

In the ultra-relativistic limit $v \rightarrow 1$, equation (203) becomes

$$qn_{\text{ion}}E = \left[(\rho + p - 2\xi) \frac{1-u}{1+u} \right]' . \quad (204)$$

Simultaneously, Maxwell equation (12) lead to

$$E' = qn_{\text{ion}} \frac{u}{1-u} . \quad (205)$$

By multiplying equation (204) with equation (205) and integrating the result with respect to ζ , we have

$$\int d(E^2) = \int d \left[(\rho + p - 2\xi) - n_{\text{ion}}^2 \frac{\rho + p - 2\xi}{n^2} \right] - \int \frac{2(\rho + p - 2\xi)}{n} dn . \quad (206)$$

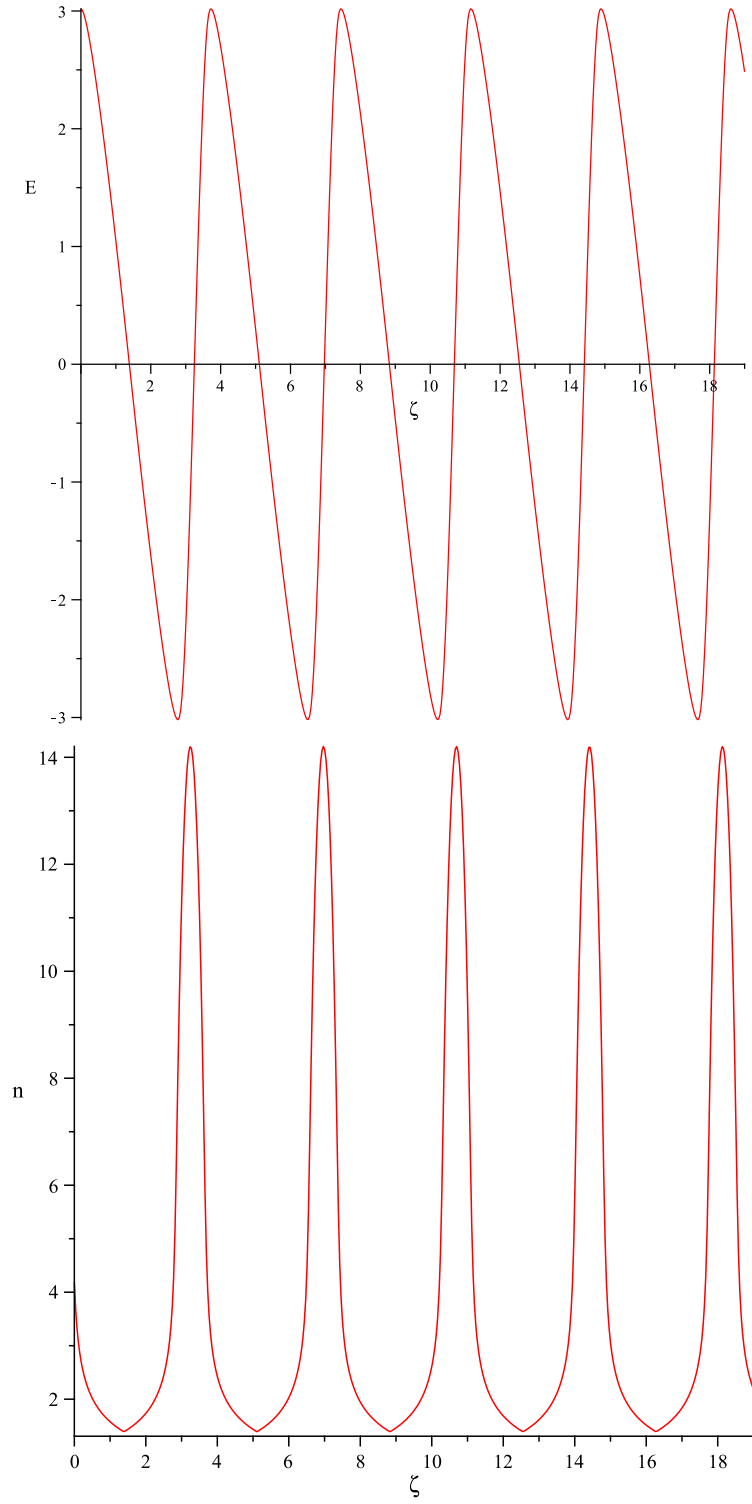


FIG. 5: E and n with respect to ζ (the upper one is E and the lower one is n , and the parameters are chosen as $n_{\text{ion}} = \frac{8\pi}{3}$, $m = 1$, $R = 1$, $\alpha = 2$, $q = 1$, $v = 0.99$)

The behaviour of the electrostatic oscillation is demonstrated in Fig. 5. Compared with a cold plasma that has its proper mass density $\rho = n$, pressure $p = 0$ and the maximum possible value of the proper number density $n_{\max} = \infty$, waterbag-distributed plasmas have non-zero pressure p and finite maximum proper number density n_{\max} . Further calculation illustrated by Fig. 5 shows that $E = -E_{\max}$ when $n = n_{\text{ion}}$ and $E = 0$ when $n = n_{\max}$. Hence, we obtain the following expression for E_{\max} ,

$$E_{\max}^2 = \left[-(\rho + p - 2\xi) + n_{\text{ion}}^2 \frac{\rho + p - 2\xi}{n^2} \right] \Big|_{n_{\text{ion}}}^{n_{\max}} + \int_{n_{\text{ion}}}^{n_{\max}} \frac{2(\rho + p - 2\xi)}{n} dn \quad (207)$$

Wave-breaking limits appear when electrostatic oscillations have large amplitudes and as a result, the maximum proper number density $n_{\max} \rightarrow \infty$. Thus, we are interested in the maximum value of electric fields when $n_{\max} \rightarrow \infty$.

For a 1-D waterbag, the EOS is

$$\begin{aligned} \rho &= m\alpha \left[\frac{n}{2\alpha} \sqrt{1 + \left(\frac{n}{2\alpha}\right)^2} + \sinh^{-1} \left(\frac{n}{2\alpha}\right) \right] \\ &\approx m\alpha \left[\frac{n}{2\alpha} \left(\frac{n}{2\alpha} + \frac{\alpha}{n}\right) + \ln \left(\frac{n}{2\alpha}\right) + \ln 2 \right] \\ &= \frac{mn^2}{4\alpha} + \frac{m\alpha}{2} + \ln \left(\frac{n}{2\alpha}\right) + \ln 2, \end{aligned} \quad (208)$$

$$\begin{aligned} p &= m\alpha \left[\frac{n}{2\alpha} \sqrt{1 + \left(\frac{n}{2\alpha}\right)^2} - \sinh^{-1} \left(\frac{n}{2\alpha}\right) \right] \\ &\approx m\alpha \left[\frac{n}{2\alpha} \left(\frac{n}{2\alpha} + \frac{\alpha}{n}\right) - \ln \left(\frac{n}{2\alpha}\right) - \ln 2 \right] \\ &= \frac{mn^2}{4\alpha} + \frac{m\alpha}{2} - \ln \left(\frac{n}{2\alpha}\right) - \ln 2 \end{aligned} \quad (209)$$

$$\xi = 0, \quad (210)$$

so $\rho + p - 2\xi = \frac{mn^2}{2\alpha} + m\alpha$ and the maximum electric field is

$$\begin{aligned}
E_{\max}^2 &= \left[-(\rho + p - 2\xi) + n_{\text{ion}}^2 \frac{\rho + p - 2\xi}{n^2} \right] \Big|_{n_{\text{ion}}}^{n_{\max}} + \int_{n_{\text{ion}}}^{n_{\max}} \frac{2(\rho + p - 2\xi)}{n} dn \\
&\approx -\frac{m}{2\alpha}(n_{\max}^2 - n_{\text{ion}}^2) - m\alpha + m\alpha \frac{n_{\text{ion}}^2}{n_{\max}^2} \\
&\quad + \frac{m}{2\alpha}(n_{\max}^2 - n_{\text{ion}}^2) + 2m\alpha(\ln n_{\max} - \ln n_{\text{ion}}) \\
&\approx m\alpha \ln \frac{n_{\max}^2}{n_{\text{ion}}^2} - m\alpha + m\alpha \frac{n_{\text{ion}}^2}{n_{\max}^2} .
\end{aligned} \tag{211}$$

In the case of the 3-D ellipsoid waterbag, the zero component (122) leads to a zero heat flux

$$\xi = 0 . \tag{212}$$

To obtain the expression for $\rho + p$ with respect to n , we expand the expressions of ρ and p in equations (181) and (183) about a large l ($l \gg 1$) as follows,

$$\begin{aligned}
\rho &= m\pi\alpha R^4 \left[\left(\frac{l}{2} - \frac{1}{4l} \right) \sqrt{1+l^2} + \left(1 + \frac{1}{4l^2} \right) \sinh^{-1} l \right] \\
&\approx m\pi\alpha R^4 \left[\left(\frac{l^2}{2} - \frac{3}{16l^2} + \frac{1}{16l^4} \right) + \left(\ln l + \ln 2 + \frac{1}{4l^2} + \frac{\ln l + \ln 2}{4l^2} - \frac{1}{32l^4} \right) \right] ,
\end{aligned} \tag{213}$$

$$\begin{aligned}
p &= m\pi\alpha R^4 \left[\left(\frac{l}{2} + \frac{3}{4l} \right) \sqrt{1+l^2} - \left(1 + \frac{3}{4l^2} \right) \sinh^{-1} l \right] \\
&\approx m\pi\alpha R^4 \left[\left(\frac{l^2}{2} + 1 + \frac{5}{16l^2} - \frac{1}{16l^4} \right) - \left(\ln l + \ln 2 + \frac{1}{4l^2} + \frac{3\ln l + 3\ln 2}{4l^2} + \frac{3}{32l^4} \right) \right] .
\end{aligned} \tag{214}$$

With

$$l = \frac{3n}{4\pi\alpha R^2} , \tag{215}$$

it can be seen from equation (179) that we get the following maximum electric field for the 3-D ellipsoid waterbag-distributed electron fluid,

$$\begin{aligned}
E_{\max}^2 &= \left[-(\rho + p - 2\xi) + n_{\text{ion}}^2 \frac{\rho + p - 2\xi}{n^2} \right] \Big|_{n_{\text{ion}}}^{n_{\max}} + \int_{n_{\text{ion}}}^{n_{\max}} \frac{2(\rho + p - 2\xi)}{n} dn \\
&\approx m\pi\alpha R^4 \ln \frac{n_{\max}^2}{n_{\text{ion}}^2} - m\pi\alpha R^4 - \frac{8}{9} m\pi^3 \alpha^3 R^8 \frac{\ln n_{\text{ion}}}{n_{\text{ion}}^2} + \frac{8}{9} m\pi^3 \alpha^3 R^8 \frac{\ln n_{\max}}{n_{\max}^2} \\
&\quad + m\pi\alpha R^4 \frac{n_{\text{ion}}^2}{n_{\max}^2}. \tag{216}
\end{aligned}$$

The EOS for 3-D gourd waterbag differs as it has a non-zero heat flux ξ . By evaluating the moment integrals using a numerical method with Maple, we get the following EOS for a large n ,

$$\rho + p - 2\xi \approx \frac{mn^2b}{n_{\text{ion}}} \left(1 + 8e^{-\frac{2}{3}\frac{n^2b^2}{n_{\text{ion}}^2} - \frac{5}{2}} \right) + \frac{13}{b} mn_{\text{ion}} e^{-\frac{2}{3}\frac{n^2b^2}{n_{\text{ion}}^2} - \frac{5}{2}}, \tag{217}$$

where $b = \frac{5k_B T_{\parallel\text{eq}}}{m}$ is a dimensionless constant, which can be checked from the definition of $T_{\parallel\text{eq}}$ in equation (66). We then get the following maximum electric field

$$\begin{aligned}
E_{\max}^2 &= \left[-(\rho + p - 2\xi) + n_{\text{ion}}^2 \frac{\rho + p - 2\xi}{n^2} \right] \Big|_{n_{\text{ion}}}^{n_{\max}} + \int_{n_{\text{ion}}}^{n_{\max}} \frac{2(\rho + p - 2\xi)}{n} dn \\
&\approx \frac{2mn_{\text{ion}}}{b\varepsilon_0} \left(6 + \frac{13}{b} \right) e^{-\frac{2}{3}\frac{n^2b^2}{n_{\text{ion}}^2} - \frac{5}{2}} - \frac{8bmn_{\max}^2}{\varepsilon_0 n_{\text{ion}}} e^{-\frac{2}{3}\frac{n_{\max}^2b^2}{n_{\text{ion}}^2} - \frac{5}{2}} \\
&\quad + \frac{mn_{\text{ion}}}{\varepsilon_0} \left(8b - \frac{25}{b} \right) e^{-\frac{2}{3}\frac{n_{\max}^2b^2}{n_{\text{ion}}^2} - \frac{5}{2}} + \frac{13mn_{\text{ion}}^3}{b\varepsilon_0 n_{\max}^2} e^{-\frac{2}{3}\frac{n_{\max}^2b^2}{n_{\text{ion}}^2} - \frac{5}{2}} \\
&\approx \frac{2mn_{\text{ion}}}{b\varepsilon_0} \left(6 + \frac{13}{b} \right) e^{-\frac{2}{3}\frac{n^2b^2}{n_{\text{ion}}^2} - \frac{5}{2}} + O\left(e^{-\frac{2}{3}\frac{n_{\max}^2b^2}{n_{\text{ion}}^2} - \frac{5}{2}} \right). \tag{218}
\end{aligned}$$

By checking the dominant terms in equations (211)-(218), we see that when $n_{\max} \rightarrow \infty$, a 1-D waterbag or a 3-D ellipsoid waterbag-distributed electron fluid does not have a maximum wave-breaking limit (i.e. $E_{\max} \rightarrow \infty$), while the wave-breaking limit E_{\max} is finite for a 3-D gourd distributed electron fluid. As stated in Section ID, a 1-D waterbag or a 3-D ellipsoid waterbag model shows its merit in working well in a larger possible region than a 3-D gourd waterbag model.

3. *Trapped Particles*

As stated in Section ID, once an oscillating particle is trapped, the particle will not continue to go back and forth any more and will be accelerated by the wave. Section ID suggests that a considerable fraction of trapped particles required by experiments will cause a large energy shift from electric fields of the wave to the trapped particles. As a result, there seems to be a higher probability for a 1-D or a 3-D ellipsoid waterbag, rather than a 3-D gourd waterbag, to allow the existence of a stronger electric field for supporting considerable fractions of trapped particles.

It should be noted that the 3-D ellipsoid waterbag is a solution to (lower order) moment equations, but not to the Vlasov equation (87), whereas the 1-D waterbag and 3-D gourd waterbag are solutions to the Vlasov equation (87) [6]. The comparison of different waterbags shows that the 1-D waterbag owns the merits of being a solution to the Vlasov equation and having a stronger electric field for supporting a considerable fraction of trapped particles.

Additionally, we can draw some conclusions for more generally distributed electron fluids by tracing the origin of the infinity of the maximum electric field from equations (207), (211), (216). We find that the n^2 terms in the $\rho+p-2\xi$ cancel each other between the first and the second terms on the right side of equation (207). The integral or summation of the next order term, namely, the constant term in $\rho+p-2\xi$, contributes to a $\ln n_{\max}$ term that diverges when $n_{\max} \rightarrow \infty$. A general calculation shows that, for any EOS $\rho+p-2\xi$ consisting of $C_1 n^2 + C_2 + O(C_2)$ (with C_1, C_2 constants), the leading term of the maximum electric field (when $n_{\max} \rightarrow \infty$) will be proportional to $C_2 \ln n_{\max}$, which tends to infinity and is likely to accelerate considerable fractions of trapped particles. Here we see that the 3-D gourd waterbag is a special case with $C_2 = 0$, which, for an arbitrary initial distribution, can only be for some special reason or a choice of fine-tuning.

Therefore, we could postulate that a considerable fraction of trapped particles are allowed for an arbitrary initial condition with its EOS $\rho + p - 2\xi$ leading to a form $C_1 n^2 + C_2 + O(C_2)$.

4. *The Fraction of the Trapped Particles in the 3-D Ellipsoid Waterbag-Distributed Fluid*

We now go back to the 3-D ellipsoid waterbag-distributed fluid due to its advantage of having the analytical expressions (120)-(133) of the moments in terms of the length of the waterbag l . With these analytical expressions, we are able to calculate the relative velocities of the wave with respect to the bulk motion of fluid. This enables us to obtain the fraction of the trapped particles among all the particles in the fluid. The reason is that the fraction of trapped particles is just the fraction of the geometric volume of the ellipsoid head cut by the wave over the volume of the whole waterbag ellipsoid. The details are shown in the rest of this subsection (here terms “fluid”, “waterbag” and “axes of waterbag” are used to refer to the same object).

We now observe the following 4-velocity of the wave with its phase speed v in the ion (or lab) frame,

$$W = \frac{1}{\sqrt{1-v^2}} \left(\frac{\partial}{\partial x^0} + v \frac{\partial}{\partial x^3} \right). \quad (219)$$

In order to understand how fast the wave travels with respect to the bulk motion of fluid (along \hat{x}^3 in the fiber space), we calculate the velocity vector pointing from the axial center of the waterbag to the wave.

The unit vector $X_{\hat{3}}$ points along $\frac{\partial}{\partial x^3}$ and lies in the instantaneous rest frame of a field of observers with 4-velocity $V = X_{\hat{0}}$, i.e. a fields of observers adapted to the bulk motion of the fluid. The vector field $X_{\hat{3}}$, defined in (138), is written explicitly as,

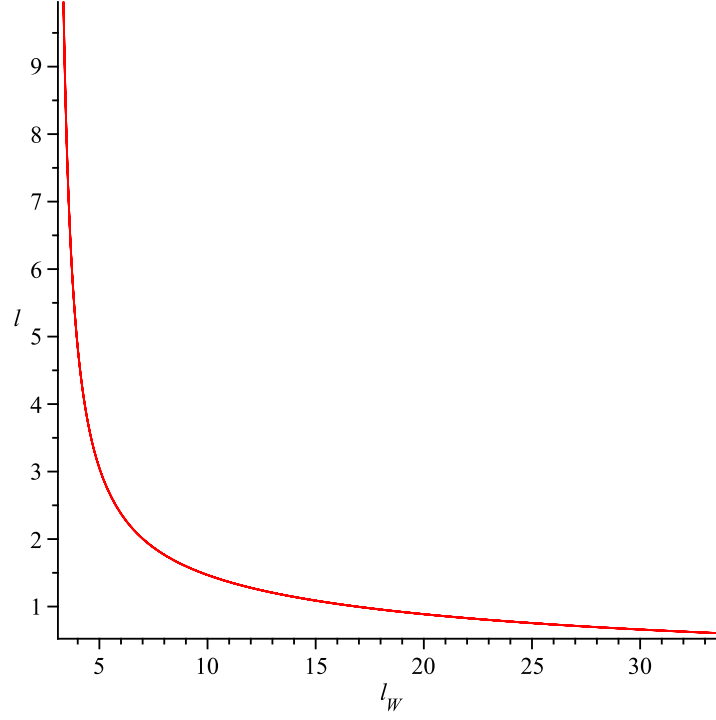


FIG. 6: The relation between l and l_W (the parameters are chosen as $n_{\text{ion}} = \frac{8\pi}{3}$, $m = 1$, $R = 1$, $\alpha = 2$, $q = 1$, $v = 0.99$)

$$X_{\hat{3}} = V^3 \frac{\partial}{\partial x^0} + V^0 \frac{\partial}{\partial x^3} . \quad (220)$$

Then the proper velocity $l_W(\zeta)$ of the wave observed from the bulk of fluid is expressed as follows,

$$\begin{aligned} l_W(\zeta) &= g(W, X_{\hat{3}}) \\ &= \gamma(vV^0 - V^3) . \end{aligned} \quad (221)$$

Obviously, the condition $l_W \leq l$ indicates the existence of the "trapped particles". And when the phenomenon "particle-trapping" exist, the value of $l - l_W$ suggests the height of the upper part of the waterbag, which represents the trapped part of the particles.

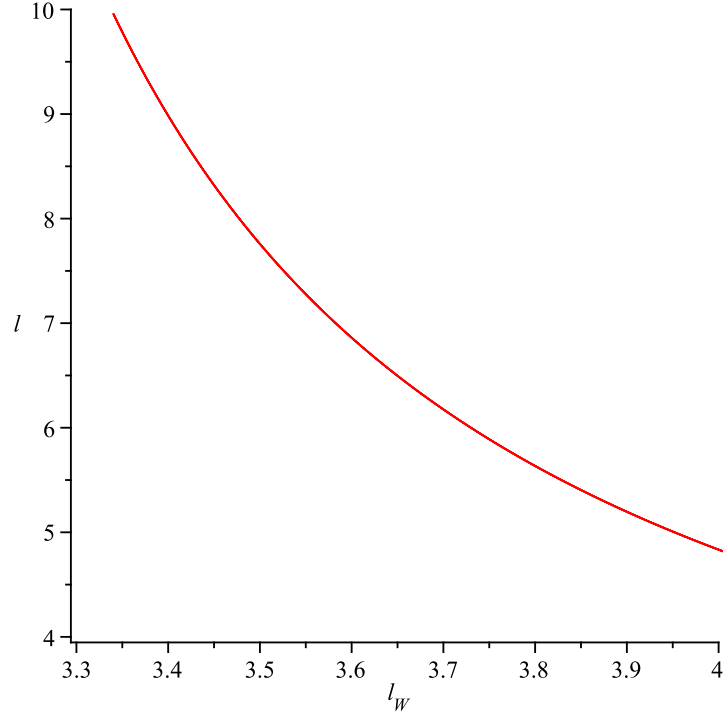


FIG. 7: The relation between l and l_W when $l_W < l$ (the parameters are chosen as $n_{\text{ion}} = \frac{8\pi}{3}$, $m = 1$, $R = 1$, $\alpha = 2$, $q = 1$, $v = 0.99$)

It should be noted that l and l_W depend on ζ . Further calculation illustrated by Fig. 6 shows that l_W monotonously decays with respect to l . The narrow region on the left of Fig. 6 (where $l_W < l$) shows the presence of trapped particles whereas the region on the right of Fig. 6 (where $l_W > l$) indicates the absence of trapped particles. When there are trapped particles, we stretch the narrow region on the left for a closer sight of the relation between l_W and l (shown in Fig. 7).

Concerning the relation between l and l_W , we obtain the fraction of trapped particles over the whole waterbag by calculating the geometric volume of the upper part of the waterbag (over the volume of the whole waterbag $\frac{4}{3}\pi R^2 l$). Considering $l \gg R$, the volume fraction tends to the length fraction $\frac{l - l_W}{2l}$ for the part of the waterbag representing trapped particles. We plot the fraction of the trapped

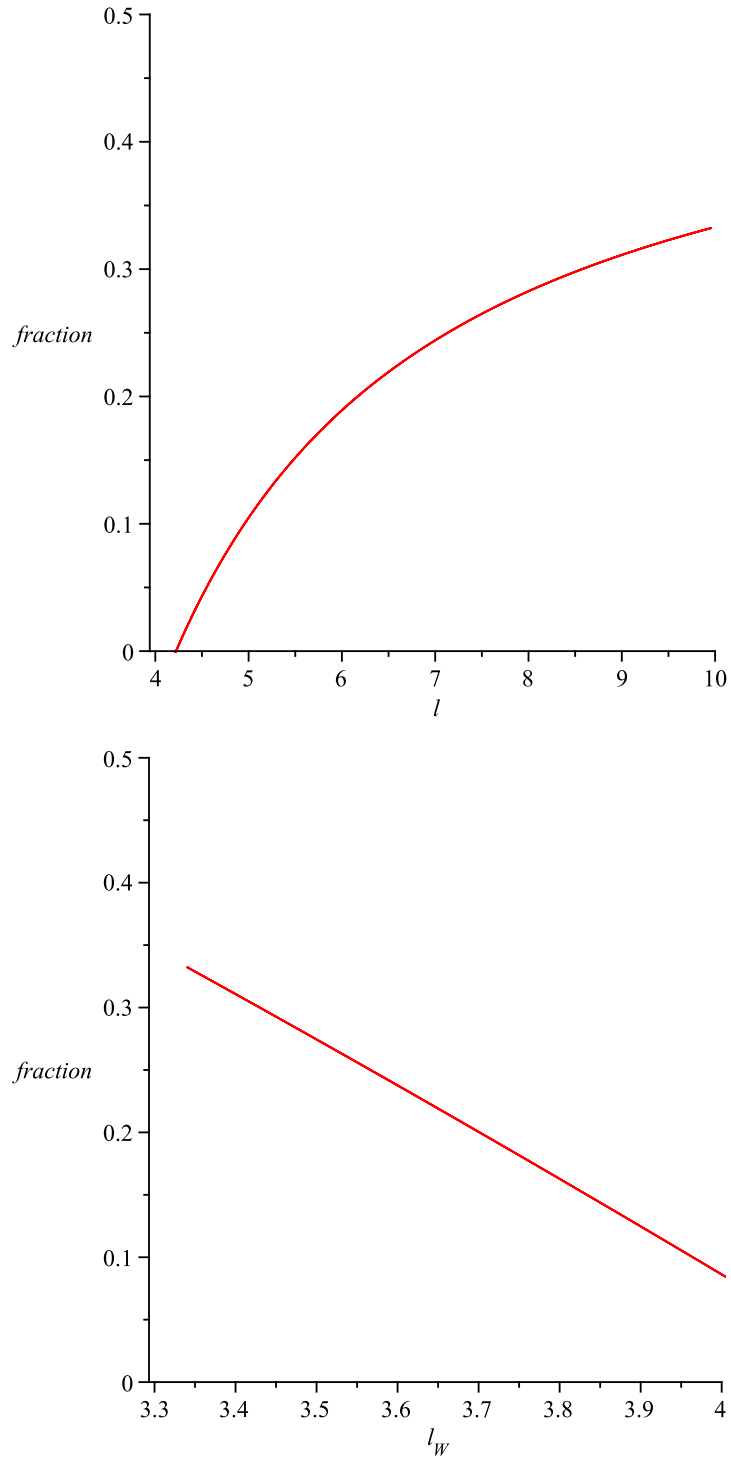


FIG. 8: The fraction of trapped particles with respect to l (upper) and l_W (lower) (the parameters are chosen as $n_{\text{ion}} = \frac{8\pi}{3}$, $m = 1$, $R = 1$, $\alpha = 2$, $q = 1$, $v = 0.99$)

particles $\frac{l - l_W}{2l}$ in Fig. 8, from which we see that the fraction grows with respect to l and decays with respect to l_W . Quantitative comparison shows the consistency between the fraction plotted in Fig. 8 and the fraction indicated from the $l - l_W$ relations in Fig. 6 and Fig. 7.

IV. A BRIEF EXPLORATION OF A QUANTUM PLASMA

Investigations of low temperature and high density plasmas, may require understanding the concept of a quantum plasma, which was first studied in the 1960's by Pines [68] [69].

We adopt the phenomenological approach recently introduced by Eliasson and Shukla [71] and represent the electron fluid using a complex scalar field Ψ . This model attempts to capture the quantum interference of each electron with itself, but does not consider the interactions between electrons from a full quantum perspective, and therefore it is a semi-classical effective model only.

The Klein-Gordon equation with $\Psi = ae^{\frac{i}{\hbar}S}$ as the formal solution with the amplitude a and the phase factor S and U(1) field \mathcal{A} as its potential 1-form is:

$$\mathcal{D} \star \mathcal{D}\Psi = \frac{m^2}{\hbar^2} \Psi \star 1, \quad (222)$$

$$\mathcal{D} = d + \frac{i}{\hbar} q \mathcal{A}, \quad (223)$$

where m and q are the mass and charge of a scalar field particle.

The corresponding Maxwell equations is as follows,

$$d\mathcal{F} = 0, \quad (224)$$

$$d \star \mathcal{F} = qn_{\text{ion}} \star \tilde{V}_{\text{ion}} - \text{Im}(\bar{\Psi} \star \mathcal{D}\Psi), \quad (225)$$

where $\mathcal{F} = d\mathcal{A}$.

We now carry out $\mathcal{D} \star \mathcal{D}$ on the above formal solution Ψ :

$$\mathcal{D}\Psi = e^{\frac{i}{\hbar}S} da + \frac{i}{\hbar}\Psi dS + \frac{i}{\hbar}\Psi q\mathcal{A}, \quad (226)$$

$$\star \mathcal{D}\Psi = e^{\frac{i}{\hbar}S} \star da + \frac{i}{\hbar}\Psi \star dS + \frac{i}{\hbar}\Psi \star (q\mathcal{A}), \quad (227)$$

$$\begin{aligned} \mathcal{D} \star \mathcal{D}\Psi &= \frac{i}{\hbar} e^{\frac{i}{\hbar}S} dS \wedge \star da + e^{\frac{i}{\hbar}S} d \star da + \frac{i}{\hbar} e^{\frac{i}{\hbar}S} da \wedge \star dS - \frac{1}{\hbar^2} \Psi dS \wedge \star dS + \frac{i}{\hbar} \Psi d \star dS \\ &\quad + \frac{i}{\hbar} e^{\frac{i}{\hbar}S} da \wedge \star (q\mathcal{A}) - \frac{1}{\hbar^2} \Psi dS \wedge \star (q\mathcal{A}) + \frac{i}{\hbar} \Psi d \star (q\mathcal{A}) \\ &\quad + \frac{i}{\hbar} e^{\frac{i}{\hbar}S} q\mathcal{A} \wedge \star da - \frac{1}{\hbar^2} \Psi q\mathcal{A} \wedge \star dS - \frac{1}{\hbar^2} \Psi q\mathcal{A} \wedge \star (q\mathcal{A}) \\ &= \left(\frac{2i}{\hbar} e^{\frac{i}{\hbar}S} da \cdot dS - e^{\frac{i}{\hbar}S} \delta da - \frac{1}{\hbar^2} \Psi dS \cdot dS - \frac{i}{\hbar} \Psi \delta dS \right. \\ &\quad \left. + \frac{2i}{\hbar} e^{\frac{i}{\hbar}S} da \cdot (q\mathcal{A}) - \frac{2}{\hbar^2} \Psi dS \cdot (q\mathcal{A}) - \frac{i}{\hbar} \Psi \delta (q\mathcal{A}) - \frac{1}{\hbar^2} \Psi (q\mathcal{A}) \cdot (q\mathcal{A}) \right) \star 1, \end{aligned} \quad (228)$$

where the operator $\delta = \star d \star$ and the notation \cdot represents the inner multiplication with respect to the metric g so that

$$da \cdot (q\mathcal{A}) = g^{-1}(da, q\mathcal{A}). \quad (229)$$

Comparing the real part and the imaginary part of Klein-Gordon equation separately we get:

$$m^2 + \hbar^2 a^{-1} \delta da + (dS + q\mathcal{A}) \cdot (dS + q\mathcal{A}) = 0, \quad (230)$$

$$2da \cdot dS + 2da \cdot (q\mathcal{A}) - a\delta dS - a\delta(q\mathcal{A}) = 0. \quad (231)$$

Again we will explore non-linear electrostatic oscillations. Let

$$\tilde{V} = f(dS + q\mathcal{A}), \quad (232)$$

where f is defined so that $g(V, V) = -1$, then it becomes

$$m^2 + \hbar^2 a^{-1} \delta da + \frac{\tilde{V}}{f} \cdot \frac{\tilde{V}}{f} = 0, \quad (233)$$

$$2da \cdot \frac{\tilde{V}}{f} - a\delta \frac{\tilde{V}}{f} = 0. \quad (234)$$

We get f by:

$$\begin{aligned} g(\tilde{V}, \tilde{V}) &= f^2(dS + q\mathcal{A}) \cdot (dS + q\mathcal{A}) = -1, \\ f &= (m^2 + \hbar^2 a^{-1} \delta da)^{-\frac{1}{2}}, \end{aligned} \quad (235)$$

then

$$\begin{aligned} \nabla_V \tilde{V} &= i_V d\tilde{V} - \frac{1}{2} dg(V, V) \\ &= i_V d\tilde{V} \\ &= i_V df \wedge \left(\frac{\tilde{V}}{f}\right) + f i_V d(q\mathcal{A}). \end{aligned} \quad (236)$$

Equations (232) and (236) lead to

$$d\tilde{V} = df \wedge \left(\frac{\tilde{V}}{f}\right) + f d(q\mathcal{A}). \quad (237)$$

To solve the system, we write equation (237) in a particular frame (e^1, e^2) , where $e^1 = dx^0 - v dx^3$ and $e^2 = dx^3 - v dx^0$. We then seek travelling wave solution by assuming all the physical quantities a , \mathcal{F} , V depend on $\zeta = x^3 - vx^0$ only. Thus, $\mathcal{F} = E dx^0 \wedge dx^3$ and $\delta da = -(1-v^2)a'' = -\gamma^{-2}a''$, where the Lorentz factor $\gamma = \frac{1}{\sqrt{1-v^2}}$. Hence, formula (235) is written explicitly as,

$$f = \frac{1}{\sqrt{m^2 - \frac{\hbar^2 a''}{\gamma^2 a}}}. \quad (238)$$

In a spacetime manifold with the Minkowski metric, we assume $\tilde{V}(\zeta) = \mu e^1 - \sqrt{\mu^2 - \gamma^2} e^2$, where $\mu = \mu(\zeta)$. Then the left side of the above equation (237) is written as

$$\begin{aligned} d\tilde{V} &= \mu' e^2 \wedge e^1 \\ &= \mu' \gamma^{-2} dx^0 \wedge dx^3, \end{aligned} \quad (239)$$

and the right side of (237)

$$\begin{aligned} df \wedge \left(\frac{\tilde{V}}{f}\right) + f d(q\mathcal{A}) &= f' e^2 \wedge \frac{1}{f} \mu e^1 + f q E dx^0 \wedge dx^3 \\ &= \left[f q E + \frac{f'}{f} \mu \gamma^{-2} \right] dx^0 \wedge dx^3, \end{aligned} \quad (240)$$

from which we get an expression for E in terms of μ and μ' as

$$\begin{aligned} E &= \frac{\mu'}{q\gamma^2 f} + \frac{f'\mu}{q\gamma^2 f^2} \\ &= \frac{1}{q\gamma^2} \left(\frac{\mu}{f} \right)' . \end{aligned} \quad (241)$$

We now try to solve the Maxwell equations (224) and (225). Since \mathcal{F} is a 2-form on subspace of forms on spacetime spanned by $\{dx^0, dx^3\}$, and furthermore, \mathcal{F} depends on ζ only, equation (224) is satisfied automatically. The left side of equation (225) reads

$$\begin{aligned} d \star (\mathcal{F} &= d \star E dx^0 \wedge dx^3) \\ &= -E' e^2 \wedge \#_{\perp} 1 , \end{aligned} \quad (242)$$

where

$$\#_{\perp} 1 = dx^1 \wedge dx^2 . \quad (243)$$

The right side of equation (225) reads

$$\begin{aligned} &qn_{\text{ion}} \star \tilde{V}_{\text{ion}} - \text{Im}(\bar{\Psi} \star \mathcal{D}\Psi) \\ &= [qn_{\text{ion}}\gamma^2(e^2 - ve^1) - \frac{|a|^2}{\hbar}(m^2 + \hbar^2 a^{-1} \delta da)^{\frac{1}{2}}(\mu e^2 - \sqrt{\mu^2 - \gamma^2} e^1)] \#_{\perp} 1 \end{aligned} \quad (244)$$

By comparing the e^2 and e^1 components of the above equations (242) and (244) we get the following ODE system

$$-E' = qn_{\text{ion}}\gamma^2 - \frac{|a|^2}{\hbar f} \mu , \quad (245)$$

$$0 = -qn_{\text{ion}}\gamma^2 v + \frac{|a|^2}{\hbar f} \sqrt{\mu^2 - \gamma^2} . \quad (246)$$

The ODE system consisting of equations (241), (245) and (246) expresses the behaviour of the nonlinear electrostatic oscillations of a quantum plasma.

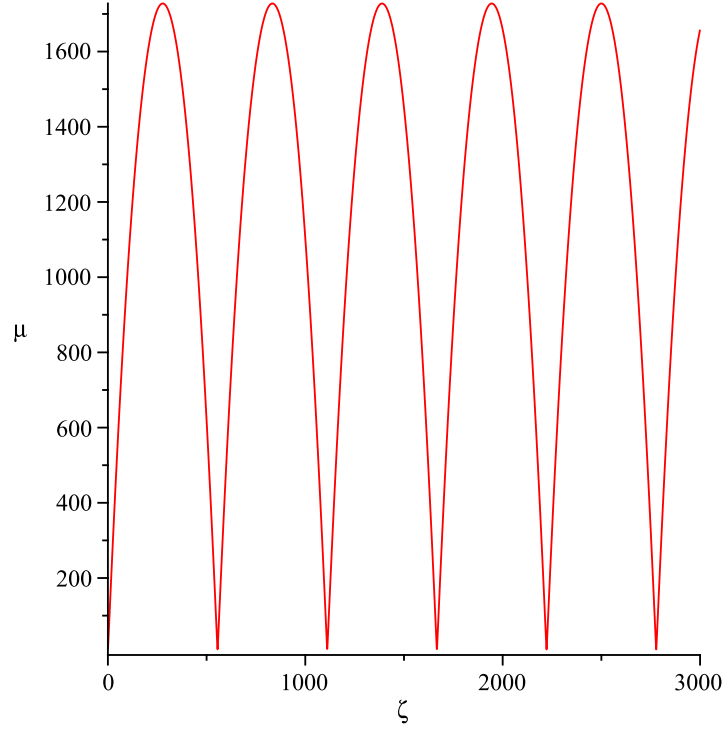


FIG. 9: The relation between μ and ζ when $\hbar = 0$ (where the parameters are chosen as $m = 1$, $q = 0.01$, $n = 9$)

In the classical limit $\hbar \rightarrow 0$, we have $f \propto \frac{1}{m}$ and $f' \propto O(\hbar)$. The field system then reduces to the classical Maxwell-Lorentz system (11), (12), (37) and (38). A solution to the corresponding ODE system which describes electrostatic waves is shown in Fig. 9. Hence the result for the wave-breaking limit is [29]

$$E_{\max}^M = \frac{m\omega_{pe}c}{|q|} \sqrt{2(\gamma - 1)}, \quad (247)$$

where the plasma electron frequency ω_{pe} is

$$\omega_{pe} = \sqrt{\frac{q^2 n_{\text{ion}}}{m\varepsilon_0}}. \quad (248)$$

For a quantum plasma, from equation (246) we get

$$\frac{|a|^2}{\hbar f} = \frac{qn_{\text{ion}}\gamma^2 v}{\sqrt{\mu^2 - \gamma^2}}, \quad (249)$$

or

$$\frac{1}{f} = \frac{\hbar q n_{\text{ion}} \gamma^2 v}{a^2 \sqrt{\mu^2 - \gamma^2}}, \quad (250)$$

where $a^2 = |a|^2$ as $a(\zeta)$ is a real function. By substituting the expression (249) into (245) we find that the Maxwell equation (225) turns out to be

$$E' = q n_{\text{ion}} \gamma^2 \left(\frac{v \mu}{\sqrt{\mu^2 - \gamma^2}} - 1 \right). \quad (251)$$

Similarly, substituting the expression (250) into (240) leads to an electric field E of the form

$$\begin{aligned} E &= \frac{1}{q \gamma^2} \left(\frac{\hbar q n_{\text{ion}} \gamma^2 v \mu}{a^2 \sqrt{\mu^2 - \gamma^2}} \right)' \\ &= \hbar n_{\text{ion}} \left(\frac{v \mu}{a^2 \sqrt{\mu^2 - \gamma^2}} \right)'. \end{aligned} \quad (252)$$

By letting $\nu = \frac{\mu}{m f}$ and considering formulae (238) and (250), we rewrite equations (251) and (252) as follows,

$$E' = q n_{\text{ion}} \gamma^2 \left(\frac{v \nu}{\sqrt{\nu^2 - \frac{\gamma^2}{m^2 f^2}}} - 1 \right), \quad (253)$$

$$E = \frac{m}{q \gamma^2} \nu'. \quad (254)$$

For clarity, we now restore the dependence of the physical quantities on ζ explicitly and summarize the final ODE system to be solved as follows,

$$E(\zeta)' = q n_{\text{ion}} \gamma^2 \left(\frac{v \nu(\zeta)}{\sqrt{\nu(\zeta)^2 - \frac{\gamma^2}{m^2 f(\zeta)^2}}} - 1 \right), \quad (255)$$

$$E(\zeta) = \frac{m}{q \gamma^2} \nu(\zeta)', \quad (256)$$

$$\hbar q n_{\text{ion}} \gamma^2 v = m a(\zeta)^2 \sqrt{\nu(\zeta)^2 - \frac{\gamma^2}{m^2 f(\zeta)^2}}, \quad (257)$$

$$f(\zeta) = \frac{1}{\sqrt{m^2 - \frac{\hbar^2 a(\zeta)''}{\gamma^2 a(\zeta)}}}. \quad (258)$$

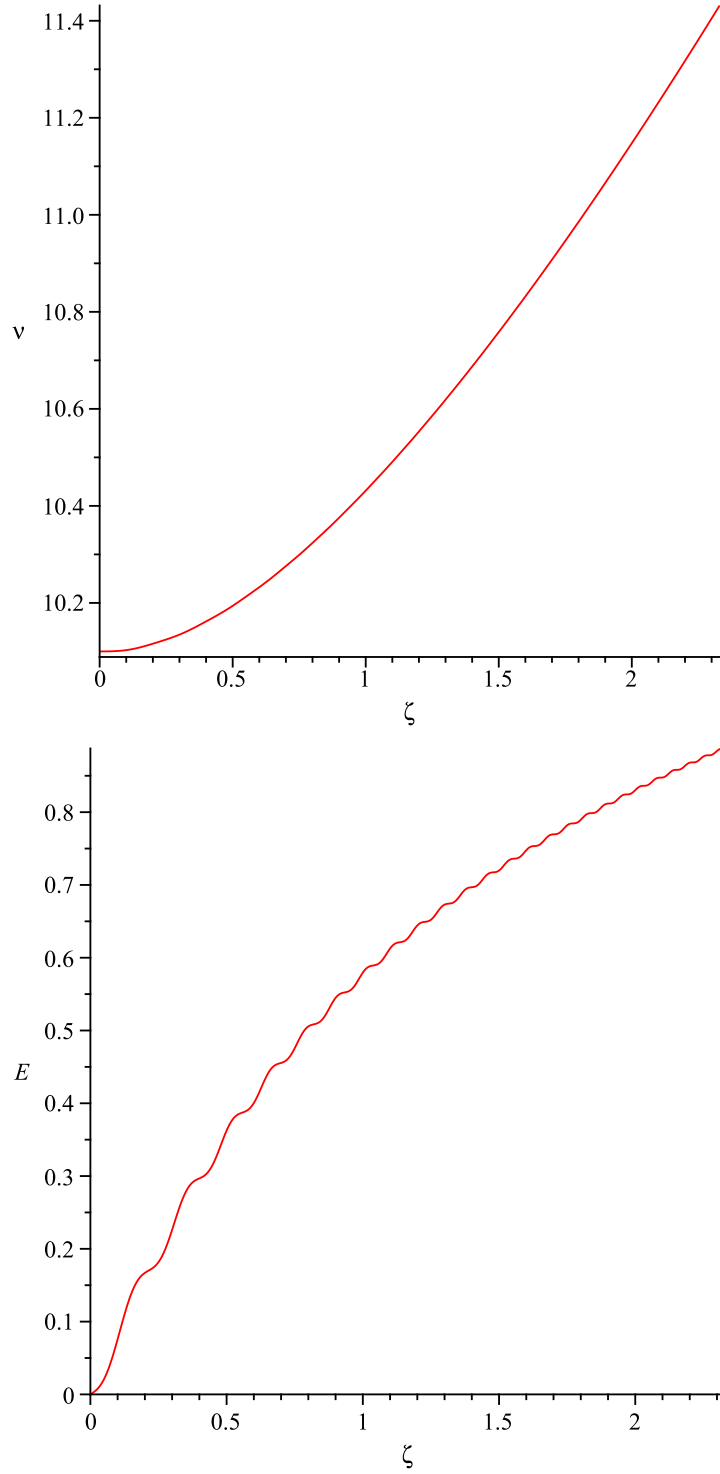


FIG. 10: ν (upper graph) and E (lower graph) with respect to ζ , respectively (where the parameters are chosen as: $m = 1$, $q = 0.001$, $n = 10$, $\hbar = 0.098$, $\gamma = 10$)

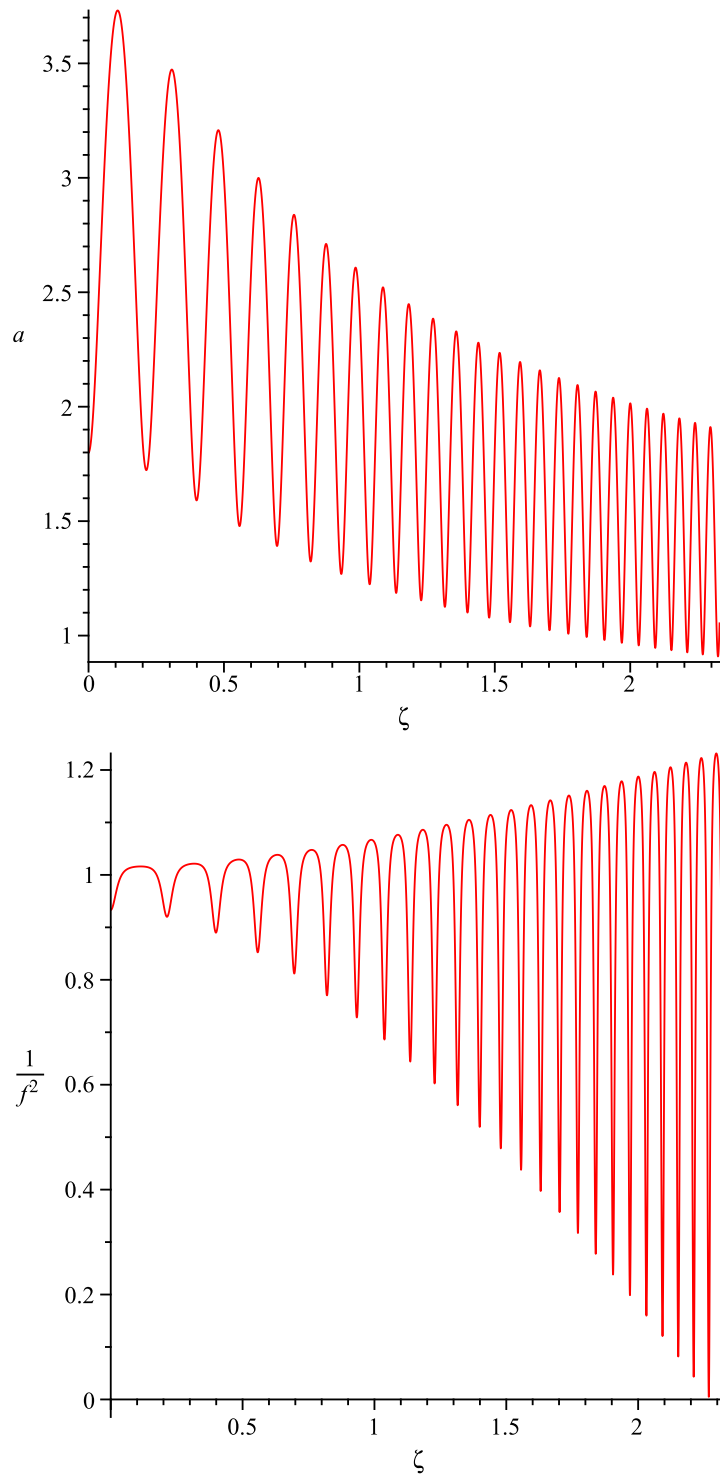


FIG. 11: a (upper graph) and $\frac{1}{f^2}$ (lower graph) with respect to ζ , respectively (where the parameters are chosen as: $m = 1$, $q = 0.001$, $n = 10$, $\hbar = 0.098$, $\gamma = 10$)

For a quantum plasma with $\hbar > 0$, it is not easy to obtain an analytical solution to the ODE system. Numerical calculation illustrated by the upper graph in Fig. 10 shows that $\nu(\zeta)$ monotonously grows until reaching a particular value at a certain ζ where the numerical integrator gives up. As a result, $E(\zeta)$ also monotonously grows and terminates (shown in the lower graph in Fig. 10). The reason that the integrator gives up is that as ζ increases, the oscillations of $a(\zeta)$ become increasingly faster (see the upper graph in Fig. 11) and $\frac{1}{f^2} \rightarrow 0$ (shown in the lower graph in Fig. 11). At present, it is not clear how to consistently calculate the maximum amplitude of electrostatic oscillations in this model.

V. BORN-INFELD PLASMAS

A. Wave-Breaking Limit and Period of a Maximum Electrostatic Oscillation

As stated in Section ID, the wave-breaking limit E_{\max} is the maximum electric field allowed in our model. The maximum electric field for a cold Born-Infeld plasma without external magnetic fields is obtained by Burton, et al [61]. Thus, we generalise their study to a magnetised cold Born-Infeld plasmas, where the external magnetic field B is constant.

We again consider a large amplitude electrostatic wave in a resting ion background ($V_{\text{ion}} = \frac{\partial}{\partial x^0}$) in a magnetised plasma with the constant external magnetic field B pointing in the x^3 direction. Again, we conveniently assume that all the physical quantities depend on

$$\zeta = x^3 - vx^0 \quad (259)$$

only (where v is the phase speed of the wave), and we choose the varying electric field and constant magnetic field to point along the positive or negative x^3 direction and restrict the electromagnetic field strength 2-form F as

$$F(\zeta) = E(\zeta)dx^0 \wedge dx^3 - Bdx^1 \wedge dx^2 . \quad (260)$$

As stated in Section IE, the excitation 2-form G is defined as

$$\star G = 2 \left(\frac{\partial \mathcal{L}}{\partial X} \star F + \frac{\partial \mathcal{L}}{\partial Y} F \right) , \quad (261)$$

and we write it explicitly below.

According to the definition of X and Y ((29) and (30)), we have

$$X(\zeta) = E(\zeta)^2 - B^2 \quad (262)$$

$$Y(\zeta) = 2BE(\zeta) , \quad (263)$$

which leads to

$$\begin{aligned}\mathcal{L} &= \frac{1}{\kappa^2} \left(1 - \sqrt{1 - \kappa^2 X - \frac{\kappa^4}{4} Y^2} \right) \\ &= \frac{1}{\kappa^2} (1 - \sqrt{1 + \kappa^2 B^2} \sqrt{1 - \kappa^2 E^2})\end{aligned}\quad (264)$$

$$\begin{aligned}\frac{\partial \mathcal{L}}{\partial X} &= \frac{1}{2} \frac{1}{\sqrt{1 - \kappa^2 X - \frac{\kappa^4}{4} Y^2}} \\ &= \frac{1}{2} \frac{1}{\sqrt{1 + \kappa^2 B^2}} \frac{1}{\sqrt{1 - \kappa^2 E^2}}\end{aligned}\quad (265)$$

$$\begin{aligned}\frac{\partial \mathcal{L}}{\partial Y} &= \frac{\kappa^2}{4} \frac{Y}{\sqrt{1 - \kappa^2 X - \frac{\kappa^4}{4} Y^2}} \\ &= \frac{1}{2} \frac{\kappa^2 B}{\sqrt{1 + \kappa^2 B^2}} \frac{E}{\sqrt{1 - \kappa^2 E^2}},\end{aligned}\quad (266)$$

and further we obtain

$$\star G = \frac{1}{\sqrt{1 + \kappa^2 B^2}} \frac{1}{\sqrt{1 - \kappa^2 E^2}} \star F + \frac{\kappa^2 B}{\sqrt{1 + \kappa^2 B^2}} \frac{E}{\sqrt{1 - \kappa^2 E^2}} F. \quad (267)$$

Again we write the 4-velocity of electrons in the following form

$$\tilde{V}(\zeta) = \mu(\zeta) e^1 + \psi(\zeta) e^2, \quad (268)$$

where

$$e^1 = v dx^3 - dx^0 \quad (269)$$

$$e^2 = dx^3 - v dx^0. \quad (270)$$

As before, the timelike and future-directed requirements lead to

$$\psi(\zeta) = -\sqrt{\mu(\zeta)^2 - \gamma^2} e^2. \quad (271)$$

Then, from the Lorentz equation $\nabla_V \tilde{V} = \frac{q}{m} \iota_V F$ and assumptions of expressions (260) and (268) we get

$$E(\zeta) = \frac{1}{\gamma^2} \frac{m}{q} \mu'(\zeta). \quad (272)$$

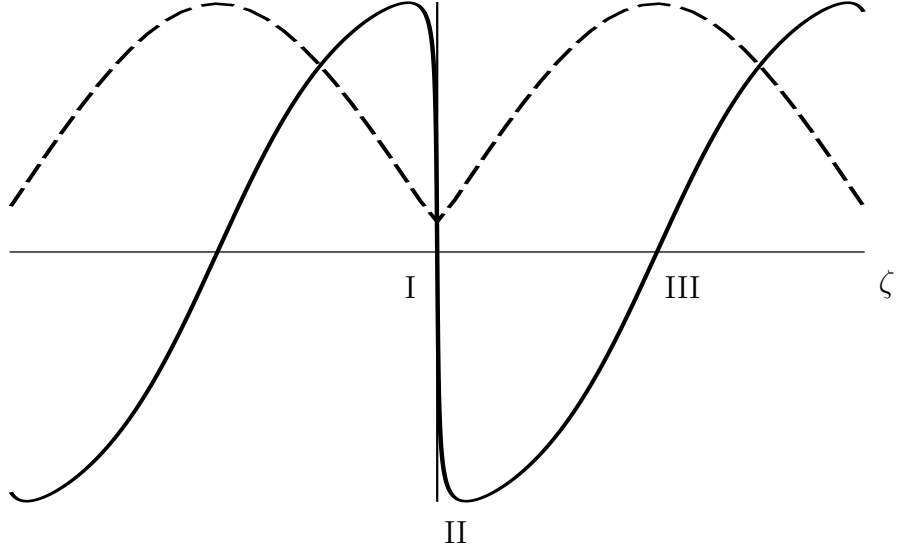


FIG. 12: E and μ with respect to ζ (the solid and the dashed line show E and μ , respectively, see [6])

Fig. 12 describes the periodic behaviour of E and μ and shows their relation (272).

For a plasma with ions and electrons, $j = -q \star \tilde{N} + q \star \tilde{N}_{\text{ion}}$ in the Born-Infeld equation. According to our assumptions, we have $N_{\text{ion}} = n_{\text{ion}} \frac{\partial}{\partial x^0}$ and $N = nV$

Since $E(\zeta)$ is independent of x^1 and x^2 , and B is a constant, the form of the electromagnetic field (260) gives that the field equation (34) is satisfied automatically. Based on equations (267)-(272), the field equation (35) can be turned into the following equation,

$$\left[2 \frac{\partial \mathcal{L}}{\partial X} \mu'(\zeta) + 2 \frac{\gamma^2 q}{m} B \frac{\partial \mathcal{L}}{\partial Y} \right]' = \frac{q^2 n_{\text{ion}} \gamma^4}{m} \left(\frac{v \mu(\zeta)}{\sqrt{\mu(\zeta)^2 - \gamma^2}} - 1 \right), \quad (273)$$

which we write as

$$\frac{\sqrt{1 + \kappa^2 B^2}}{(1 - \kappa^2 E(\zeta)^2)^{\frac{3}{2}}} E'(\zeta) = q n_{\text{ion}} \gamma^2 \left(\frac{v \mu(\zeta)}{\sqrt{\mu(\zeta)^2 - \gamma^2}} - 1 \right). \quad (274)$$

We will focus on the above field equation (274) in the next section, so as to obtain the wave-breaking limit of the Born-Infeld plasma in our scenario.

1. *Wave-Breaking Limit*

Multiplying equation (274) by $\frac{m}{q\gamma^2}\mu'$ and integrating it from ζ_I to ζ_{II} , we get

$$\left[\frac{1}{\kappa^2} \frac{\sqrt{1 + \kappa^2 B^2}}{\sqrt{1 - \kappa^2 E(\zeta)^2}} \right] \Big|_{\zeta_I}^{\zeta_{II}} = [mn_{\text{ion}}(v\sqrt{\mu(\zeta)^2 - \gamma^2} - \mu(\zeta))] \Big|_{\zeta_I}^{\zeta_{II}}. \quad (275)$$

The square root on the right side of equation (275) puts a lower limit on $\mu(\zeta)$ at $\zeta = \zeta_I$:

$$\mu_I = \gamma, \quad (276)$$

where $\mu_I \equiv \mu(\zeta_I)$. Since the minimum value $\mu_{\text{min}} = \mu_I$ is a turning point of $\mu(\zeta)$ and $E_I \propto \mu'(\zeta_I)$, we get

$$E_I = 0, \quad (277)$$

where $E_I \equiv E(\zeta_I)$. As we are interested in the maximum E and $\zeta = \zeta_{II}$ is a stationary point of $E(\zeta)$, we have

$$E_{II} = -E_{\text{max}}, \quad (278)$$

$$E'(\zeta_{II}) = 0. \quad (279)$$

At $\zeta = \zeta_{II}$, both sides of equation (274) become

$$\frac{\sqrt{1 + \kappa^2 B^2}}{(1 - \kappa^2 E_{\text{max}}^2)^{\frac{3}{2}}} E'(\zeta_{II}) = qn_{\text{ion}}\gamma^2 \left(\frac{v\mu_{II}}{\sqrt{\mu_{II}^2 - \gamma^2}} - 1 \right). \quad (280)$$

Both sides of the above equation are zero because $E'_{II} = 0$. This leads to the following equation

$$v\mu_{II} = \sqrt{\mu_{II}^2 - \gamma^2}. \quad (281)$$

μ_{II} can be obtained from equation (281) as

$$\mu_{II} = \gamma^2, \quad (282)$$

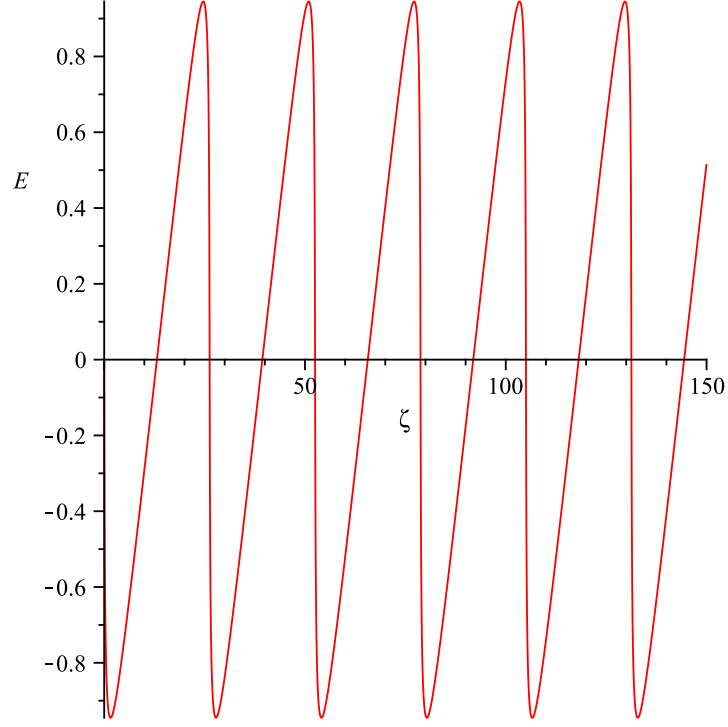


FIG. 13: Electric field calculated in Maxwell electrodynamics

where we give up the other solution $\mu_{\text{II}} = -\gamma^2$ because $\mu(\zeta)$ should be positive.

Through (275)-(278) we get

$$\frac{1}{\kappa^2 \sqrt{1 - \kappa^2 E_{\text{max}}^2}} - \frac{1}{\kappa^2} = \frac{mn_{\text{ion}}}{\sqrt{1 + \kappa^2 B^2}} (\gamma - 1). \quad (283)$$

We then get the following $E_{\text{max}} = E_{\text{max}}^{\text{BI}}$ in Born-Infeld electrodynamics

$$E_{\text{max}}^{\text{BI}^2} = \frac{1}{\kappa^2} \left[1 - \frac{1}{\left(1 + \frac{\kappa^2}{2} \frac{E_{\text{max}}^{\text{M}^2}}{\sqrt{1 + \kappa^2 B^2}} \right)^2} \right], \quad (284)$$

where

$$E_{\text{max}}^{\text{M}} = \frac{m\omega_{pe}c}{|q|} \sqrt{2(\gamma - 1)}, \quad (285)$$

is the wave-breaking limit calculated in Maxwell electrodynamics, which was first obtained by Akhiezer et al [29]. The angular frequency ω_{pe} in equation (285) is

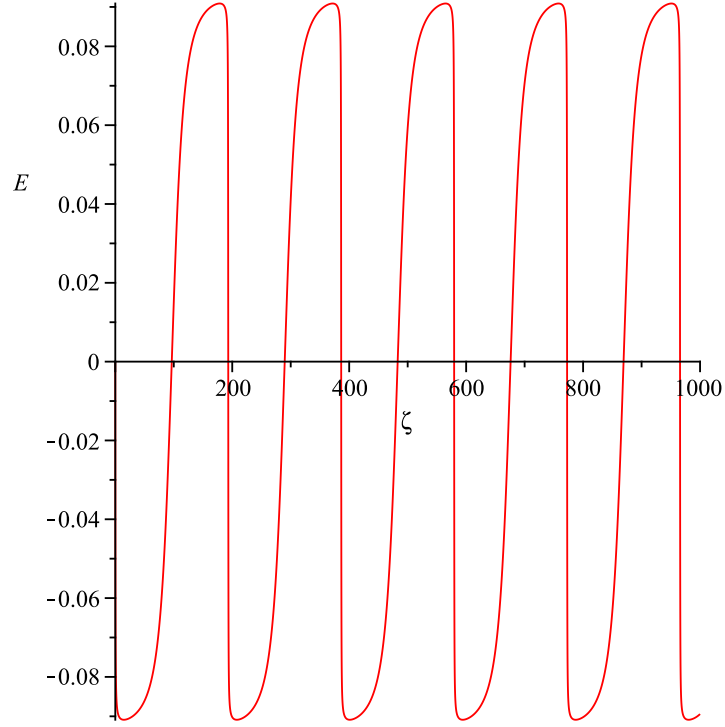


FIG. 14: Electric field calculated in Born-Infeld electrodynamics

defined as

$$\omega_{pe} = \sqrt{\frac{q^2 n_{\text{ion}}}{m \varepsilon_0}} . \quad (286)$$

and is the plasma frequency for electron oscillation (due to a perturbative displacement) without any external fields, where the speed of light c and the permittivity of the vacuum ε_0 have been restored. We find that $E_{\text{max}}^{\text{BI}} \rightarrow E_{\text{max}}^{\text{M}}$ when we let $\kappa \rightarrow 0$, which means Maxwell electrodynamics is restored when the Born-Infeld parameter κ is negligible.

With the above results, we plot Fig. 13 and Fig. 14 to show the electric field in a magnetised plasma calculated in Maxwell electrodynamics and in Born-Infeld electrodynamics. The relations between $\kappa E_{\text{max}}^{\text{BI}}$, $\kappa E_{\text{max}}^{\text{M}}$ and κBc are also plotted in Fig. 15 and Fig. 16.

From the four figures, we can see that the electric field in a magnetised plasma

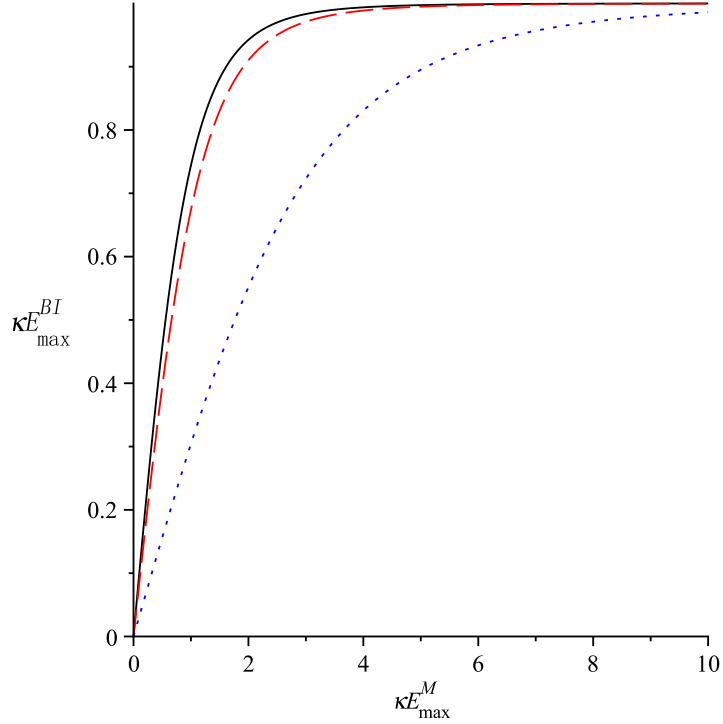


FIG. 15: κE_{\max}^{BI} with respect to κE_{\max}^M when κBc takes the value 0.1 (black solid), 1 (red dashed) and 10 (blue dotted), respectively

calculated in Born-Infeld electrodynamics is weaker and smoother than that in Maxwell electrodynamics. The smoothness is in accordance with the non-singular (albeit the non-smooth) nature of the electric field at a point charge in Born-Infeld electrodynamics [54]. The four figures also demonstrate that the magnetic field reduces the wave-breaking limit of the electric field. The effect of reduction begins to be important when the magnetic field is stronger, or when the number density of ions n_{ion} , or the Lorentz factor γ of the wave phase speed v is large.

2. Period of the Maximum Amplitude Oscillation

By choosing the initial conditions (276), (277) on $\mu(\zeta)$, we get a first integral of equation (274). In order to do that, we follow the same method as we used to

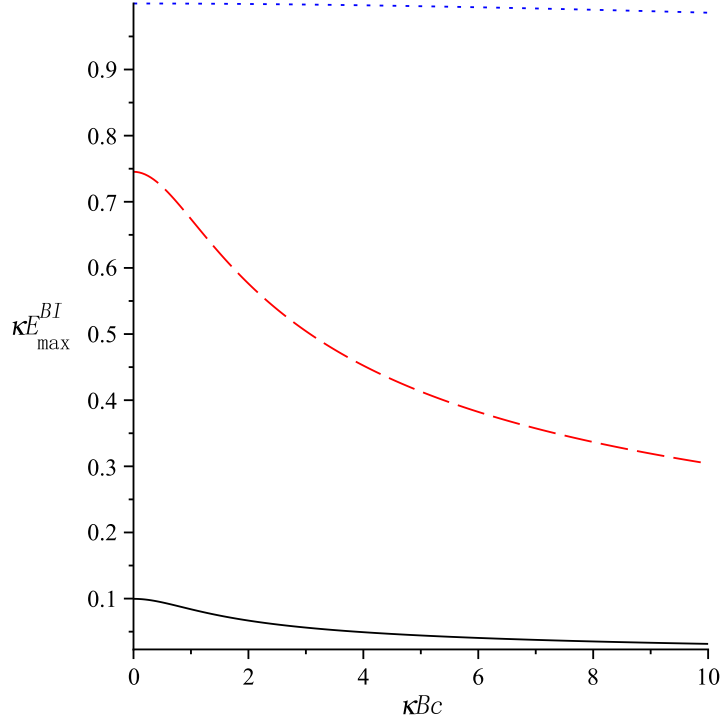


FIG. 16: κE_{\max}^{BI} with respect to $\kappa B c$ when κE_{\max}^M takes the value 0.1 (black solid), 1 (red dashed) and 10 (blue dotted), respectively

derive equation (275) and get

$$\frac{1}{\kappa^2} \sqrt{1 + \kappa^2 B^2} \left(\frac{1}{\sqrt{1 - \kappa^2 E(\zeta)^2}} - 1 \right) = m n_{\text{ion}} (v \sqrt{\mu(\zeta)^2 - \gamma^2} - \mu(\zeta) + \gamma) \quad (287)$$

where $\mu(\zeta_I) = \gamma$ and $E(\zeta_I) = 0$ have been used. Based on equations (272) and (287), we express $\left(\frac{d\mu(\zeta)}{d\zeta} \right)^2$ below,

$$\left(\frac{d\mu(\zeta)}{d\zeta} \right)^2 = \frac{q^2 \gamma^4}{m^2 \kappa^2} \left\{ 1 - \left[\frac{\kappa^2}{\sqrt{1 + \kappa^2 B^2}} m n_{\text{ion}} (v \sqrt{\mu^2 - \gamma^2} - \mu + \gamma) + 1 \right]^{-2} \right\}. \quad (288)$$

The stationary points of $\mu(\zeta)$ in equation (288) lead to

$$\mu(\zeta_I) \leq \mu \leq \mu(\zeta_{\text{III}}), \quad (289)$$

$$\mu(\zeta_{\text{III}}) = \gamma^3 (1 + v^2). \quad (290)$$

Examination of Fig. 12 gives the spatial period (wavelength) λ below,

$$\begin{aligned}
\lambda &= 2(\zeta_{\text{III}} - \zeta_{\text{I}}) \\
&= \frac{2m\kappa}{q\gamma^2} \int_{\gamma}^{\gamma^3(1+v^2)} \frac{1}{\sqrt{1 - \left[\frac{\kappa^2}{\sqrt{1+\kappa^2 B^2}} mn_{\text{ion}} (v\sqrt{\mu^2 - \gamma^2} - \mu + \gamma) + 1 \right]^{-2}}} d\mu \\
&= \frac{2(1 + \kappa^2 B^2)^{\frac{1}{4}}}{\omega_{pe} \gamma^2} \int_{\gamma}^{\gamma^3(1+v^2)} \frac{\hat{\kappa}}{\sqrt{1 - \left[\hat{\kappa}^2 (v\sqrt{\mu^2 - \gamma^2} - \mu + \gamma) + 1 \right]^{-2}}} d\mu \quad (291)
\end{aligned}$$

where $\hat{\kappa} = \frac{\kappa m \omega_{pe}}{|q|(1 + \kappa^2 B^2)^{\frac{1}{4}}}$.

Since the function $\mu(\zeta)$ depends on $\zeta = x^3 - vx^0$ only, the temporal period T and spatial period λ of the wave are related as $\lambda = vT$. Hence, the angular frequency $\omega^{\text{BI}} \equiv \frac{2\pi}{T}$ of the wave in the lab frame is

$$\omega^{\text{BI}} = \frac{2\pi v}{\lambda}. \quad (292)$$

Considering equation (292), we expand equation (291) about the dimensionless small parameter $\frac{\kappa m \omega_{pe}}{2|q|}$ and obtain

$$\omega^{\text{BI}} \approx \frac{\omega^{\text{M}}}{(1 + \kappa^2 B^2)^{\frac{1}{4}}} \left[1 - \left(\frac{\kappa m \omega_{pe}}{2q} \right)^2 \frac{\gamma}{\sqrt{1 + \kappa^2 B^2}} \right], \quad (293)$$

where $\omega^{\text{M}} = \frac{\pi}{2\sqrt{2}\gamma} \omega_{pe}$ is the angular frequency of the wave in the lab frame when $\kappa = 0$. The expression $\omega^{\text{M}} = \frac{\pi}{2\sqrt{2}\gamma} \omega_{pe}$ for the angular frequency of a plasma wave with $\gamma \gg 1$ was first derived by Akhiezer et al. [29].

We then get the following period of the maximum amplitude oscillation

$$\begin{aligned}
\lambda &= \frac{2\pi}{\frac{\omega^{\text{M}}}{(1 + \kappa^2 B^2)^{\frac{1}{4}}} \left[1 - \left(\frac{\kappa m \omega_{pe}}{2q} \right)^2 \frac{\gamma}{\sqrt{1 + \kappa^2 B^2}} \right]} \\
&= \frac{2\pi c}{\frac{\omega^{\text{M}}}{(1 + \kappa^2 B^2 c^2)^{\frac{1}{4}}} \left[1 - \left(\frac{\kappa m \omega_{pe} c}{2q} \right)^2 \frac{\gamma}{\sqrt{1 + \kappa^2 B^2 c^2}} \right]}, \quad (294)
\end{aligned}$$

where the speed of light c has been restored.

3. Comparison of the Maximum Energy Gain with Maxwell Theory

We now compare the maximum energy gain a test electron can obtain in Born-Infeld electrodynamics with that in Maxwell electrodynamics. From Fig. 12 we find that the maximum energy change a test electron ($q < 0$) may obtain is the consequence of its acceleration from the electric field over the half wavelength region (ζ_I, ζ_{III}). Using equations (272), (276) and (290), we obtain

$$\begin{aligned}
 q \int_{\xi_I}^{\xi_{III}} E d\xi &= q \int_{(\gamma\zeta_I)}^{(\gamma\zeta_{III})} E(\zeta) d(\gamma\zeta) \\
 &= \frac{m}{\gamma^2} \int_{\zeta_I}^{\zeta_{III}} \gamma \mu'(\zeta) d\zeta \\
 &= \frac{m}{\gamma^2} \int_{\mu_I}^{\mu_{III}} \gamma d\mu \\
 &= 2mv^2 \gamma^2, \tag{295}
 \end{aligned}$$

where $\xi = \gamma\zeta = \gamma(x^3 - vx^0)$ is a unit normalised spatial coordinate adapted to an inertial frame moving with the wave.

Equation (295) represents the energy gained by the electron in the frame of the wave. As the result $2mv^2\gamma^2$ is the same for the cases of both Maxwell electrodynamics and Born-Infeld electrodynamics, equation (295) reveals that the Born-Infeld parameter κ does not contribute to the maximum energy that a test electron may obtain. In other words, Born-Infeld electrodynamics gives the same prediction as Maxwell electrodynamics for the maximum energy that a test electron may obtain. However, we expect κ to affect the properties of electromagnetic waves, which will be discussed in the next section.

B. Dispersion Relation in Born-Infeld Electrodynamics

In a resting ion background $V_{\text{ion}} = \frac{\partial}{\partial t}$ (in Section VB and Section VC we will use the frame $t = x^0, x = x^1, y = x^2$ and $z = x^3$ for simplicity and a more

direct physical expression), we consider electrons (number density $n = n_{\text{ion}} + \epsilon\mathcal{N}$) travelling in a strong constant magnetic field (so that non-linear effects arising from Born-Infeld electrodynamics may apply) pointing in the z direction. We now examine the cases of electrostatic waves caused by the displacement of electrons from their equilibrium and the electromagnetic waves coupled to the motion of the electrons. For the electromagnetic waves, we classify them by the direction of propagation of the waves. In the case of the waves travelling parallel to the z (external magnetic field) direction, we express the waves on the basis of right and left circularly polarised waves and the phenomenon of Faraday Rotation will result for general waves attained as a linear superposition of both left and right circularly polarised waves. In the case of the wave travelling perpendicular to the z (external magnetic field) direction, there are “ordinary” modes (electric field parallel to external magnetic field) and “extraordinary” modes (electric field perpendicular to external magnetic field). For convenience, we use “R”, “L”, “O” and “X” modes to represent right circularly polarised, left circularly polarised, “ordinary” and “extraordinary” modes. Here we contrast the four modes.

1. Wave Traveling Parallel to the External Magnetic Field

For the wave travelling parallel to the z (external magnetic field) direction, there is a basis of left and right circularly polarised waves, where the electric field vector of the wave is seen to trace a right or left handed circle when the wave is observed head on.

1. “R” Mode: Right Handed Circularly Polarised Wave

Assuming that all the physical properties depend on z and t only, we calculate the dispersion relation by investigating the perturbation of the velocity field of

electrons in the transverse direction to the magnetic field, which we express as

$$V = \frac{\partial}{\partial t} + \epsilon U + O(\epsilon^2) , \quad (296)$$

where the transverse perturbation is assumed as

$$\tilde{U} = \cos(kz - \omega t)dx + \sin(kz - \omega t)dy . \quad (297)$$

The normalisation formula for the 4-velocity V is

$$-1 = g(V, V) = -1 + 2\epsilon g(U, \frac{\partial}{\partial t}) + O(\epsilon^2), \quad (298)$$

which leads to

$$g(U, \frac{\partial}{\partial t}) = 0 \quad (299)$$

by equating equal powers of ϵ .

We write the field strength tensors as

$$F = \mathcal{B} + \epsilon \mathcal{F} + O(\epsilon^2) \quad (300)$$

$$G = \mathcal{H} + \epsilon \mathcal{G} + O(\epsilon^2) , \quad (301)$$

where $\mathcal{B} = Bdx \wedge dy$.

The Lorentz equation that the electrons satisfy in our theory of Born-Infeld plasma is the same as in Maxwell electrodynamics (i.e. equation (37))

$$\epsilon \nabla_{\frac{\partial}{\partial t}} \tilde{U} + O(\epsilon^2) = \epsilon \frac{q}{m} \iota_{\frac{\partial}{\partial t}} \mathcal{F} + \epsilon \frac{q}{m} \iota_U \mathcal{B} + O(\epsilon^2) , \quad (302)$$

which turns out to be

$$\nabla_{\frac{\partial}{\partial t}} \tilde{U} = \frac{q}{m} \iota_{\frac{\partial}{\partial t}} \mathcal{F} + \frac{q}{m} \iota_U \mathcal{B} \quad (303)$$

by equating equal powers of ϵ .

Writing the number density in a perturbative form $n = n_{\text{ion}} + \epsilon \mathcal{N}$, we divide the field equations in Born-Infeld electrodynamics

$$dF = 0 \quad (304)$$

$$d \star G = -qn \star \tilde{V} + qn_{\text{ion}} \star \tilde{V}_{\text{ion}} \quad (305)$$

into the zeroth order equations (with respect to ϵ)

$$d\mathcal{B} = 0 \quad (306)$$

$$d \star \mathcal{H} = 0, \quad (307)$$

and the first order equations (with respect to ϵ)

$$\epsilon d\mathcal{F} = 0, \quad (308)$$

$$\epsilon d \star \mathcal{G} = -\epsilon q \mathcal{N} \star \frac{\tilde{\partial}}{\partial t} - \epsilon q n_{\text{ion}} \star \tilde{U}. \quad (309)$$

Equation (306) is satisfied automatically. Thus we get the dispersion relation from the equation set that consists of field equations (307), (308), (309), Lorentz equation (303) and the velocity normalisation equation (298).

We now try a formal solution for the field strength tensor as $\mathcal{F} = \mathcal{F}_{tx} dt \wedge dx + \mathcal{F}_{ty} dt \wedge dy + \mathcal{F}_{xz} dx \wedge dz + \mathcal{F}_{yz} dy \wedge dz$, which corresponds to the physical situation with no electric or magnetic field components in the z direction, apart from the background fields. We get the constraints on \mathcal{F}_{tx} and \mathcal{F}_{ty} from the Lorentz equation (303) as

$$\mathcal{F}_{tx} = \left(\frac{m}{q} \omega + B \right) \sin(kz - \omega t) \quad (310)$$

$$\mathcal{F}_{ty} = - \left(\frac{m}{q} \omega + B \right) \cos(kz - \omega t), \quad (311)$$

and then get the constraints on \mathcal{F}_{xz} and \mathcal{F}_{yz} from the field equation (308) as

$$\frac{\partial \mathcal{F}_{xz}}{\partial t} = -k \left(\frac{m}{q} \omega + B \right) \cos(kz - \omega t) \quad (312)$$

$$\frac{\partial \mathcal{F}_{yz}}{\partial t} = -k \left(\frac{m}{q} \omega + B \right) \sin(kz - \omega t). \quad (313)$$

According to Born-Infeld electrodynamics, we have

$$\star G = 2 \left(\frac{\partial \mathcal{L}}{\partial X} \star F + \frac{\partial \mathcal{L}}{\partial Y} F \right) \quad (314)$$

$$\mathcal{L} = \frac{1}{\kappa^2} \left(1 - \sqrt{1 - \kappa^2 X - \frac{\kappa^4}{4} Y^2} \right) \quad (315)$$

$$X = \star(F \wedge \star F) \quad (316)$$

$$Y = \star(F \wedge F) . \quad (317)$$

Then the zeroth and first order components with respect to ϵ of the above equation are

$$\star \mathcal{H} = \frac{1}{\sqrt{1 - \kappa^2 X - \frac{\kappa^4}{4} Y^2}_{(0)}} \star \mathcal{B} + \frac{\kappa^2}{2} \frac{Y}{\sqrt{1 - \kappa^2 X - \frac{\kappa^4}{4} Y^2}_{(0)}} \mathcal{B} \quad (318)$$

$$\begin{aligned} \star \mathcal{G} &= \frac{1}{\sqrt{1 - \kappa^2 X - \frac{\kappa^4}{4} Y^2}_{(0)}} \star \mathcal{F} + \frac{\kappa^2}{2} \frac{Y}{\sqrt{1 - \kappa^2 X - \frac{\kappa^4}{4} Y^2}_{(0)}} \mathcal{F} \\ &+ \frac{1}{\sqrt{1 - \kappa^2 X - \frac{\kappa^4}{4} Y^2}_{(1)}} \star \mathcal{B} + \frac{\kappa^2}{2} \frac{Y}{\sqrt{1 - \kappa^2 X - \frac{\kappa^4}{4} Y^2}_{(1)}} \mathcal{B} , \end{aligned} \quad (319)$$

where the subscript $_{(0)}$ and $_{(1)}$ are defined below,

$$\begin{aligned} f_{(0)} &= f|_{\epsilon=0} \\ f_{(1)} &= \left. \frac{df}{d\epsilon} \right|_{\epsilon=0} \end{aligned} \quad (320)$$

and \mathcal{H} and \mathcal{G} are defined in (300) and (301).

From the zeroth and the first order of field equations (307) and (309), we get

$$d \star \mathcal{H} = d \left(\frac{1}{\sqrt{1 - \kappa^2 X - \frac{\kappa^4}{4} Y^2}} \star \mathcal{B} \right) + \frac{\kappa^2}{2} d \left(\frac{Y}{\sqrt{1 - \kappa^2 X - \frac{\kappa^4}{4} Y^2}} \mathcal{B} \right) = 0 \quad (321)$$

$$\begin{aligned} d \star \mathcal{G} &= d \left(\frac{1}{\sqrt{1 - \kappa^2 X - \frac{\kappa^4}{4} Y^2}} \star \mathcal{F} \right) + \frac{\kappa^2}{2} d \left(\frac{Y}{\sqrt{1 - \kappa^2 X - \frac{\kappa^4}{4} Y^2}} \mathcal{F} \right) \\ &\quad + d \left(\frac{1}{\sqrt{1 - \kappa^2 X - \frac{\kappa^4}{4} Y^2}} \star \mathcal{B} \right) + \frac{\kappa^2}{2} d \left(\frac{Y}{\sqrt{1 - \kappa^2 X - \frac{\kappa^4}{4} Y^2}} \mathcal{B} \right) \\ &= -\epsilon q \mathcal{N} \star \frac{\tilde{\partial}}{\partial t} - \epsilon q n_{\text{ion}} \star \tilde{U} . \end{aligned} \quad (322)$$

Since $\mathcal{B} \wedge \star \mathcal{F} = 0$, according to our assumptions above, we simplify the components of field equations (321) and (322) by writing X and Y as follows

$$\begin{aligned} X &= \star(F \wedge \star F) \\ &= \star(\mathcal{B} \wedge \star \mathcal{B}) + O(\epsilon^2) \\ &= -B^2 + O(\epsilon^2) \end{aligned} \quad (323)$$

$$\begin{aligned} Y &= \star(F \wedge F) \\ &= 2\epsilon \star(\mathcal{B} \wedge \star \mathcal{F}) + O(\epsilon^2) \\ &= O(\epsilon^2) . \end{aligned} \quad (324)$$

We then get

$$\star \mathcal{H} = \frac{1}{\sqrt{1 + \kappa^2 B^2}} \star \mathcal{B} \quad (325)$$

$$\star \mathcal{G} = \frac{1}{\sqrt{1 + \kappa^2 B^2}} \star \mathcal{F} . \quad (326)$$

By investigating field equations (321) and (322), we find that (321) is trivial and

(322) gives

$$\mathcal{N} = 0 \quad (327)$$

$$\frac{1}{\sqrt{1 + \kappa^2 B^2}} \left[\left(\frac{m}{q} \omega + B \right) \omega \cos(kz - \omega t) - \frac{\partial \mathcal{F}_{xz}}{\partial z} \right] = q n_{\text{ion}} \cos(kz - \omega t) \quad (328)$$

$$\frac{1}{\sqrt{1 + \kappa^2 B^2}} \left[\left(\frac{m}{q} \omega + B \right) \omega \sin(kz - \omega t) - \frac{\partial \mathcal{F}_{yz}}{\partial z} \right] = q n_{\text{ion}} \sin(kz - \omega t) \quad (329)$$

where equation (327) also means

$$n = n_{\text{ion}} + O(\epsilon^2) . \quad (330)$$

We find that the solutions for \mathcal{F}_{xz} and \mathcal{F}_{yz}

$$\mathcal{F}_{xz} = \frac{k}{\omega} \left(\frac{m}{q} \omega + B \right) \sin(kz - \omega t) \quad (331)$$

$$\mathcal{F}_{yz} = -\frac{k}{\omega} \left(\frac{m}{q} \omega + B \right) \cos(kz - \omega t) \quad (332)$$

satisfy all of the conditions (312), (313), (328) and (329). Then equations (328) and (331), or equations (329) and (332) give the following dispersion relation in Born-Infeld electrodynamics:

$$k = \left[\frac{(m\omega + qB)\omega^2 - q^2 n_{\text{ion}} \omega \sqrt{1 + \kappa^2 B^2}}{m\omega + qB} \right]^{\frac{1}{2}} . \quad (333)$$

Using the above dispersion relation, we obtain the index of refraction n (its square in the following formula) as follows,

$$\begin{aligned} n^2 &= \frac{k^2}{\omega^2} \\ &= 1 - \frac{\frac{q^2 n_{\text{ion}}}{m} \sqrt{1 + \kappa^2 B^2}}{\omega^2 \left(1 + \frac{qB}{m\omega} \right)} \\ &= 1 - \frac{\omega_{pe}^2 \sqrt{1 + \kappa^2 B^2}}{\omega^2 \left(1 - \frac{\omega_{ce}}{\omega} \right)} , \end{aligned} \quad (334)$$

where the cyclotron frequency $\omega_{ce} = -\frac{qB}{m}$.

As the electric field vector of the above wave is seen to trace a right handed circle when the wave is observed head on, we call it a right handed circularly polarised wave. In terms of a frequency $\omega \ll \omega_{ce} \ll \omega_{pe}$, we have

$$n^2 = \frac{\omega_{pe}^2 \sqrt{1 + \kappa^2 B^2}}{\omega \omega_{ce}} . \quad (335)$$

Since $n^2 = \frac{k^2}{\omega^2}$, we rewrite equation (335) as

$$\omega = \frac{\omega_{ce} k^2}{\omega_{pe}^2 \sqrt{1 + \kappa^2 B^2}} , \quad (336)$$

which leads to the group velocity

$$\begin{aligned} v_g &= \frac{d\omega}{dk} \\ &= \frac{2\omega_{ce}}{\omega_{pe}^2 \sqrt{1 + \kappa^2 B^2}} k \end{aligned} \quad (337)$$

$$= \frac{2\sqrt{\omega_{ce}}}{\omega_{pe} (1 + \kappa^2 B^2)^{\frac{1}{4}}} \sqrt{\omega} , \quad (338)$$

and the phase velocity

$$\begin{aligned} v_p &= \frac{\omega}{k} \\ &= \frac{\omega_{ce}}{\omega_{pe}^2 \sqrt{1 + \kappa^2 B^2}} k \end{aligned} \quad (339)$$

$$= \frac{\sqrt{\omega_{ce}}}{\omega_{pe} (1 + \kappa^2 B^2)^{\frac{1}{4}}} \sqrt{\omega} . \quad (340)$$

From the above equation (340) we see that in a wave packet consisting of components with different phase velocities, a higher frequency component wave travels faster than a lower frequency component wave. In other words, the frequency that a receiver gets is descending like a whistle, hence it is called a "whistler mode".

When the frequency of the wave is ascending, the index of refraction n is descending. As a result the motion of the wave will be terminated when n tends to zero. We then get the cutoff frequency from $n = 0$ in equation (334) as follows

$$\omega_R = \frac{\omega_{ce}}{2} + \sqrt{\omega_{pe}^2 \sqrt{1 + \kappa^2 B^2} + \frac{\omega_{ce}^2}{4}} . \quad (341)$$

Comparing with the traditional calculations in Maxwell electrodynamics $\omega_R^M = \frac{\omega_{ce}}{2} + \sqrt{\omega_{pe}^2 + \frac{\omega_{ce}^2}{4}}$, Born-Infeld electrodynamics differs by the replacement $\omega_{pe}^2 \rightarrow \omega_{pe}^2 \sqrt{1 + \kappa^2 B^2}$.

2. “L” Mode: Left Handed Circularly Polarised Wave

Correspondingly, the left circularly polarised wave solution (i.e. the electric field vector traces a left handed circle when viewed facing the wave) is

$$\begin{aligned} n^2 &= \frac{k^2}{\omega^2} \\ &= 1 - \frac{\frac{q^2 n_{\text{ion}}}{m} \sqrt{1 + \kappa^2 B^2}}{\omega^2 \left(1 - \frac{qB}{m\omega}\right)} \\ &= 1 - \frac{\omega_{pe}^2 \sqrt{1 + \kappa^2 B^2}}{\omega^2 \left(1 + \frac{\omega_{ce}}{\omega}\right)}, \end{aligned} \quad (342)$$

and the corresponding cutoff is

$$\omega_L = -\frac{\omega_{ce}}{2} + \sqrt{\omega_{pe}^2 \sqrt{1 + \kappa^2 B^2} + \frac{\omega_{ce}^2}{4}}. \quad (343)$$

We find that in the “L” mode case, Born-Infeld plasmas differ from Maxwell plasmas by the replacement $\omega_{pe}^2 \rightarrow \omega_{pe}^2 \sqrt{1 + \kappa^2 B^2}$, which is the same as the “R” mode case. This is similar to the fact that electromagnetic waves with different polarisations travel with the same phase speed in vacuum Born-Infeld electrodynamics.

3. Faraday Rotation for a Mixture of “R” and “L” Modes

In terms of a general wave with both left and right circularly polarised compo-

nents,

$$E_L = (dx - idy)E_0e^{i(k_Lz - \omega t)} , \quad (344)$$

$$E_R = (dx + idy)E_0e^{i(k_Rz - \omega t)} , \quad (345)$$

$$\begin{aligned} E &= E_L + E_R \\ &= E_0[dx(e^{ik_Lz} + e^{ik_Rz}) - idy(e^{ik_Lz} - e^{ik_Rz})]e^{-i\omega t} , \end{aligned} \quad (346)$$

$$\begin{aligned} \frac{E_x}{E_y} &= -i \frac{1 + e^{i(k_L - k_R)z}}{1 - e^{i(k_L - k_R)z}} \\ &= \cot\left(\frac{k_L - k_R}{2}z\right) . \end{aligned} \quad (347)$$

After the wave travels the distance z , the rotation angle ϕ of the electric field is

$$\begin{aligned} \phi &= \cot^{-1} \frac{\text{Re}(E_x)}{\text{Re}(E_y)} \\ &= \frac{k_L - k_R}{2}z \\ &= \frac{z}{2} \left(\sqrt{\omega_L^2 - \frac{\omega_L}{\omega_R} \omega_{pe}^2 \sqrt{1 + \kappa^2 B^2}} - \sqrt{\omega_R^2 - \frac{\omega_R}{\omega_L} \omega_{pe}^2 \sqrt{1 + \kappa^2 B^2}} \right) . \end{aligned} \quad (348)$$

2. Wave Traveling Perpendicular to the External Magnetic Field

In the case of a wave travelling along z direction, which is perpendicular to the external magnetic field in a cold Born-Infeld plasma, we introduce more general expressions for the zeroth, first order electromagnetic strength tensor and the velocity perturbation terms as follows,

$$\mathcal{B} = B_{xy}dx \wedge dy + B_{yz}dy \wedge dz + B_{zx}dz \wedge dx , \quad (349)$$

$$\begin{aligned} \mathcal{F} &= F_{tx}dt \wedge dx + F_{ty}dt \wedge dy + F_{tz}dt \wedge dz \\ &\quad + F_{xy}dx \wedge dy + F_{yz}dy \wedge dz + F_{zx}dz \wedge dx , \end{aligned} \quad (350)$$

$$\begin{aligned} \tilde{U} &= (u_x dx + u_y dy + u_z dz)e^{i\phi} \\ &= (u_x dx + u_y dy + u_z dz)e^{i(kz - \omega t)} , \end{aligned} \quad (351)$$

where all the B and F components are antisymmetric about their indices.

Similar to the “R” mode calculation, we find that in the assumptions here, the Lorentz equation (303) leads to the following equations,

$$F_{tx} = -\frac{m}{q}i\omega u_x e^{i\phi} - e^{i\phi}(u_z B_{zx} + u_y B_{yx}) , \quad (352)$$

$$F_{ty} = -\frac{m}{q}i\omega u_y e^{i\phi} - e^{i\phi}(u_x B_{xy} + u_z B_{zy}) , \quad (353)$$

$$F_{tz} = -\frac{m}{q}i\omega u_z e^{i\phi} - e^{i\phi}(u_y B_{yz} + u_x B_{xz}) , \quad (354)$$

and the Born-Infeld field equation (308) leads to the equations below,

$$\frac{\partial F_{xy}}{\partial t} = \frac{\partial F_{xy}}{\partial z} = 0 , \quad (355)$$

$$\frac{\partial F_{zx}}{\partial t} = \frac{\partial F_{tx}}{\partial z} , \quad (356)$$

$$\frac{\partial F_{zy}}{\partial t} = \frac{\partial F_{ty}}{\partial z} . \quad (357)$$

Considering that the forms of \mathcal{B} (349) and \mathcal{F} (350) lead to

$$\begin{aligned} X &= \star(F \wedge \star F) \\ &= -(B_{xy}^2 + B_{yz}^2 + B_{zx}^2) - 2\epsilon(B_{xy}F_{xy} + B_{yz}F_{yz} + B_{zx}F_{zx}) , \end{aligned} \quad (358)$$

$$\begin{aligned} Y &= \star(F \wedge F) \\ &= -2\epsilon(B_{xy}F_{tz} + B_{yz}F_{tx} + B_{zx}F_{ty}) , \end{aligned} \quad (359)$$

the Born-Infeld field equation (309) leads to the following equation,

$$\begin{aligned} &\frac{\partial F_{zx}}{\partial z} - \frac{\partial F_{tx}}{\partial t}(1 + \kappa^2 B_{yz}^2) - \kappa^2 B_{xy} B_{yz} \frac{\partial F_{tz}}{\partial t} - \kappa^2 B_{zx} B_{yz} \frac{\partial F_{ty}}{\partial t} \\ &= \sqrt{1 + \kappa^2 B^2} q n_{ion} u_x e^{i\phi} \end{aligned} \quad (360)$$

We then get the solution for different wave modes that travel perpendicular to the external magnetic field. There are ”ordinary” or ”extraordinary” wave modes with the direction of the electric field parallel or perpendicular to the external magnetic field, respectively.

4. “O” Mode: Electric Field Parallel to the External Magnetic Field

The dispersion relation for a mode for which the electric field is parallel to the external magnetic field is obtained below,

$$\omega^2 = \frac{k^2}{1 + \kappa^2 B^2} + \frac{\omega_{pe}^2}{\sqrt{1 + \kappa^2 B^2}}, \quad (361)$$

or

$$\begin{aligned} n^2 &= \frac{k^2}{\omega^2} \\ &= 1 + \kappa^2 B^2 - \frac{\omega_{pe}^2 \sqrt{1 + \kappa^2 B^2}}{\omega^2}. \end{aligned} \quad (362)$$

Letting $n \rightarrow 0$, we get the cutoff frequency of the waves below,

$$\omega = \frac{\omega_{pe}}{(1 + \kappa^2 B^2)^{\frac{1}{4}}}. \quad (363)$$

5. “X” Mode: Electric Field Perpendicular to the External Magnetic Field

Repeating the preceding method, we get the dispersion relation for a mode for which the electric field is perpendicular to the external magnetic field as,

$$\omega^2 = \frac{k^2}{1 + \kappa^2 B^2} + \omega_{pe}^2 \sqrt{1 + \kappa^2 B^2} \left(\frac{\omega^2 - \omega_{pe}^2 \sqrt{1 + \kappa^2 B^2}}{\omega^2 - \omega_{pe}^2 \sqrt{1 + \kappa^2 B^2} - \omega_{ce}^2} \right), \quad (364)$$

or

$$\begin{aligned} n^2 &= \frac{k^2}{\omega^2} \\ &= (1 + \kappa^2 B^2) \left(1 - \frac{\omega_{pe}^2 \sqrt{1 + \kappa^2 B^2}}{\omega^2} \frac{\omega^2 - \omega_{pe}^2 \sqrt{1 + \kappa^2 B^2}}{\omega^2 - \omega_{pe}^2 \sqrt{1 + \kappa^2 B^2} - \omega_{ce}^2} \right). \end{aligned} \quad (365)$$

Letting $n \rightarrow 0$, we get the cutoff frequency of the waves below,

$$\omega_{XR} = \frac{\omega_{ce}}{2} + \sqrt{\omega_{pe}^2 \sqrt{1 + \kappa^2 B^2} + \frac{\omega_{ce}^2}{4}} \quad (366)$$

$$\omega_{XL} = -\frac{\omega_{ce}}{2} + \sqrt{\omega_{pe}^2 \sqrt{1 + \kappa^2 B^2} + \frac{\omega_{ce}^2}{4}} \quad (367)$$

C. Comparisons with Cold Maxwell Plasmas

1. Wave-Breaking Limits and Dispersion Relations

Comparing the results obtained previously on the electric field calculated in Born-Infeld electrodynamics (illustrated in Fig. 14) with those obtain by traditional calculations in Maxwell electrodynamics (illustrated in Fig. 13), we see that the electric field in a magnetised plasma calculated in Born-Infeld electrodynamics is smoother than that in Maxwell electrodynamics. Besides, the maximum electric field calculated in Born-Infeld electrodynamics shown in equation (284) is weaker than that calculated in Maxwell electrodynamics. However, the maximum energy that a test electron may obtain from a cold plasma wave calculated in Born-Infeld electrodynamics is the same as that in Maxwell electrodynamics due to the cancellation from the lengthened wavelength in the Born-Infeld plasmas (though recent unpublished work by others suggested that a larger class of theories generated from local functions of the form $\mathcal{L}(X, Y)$ may have this property). It is interesting to note that Born-Infeld electrodynamics shares certain properties with Maxwell electrodynamics.

Investigation on electromagnetic waves in a cold plasma shows that the dispersion relation in the ‘‘R’’ mode (334) and ‘‘L’’ mode (342) calculated in Born-Infeld electrodynamics differs with Maxwell electrodynamics by the replacement $\omega_{pe}^2 \rightarrow \omega_{pe}^2 \sqrt{1 + \kappa^2 B^2}$. In the ‘‘X’’ mode case (365) it is more complex as the dispersion relation in a cold Born-Infeld plasma differs by the replacement

$k \rightarrow \frac{k}{\sqrt{1 + \kappa^2 B^2}}$ still with the replacement $\omega_{pe}^2 \rightarrow \omega_{pe}^2 \sqrt{1 + \kappa^2 B^2}$. On the contrary, in the “O” mode case (362) the dispersion relation in a cold Born-Infeld plasma differs by the replacement $\omega_{pe}^2 \rightarrow \frac{\omega_{pe}^2}{\sqrt{1 + \kappa^2 B^2}}$ and in the meantime the wave number k should also be replaced as $k \rightarrow \frac{k}{\sqrt{1 + \kappa^2 B^2}}$.

Further calculation shows that the cutoff frequencies of the “R” mode (341), “L” mode (343) and “X” mode (366) (367) of electromagnetic waves in Born-Infeld cold plasma are different from those in Maxwell cold plasma. As ω_{pe}^2 in the result of the cutoff frequencies in Maxwell cold plasma is replaced by $\omega_{pe}^2 \sqrt{1 + \kappa^2 B^2}$ in Born-Infeld cold plasma, the Born-Infeld cutoff frequencies are higher than the Maxwell ones. However, in the “O” mode case (363), the Born-Infeld cutoff frequencies are lower than the Maxwell ones due to the replacement of $\omega_{pe}^2 \rightarrow \frac{\omega_{pe}^2}{\sqrt{1 + \kappa^2 B^2}}$. It may be possible, therefore, to use the radiation of magnetars to test whether Born-Infeld electrodynamics meets observations better than Maxwell electrodynamics in circumstances with strong magnetic fields.

2. Decelerating and particle trapping for “O” modes

We now consider the dispersion relation (362) for an “O” mode wave and transform it into the frame that is comoving with the wave as follows,

$$t' = \gamma(t - vz) \quad (368)$$

$$x' = x \quad (369)$$

$$y' = y \quad (370)$$

$$z' = \gamma(z - vt) \quad (371)$$

$$v = \frac{\omega}{k}. \quad (372)$$

It is easy to get the expression of v as,

$$\begin{aligned} v &= \frac{\omega}{k} \\ &= \frac{1}{\sqrt{1 + \kappa^2 B^2}} \sqrt{1 + \frac{\omega_p^2}{k^2} \sqrt{1 + \kappa^2 B^2}}. \end{aligned} \quad (373)$$

We find that

$$v > 1 \quad \text{for} \quad k < \frac{\omega_p(1 + \kappa^2 B^2)^{\frac{1}{4}}}{\kappa B}, \quad (374)$$

$$v = 1 \quad \text{for} \quad k = \frac{\omega_p(1 + \kappa^2 B^2)^{\frac{1}{4}}}{\kappa B}, \quad (375)$$

$$v < 1 \quad \text{for} \quad k > \frac{\omega_p(1 + \kappa^2 B^2)^{\frac{1}{4}}}{\kappa B}, \quad (376)$$

which represent a phase speed greater than, equal to or less than the speed of light in Maxwell electrodynamics in the vacuum, respectively.

In a Maxwell plasma, the phase speed $v = 1 + \frac{\omega_{pe}}{k}$ is always greater than speed of light $c = 1$. Since any particle travelling slower than $c = 1$ is unable to catch up with a wave whose phase speed is larger than $c = 1$, a wave whose purpose is to accelerate particles has to be decelerated until its phase speed is less than $c = 1$ to trap the particles. As a result, formulae (374)-(376) suggest that for a large enough wave number in cold Born-Infeld plasmas, the deceleration is unnecessary and particle trapping in ‘‘O’’ modes may be more likely than in the cold Maxwell plasma. As a result, in strong-field environments (e.g. magnetars) we qualitatively expect that a larger number of particles may be accelerated to high energies for $\kappa > 0$ than for $\kappa = 0$, when Born-Infeld electrodynamics approaches its classical limit to Maxwell electrodynamics.

VI. SUMMARY OF THE ORIGINAL RESULTS

In this thesis we have shown some aspects of high field theory by investigating the oscillations of relativistic plasmas. These aspects are listed in the following sections.

A. Electrostatic Oscillations & Bounds on the Electric Field in the Kinetic Description

We have studied the non-linear electrostatic oscillations of waterbag-distributed plasmas for 1-D and 3-D waterbag cases in the kinetic description. Maximum electric field E_{\max} proportional to the Lorentz factor γ and the “longitudinal temperature” to the power of $-\frac{1}{4}$ ($T_{\parallel\text{eq}}^{-\frac{1}{4}}$) have been obtained, which accords with the results obtained by Burton and Nobles [50] and Katsouleas and Mori [5]. As a looser upper bound that is larger than the values obtained before, it supports other authors well.

B. Wave-Breaking Limits Calculated in a Maxwell-Moments Model

With a Maxwell-moments method (fluid description), we have obtained the maximum electric field E_{\max} when the maximum proper number density $n_{\max} \rightarrow \infty$. Results show that the maximum electric field $E_{\max} \rightarrow \infty$ for a 1-D waterbag or a 3-D ellipsoid waterbag-distributed electron fluid, while it is finite in a 3-D gourd waterbag case. It appears that, compared with a 3-D gourd waterbag, a 1-D waterbag or a 3-D ellipsoid waterbag is more likely to have a strong enough electric field to support a considerable fraction of trapped particles.

Through a more general calculation, we have found that for any EOS $\rho + p - 2\xi$ consisting of $C_1 n^2 + C_2 + O(C_2)$ (with C_1, C_2 constants), the leading term

of the maximum electric field (when $n_{\max} \rightarrow \infty$) is proportional to $C_2 \ln n_{\max}$, which tends to infinity and is likely to accelerate a considerable fraction of trapped particles. With $C_2 = 0$, the 3-D gourd waterbag is a special case. For an arbitrary initial condition with its EOS $\rho + p - 2\xi$ leading to $C_1 n^2 + C_2 + O(C_2)$, a considerable fraction of trapped particles are allowed, unless the constant term C_2 in the EOS $\rho + p - 2\xi$ vanishes for some special reason.

For a 3-D ellipsoid waterbag-distributed fluid in particular, we have obtained the fraction of trapped particles by investigating the relative velocity of the wave with respect to the bulk motion of the fluid.

C. A Brief Exploration of a Klein-Gorden Plasma

With a brief calculation of the Maxwell equations and the Klein-Gorden equation with a $U(1)$ field, we have obtained the ODE system for the electric field. Numerical calculation of the ODE system shows that electrostatic oscillations decay in a Klein-Gorden plasma.

D. Wave-Breaking Limits and Dispersion Relations for Cold Plasmas in Born-Infeld Theory

With calculations using the Born-Infeld equations and the Lorentz equation, we have investigated electrostatic oscillations and electromagnetic waves in a cold plasma in Born-Infeld electrodynamics. Below are some of the conclusions we have drawn.

For the electrostatic oscillations, the electric field of Born-Infeld electrodynamics is smoother than that of Maxwell electrodynamics. This is consistent with the non-singular (albeit the non-smooth) nature of the electric field at a point charge in Born-Infeld electrodynamics [54]. In addition, the magnetic field reduces the

wave-breaking limit of the electric field. This effect begins to be important when the magnetic field is stronger, or when the number density of ions n_{ion} , or the Lorentz factor γ of the wave phase speed v is large. However, Born-Infeld electrodynamics gives the same result as Maxwell electrodynamics for the integral of the electric field E over the spatial interval between where E takes its maximum value and where it vanishes. Therefore, Born-Infeld electrodynamics gives the same prediction as Maxwell electrodynamics for the maximum energy that a test electron may obtain.

For the electromagnetic oscillations, the dispersion relation and the cutoff frequencies of the “R”, “L”, “O” and “X” modes of electromagnetic waves in Born-Infeld cold plasmas are different from those in Maxwell cold plasmas. To obtain results in Born-Infeld plasmas from those in Maxwell plasmas that are already known, replacement $\omega_{pe}^2 \rightarrow \omega_{pe}^2 \sqrt{1 + \kappa^2 B^2}$ is needed for the “R”, “L” and “X” modes, replacement $\omega_{pe}^2 \rightarrow \frac{\omega_{pe}^2}{\sqrt{1 + \kappa^2 B^2}}$ for the “O” mode and in the meantime replacement of wave number $k \rightarrow \frac{k}{\sqrt{1 + \kappa^2 B^2}}$ as well for the “O” and “X” modes. The results for the cutoff frequency (when the index of refraction $n \rightarrow 0$) show that the factor $\omega_{pe}^2 \sqrt{1 + \kappa^2 B^2}$ makes the Born-Infeld cutoff frequencies higher than the Maxwell ones in the “R”, “L” and “X” mode oscillations, but lower (than the Maxwell ones) in the “O” mode oscillations. As a result, the “O” mode oscillation has a phase velocity less than $c = 1$, which may imply that a larger number of particles could be accelerated to high energies in a Born-Infeld plasma than in a Maxwell plasma. We suggest that the radiation of magnetars may be used to test whether Born-Infeld electrodynamics meets observations better than Maxwell electrodynamics in circumstances with strong magnetic fields.

REFERENCES

- [1] D. E. Scott, IEEE Transactions on Plasma Science, **35**, NO. 4, August (2007).
- [2] I. Langmuir, Proc. Nat. Acad. Sci. U.S., **14** 628 (1928).
- [3] J. S. Townsend, “*The theory of ionisation of gases by collision*”, Constable & Robinson Ltd., (1910).
- [4] P. Debye and E. Hueckel, Z. Physik **24** 185 (1923).
- [5] T. Katsouleas and W.B. Mori, Phys. Rev. Lett., **61** 90 (1988).
- [6] D. A. Burton, A. Noble and H. Wen Nuovo Cimento C., **32** 1 (2009).
- [7] K. Yano and S. Ishihara, “*Tangent and Cotangent Bundles*”, Marcel Dekker, INC., (1973).
- [8] A. A. Vlasov, J. Exp. Theor. Phys., **8** (3): 291 (1938).
- [9] R. A. Dandl et al., Plasma Phys., **12** 235 (1970).
- [10] T. Tajima and J. M. Dawson, Phys. Rev. Lett., **43** 267 (1979).
- [11] J. B. Rosenzweig et al., Phys. Rev. Lett., **61** 98 (1988).
- [12] D. Umstadte et al., Optics Express, **2** Issue 7, 282 (1998).
- [13] W. P. Leemans et al., Nature Physics **2** 696 (2006).
- [14] I. Blumenfeld et al., Nature **445** 741 (2007).
- [15] A. R. Choudhuri, *The physics of fluids and plasmas : an introduction for astrophysicists*, Cambridge University Press, (1998).
- [16] E. S. Weibel, Phys. Rev. Lett., **2** 83 (1959).
- [17] D. A. Diver, A A da Costa, E W Laing, C R Stark and L F A Teodoro, Mon. Not. R. Astron. Soc., **401** 613, (2010)
- [18] J. D. Jackson, “*Classical Electrodynamics*”, 3rd Edition, Wiley, (1999).
- [19] D. A. Burton, Theoret. Appl. Mech., **30** 85 (2003).
- [20] R. C. Davidson, “*Physics of Nonneutral Plasmas*”, Imperial College Press and World Scientific Publishing Co. Pte. Ltd., (2001).
- [21] D. C. DePackh, J. Electron. Control, **13** 417 (1962).

- [22] F. Hohl, Phys. Fluids, **12** No. 1, 230-234 (1969).
- [23] I. Langmuir, Phys. Rev., **26** 585 (1925).
- [24] L. Tonks and I. Langmuir, Phys. Rev., **33** 195 (1929).
- [25] D. Bohm and E. P. Gross, Phys. Rev., **75** 1851 (1949).
- [26] D. Bohm and E. P. Gross, Phys. Rev., **75** 1864 (1949).
- [27] N.G. Van Kampena, Physica **21** 949 (1955).
- [28] J. M. Dawson, Phys. Rev., **113** 383 (1959).
- [29] A I Akhiezer and R V Polovin, Sov. Phys. JETP, **3** 696, (1956)
- [30] T. P. Coffey, Phys. Fluids, **14** 1402 (1971).
- [31] B. Bezzerides and S. J. Gitomer, Phys. Fluids **26** 1359 (1983).
- [32] A. Bergmann and P. Mulser, Phys. Rev. E, **47** 3585 (1993).
- [33] A. Pukhov and J. Meyer-ter-Vehn, Appl. Phys. B, **74** 355 (2002).
- [34] S. Kiselev, A. Pukhov, and I. Kostyukov, Phys. Rev. Lett., **93** 135004 (2004).
- [35] F. S. Tsung, R. Narang, W. B. Mori et al., Phys. Rev. Lett., **93** 185002 (2004).
- [36] K. V. Lotov, Phys. Rev. E, **69** 046405 (2006).
- [37] W. Lu, C. Huang, M. Zhou, W. B. Mori, and T. Katsouleas, Phys. Rev. Lett., **96** 165002 (2006).
- [38] C. Joshi and W. B. Mori, Philos. Trans. R. Soc. London, Ser. A, **364** 577 (2006).
- [39] A. Pukhov and S. Gordienko, Philos. Trans. R. Soc. London, Ser. A, **364** 623 (2006).
- [40] V. Malka, S. Fritzler, E. Lefebvre et al., Science, **298** 1596 (2002).
- [41] S. Mangles, C. D. Murphy, Z. Najmudin et al., Nature, **431** 535 (2004).
- [42] C. Geddes, C. Toth, J. van Tilborg et al., Nature, **431** 538 (2004).
- [43] J. Faure, Y. Glinec, A. Pukhov et al., Nature, **431** 541 (2004).
- [44] M. J. Hogan, C. D. Barnes, C. E. Clayton et al., Phys. Rev. Lett., **95** 054802 (2005).
- [45] S. P. D. Mangles, A. G. R. Thomas, M. C. Kaluza et al., Phys. Rev. Lett., **96** 215001 (2006).
- [46] B. Hidding, K.-U. Amthor, B. Liesfeld et al., Phys. Rev. Lett., **96** 105004 (2006).
- [47] W. B. Mori and T. Katsouleas, Physica Scripta, **T30** 127 (1990).
- [48] R. M. G. M. Trines and P. A. Norreys, Phys. Plasmas, **13** 123102 (2006).

- [49] C. B. Schroeder, E. Esarey and B. A. Shadwick, *Phys. Rev. E.*, **72** 055401 (2005).
- [50] D. A. Burton and A. Noble, *J. Phys. A*, **43** 075502 (2010).
- [51] D. A. Burton and H. Wen, Central Laser Facility Annual Report 2010-2011, Edited by B. Wyborn (2012)
- [52] M. Marklund and J. Lundin, *Euro. Phys. J. D.*, **55** 319 (2009).
- [53] W. Heisenberg and H. Euler, *Z. Phys.*, **98**, 714 (1936).
- [54] M. Born and L. Infeld, *Proc. R. Soc. Lond. A*, **144** 425 (1934).
- [55] A. A. Tseytlin, *Nucl. Phys. B*, **501** 41 (1997).
- [56] E. S. Fradkin, A. A. Tseytlin, *Phys. Lett. B*, **163** 123 (1985).
- [57] G. W. Gibbons, C. A. R. Herdeiro, *Phys. Rev. D* **63** 064006 (2001).
- [58] R. Ferraro, *Phys. Rev. Lett.*, **99** 230401 (2007).
- [59] R. Ferraro, *J. Phys. A: Math. Theor.*, **43** 195202 (2010).
- [60] T. Dereli, R. W. Tucker, *EPL* **89** 20009 (2010).
- [61] D. A. Burton, R. M. G. M. Trines, T. J. Walton and H. Wen, *J. Phys. A: Math. Theor.*, **44** 095501 (2011).
- [62] G. Boillat, *J. Math. Phys.*, **11** 941 (1970).
- [63] J. Plebanski, *Lectures on Non-Linear Electrodynamics*, Nordita, Copenhagen, (1970).
- [64] J. D. Jackson, *Classical Electrodynamics*, 3rd ed., Wiley, New York, (1999).
- [65] D. A. Burton, H. Wen, *AIP Conf. Proc.*, **1360** 87 (2011).
- [66] D. A. Diver, A. A. da Costa, E. W. Laing, C. R. Stark and L. F. A. Teodoro, *Mon. Not. R. Astron. Soc.*, **401** 613 (2010).
- [67] D. A. Burton and A. Noble, *AIP Conf. Proc.*, **1086** 252 (2009).
- [68] D. Pines, *J. Nucl. Energy C*, **2**, 5 (1961).
- [69] D. Pines, P. Nozieres, *The Theory of Quantum Liquids* (1999).
- [70] D. A. Burton and H. Wen, *Proceedings of SPIE*, **8075** 0B (2011).
- [71] B. Eliasson and P. K. Shukla, *Phys. Rev. E.*, **83** 046407 (2011).